ERDC/CHL TR-20-6

US Army Corps
of Engineers®
Engineer Research and
Development Center

ERDC
ENGINEER RESEARCH & DEVELOPMENT CENTER

Lower Columbia River Adaptive Hydraulics (AdH) Model: Development, Water Surface Elevation Validation, and Sea Level Rise Analysis

Kimberly C. Pevey, Gaurav Savant, Hans Rod Moritz,
and Elvon O. Childs

April 2020

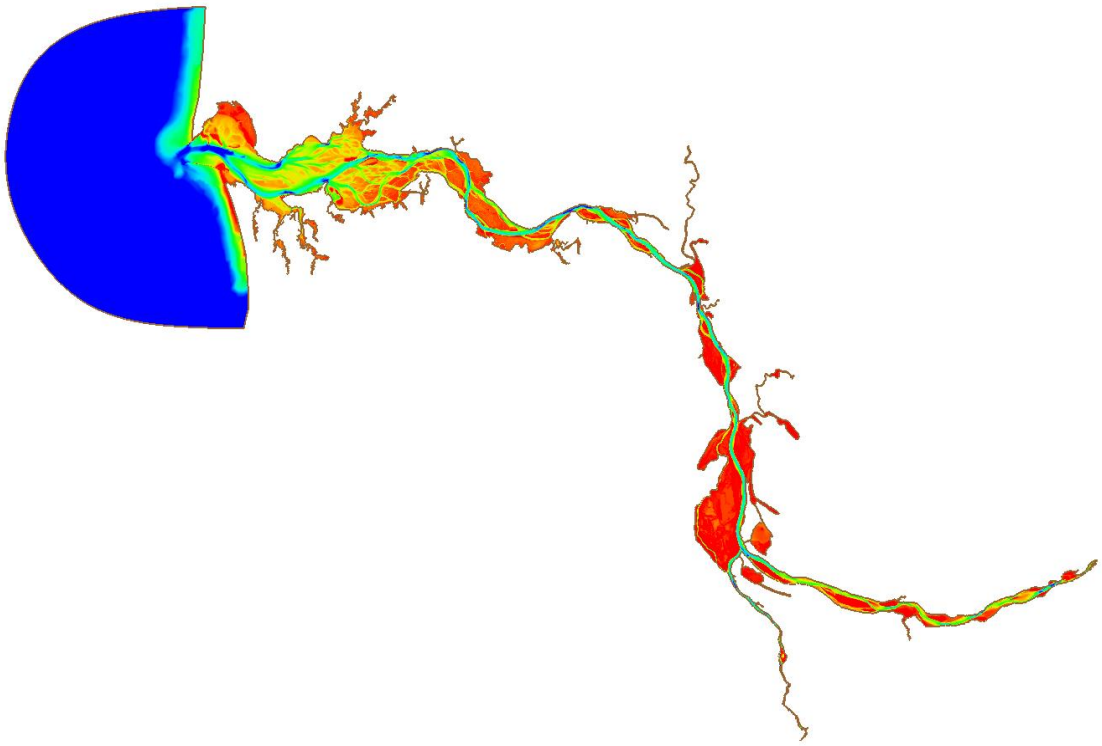

Coastal and Hydraulics Laboratory

The U.S. Army Engineer Research and Development Center (ERDC) solves the nation's toughest engineering and environmental challenges. ERDC develops innovative solutions in civil and military engineering, geospatial sciences, water resources, and environmental sciences for the Army, the Department of Defense, civilian agencies, and our nation's public good. Find out more at www.erdc.usace.army.mil.

To search for other technical reports published by ERDC, visit the ERDC online library at http://acwc.sdp.sirsi.net/client/default.

ERDC/CHL TR-20-6
April 2020

Lower Columbia River Adaptive Hydraulics (AdH) Model: Development, Water Surface Elevation Validation, and Sea Level Rise Analysis

Kimberly C. Pevey and Gaurav Savant

Coastal and Hydraulics Laboratory
U.S. Army Engineer Research and Development Center
3909 Halls Ferry Road
Vicksburg, MS 39180-6199

Hans Rod Moritz and Elvon O. Childs

U.S. Army Corps of Engineers, Portland District
333 SW First Avenue
Portland, OR 97208-2946

Final report

Prepared for U.S. Army Corps of Engineers, Portland District
333 SW First Avenue
Portland, OR 97208-2946

Under MIPR W66QKZ11602884, “Lower Columbia River Adaptive Hydraulics (AdH) Model”

Abstract

A numerical model of the Lower Columbia River, validated to water surface elevations, has been generated using the Adaptive Hydraulics (AdH) code. The model boundary conditions include an ocean tidal boundary and five inflows: the Lewis, Cowlitz, Willamette, and Sandy Rivers, and the Columbia River at Bonneville Lock and Dam. The model, which spans approximately 146 river miles, accurately reproduces water surface elevations measured in the field at several locations along the model domain.

An examination of the AdH model's Friction Library was also conducted. The Friction Library was used in this application to estimate the effects of pile dikes. Rather than model individual piles in the model mesh, the piles were modeled using the Friction Library's submerged vegetation material type. Through testing of this application, it was determined that the Friction Library approach, which enhances model run time and efficiency, can accurately reproduce the global effects of pile dike fields.

Additionally, the validated model was used to analyze three sea level rise (SLR) scenarios, which correspond to predicted SLR at Astoria, OR, at 50, 75, and 100 years from the present (0.5 meter [m], 1.0 m, and 1.5 m, respectively).

Table of Contents

Figures and Tables

Figures

Tables

Preface

This study was conducted for the U.S. Army Corps of Engineers, Portland District (NWP), under Military Interdepartmental Purchase Request W66QKZ11602884, "Lower Columbia River Adaptive Hydraulics (AdH) Model," dated 2011. Project coordination at the NWP was provided by Mr. Hans Rod Moritz of NWP.

The work described herein and the preparation of this report were performed from July 2011 through February 2012 by the U.S. Army Engineer Research and Development Center, Coastal and Hydraulics Laboratory (ERDC-CHL), Vicksburg, MS. The work was performed under the general supervision of Dr. William D. Martin, Director, ERDC-CHL, and Mr. José E. Sánchez, Deputy Directory, ERDC-CHL. Direct supervision was provided by Dr. Ty V. Wamsley, Acting Chief, Flood and Storm Protection Division, and Dr. Robert McAdory, Chief of the Estuarine Engineering Branch.

At the time of publication of this report, Mr. Jeffrey R. Eckstein was the Deputy Director of CHL, and Dr. Ty V. Wamsley was the Director.

COL Teresa A. Schlosser was the Commander of ERDC, and the Director was Dr. David W. Pittman.

1 Introduction

1.1 Background

Federally owned multipurpose dams on the Columbia River and its tributaries under the Federal Columbia River Power System (FCRPS) provide approximately 60% of the region's electric supply. Due to these hydroelectric generation activities, and to protect Endangered Species Act-listed species, the National Marine Fisheries Service and the U.S. Fish and Wildlife Service issued a set of Biological Opinions in 2000. The U.S. Army Corps of Engineers (USACE), Portland District (NWP), manages its ecosystem and habitat restoration programs with the consideration of their contribution to the FCRPS Biological Opinion, measured by the Endangered Species Units. Restoration, habitat enhancement, and habitat creation efforts are ongoing within the Lower Columbia River basin and in the estuary to mitigate the effects of human activities since the 1870s. Most recently, the Columbia River Channel Improvement Project, which deepened the navigation channel from 12.2 meters (m) to 31.1 m below the Columbia River Datum, requires ecosystem restoration as part of the adaptive management plan.

The NWP and the U.S. Army Engineer Research and Development Center (ERDC), Coastal and Hydraulics Lab (CHL), discussed the development of a regional tool that will be a platform to support a variety of NWP objectives and business lines, such as ecosystem restoration, as well as a variety of other stakeholder interests for the Lower Columbia River (LCR) system. It was determined that such a platform will provide an integrated framework that will evolve and inform decision makers of the complexities of the dominant forces and dynamic nature of the LCR. The proper tool will capture this complex and dynamic nature and provide meaningful output to both NWP and stakeholders interests.

To provide such a tool, a large-scale Adaptive Hydraulics (AdH) model, including the Lower Columbia and Willamette Rivers, was recently developed at the ERDC-CHL Estuarine Engineering Branch under the System Wide Water Resource Program (SWWRP) and was developed further at the request of NWP. AdH is the USACE next-generation multi-

dimensional, physics-based, hydrodynamic model code.[1] Planned use of AdH provides a decision support system to conduct *what-if* analyses involving circulation, salinity, sediment transport, water quality, and ecology for project sites within Columbia River Estuary during the planning phase of eco-system and habitat restoration, and other related programs.

1.2 Objective

The primary objective of this study was to enhance the existing AdH model and associated mesh of the LCR Estuary and validate it to water surface elevations at four locations. Three sea level rise (SLR) scenarios were analyzed as well as an examination of the method in which AdH models pile dikes. Additionally, demonstration of module functionally for temperature, vessel movement, salinity, and sediment transport were included.

1.3 Description of the site

The Columbia River originates in British Columbia, Canada, and flows through Washington state before it reaches its confluence with the Pacific Ocean. The Columbia River watershed stretches across seven states and two Canadian provinces in the Pacific Northwest (Simenstad et al. 1990). Flow in the river is influenced by seasonal changes. Peak spring flows are approximately 14,000 cubic meters per second (cms) while fall flows are approximately 3,000 cms (Sherwood 1990).

Tributaries into the Columbia River include the Snake River, Deschutes River, Lewis River, Cowlitz River, Sandy River, and Willamette River. The Willamette River is a major tributary of the Columbia River and contributes 12% to 15% of the total flow.

The Columbia River Estuary, where, generally, salinity intrusion exists, is located in northwest Oregon and southwest Washington states, starting at the mouth near Astoria, Oregon, and extending inland to near the eastern tip of Puget Island at River Mile (RM) 46 (Fox 1984), though tidal effects are seen all the way to Bonneville Lock and Dam (L&D).

[1] https://chl.erdc.dren.mil/adaptive-hydraulics/ ; https://chl.erdc.dren.mil/chladh

Figure 1-1. Columbia River Basin (USACE Northwestern Division).

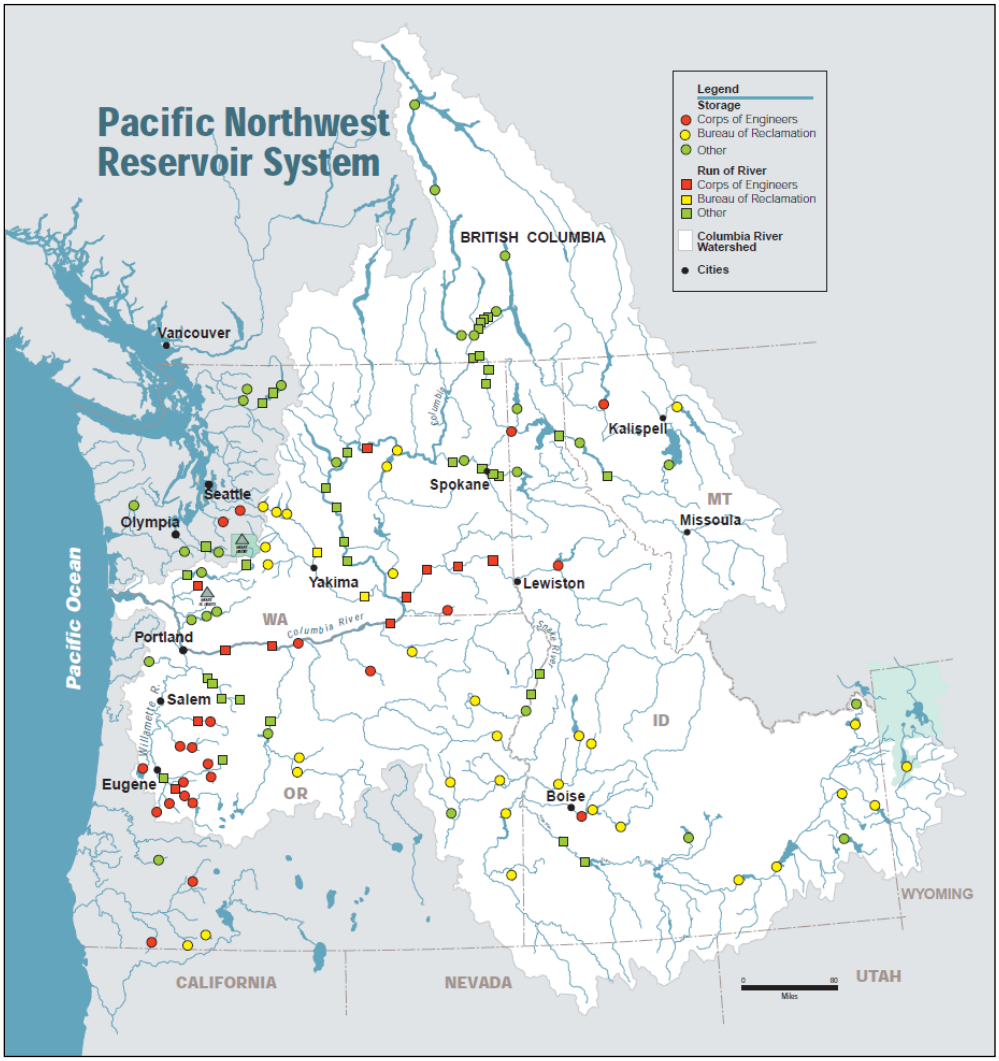

The Columbia River is a regulated waterbody with the most downstream lock and dam located at Bonneville. Below Bonneville, the river continues 146 miles before it reaches open ocean. This region, a tidally influenced estuary, is referred to as the LCR and is the focus of this work.

1.4 Approach

The approach is addressed in Chapter 2 Model Development.

2 Model Development

The numerical code used in this work is the AdH model. The AdH code uses an unstructured mesh and is both spatially and temporally adaptive. AdH can solve 2-dimensional (2D) and 3-dimensional (3D) shallow water equations, 3D Navier-Stokes equations, and 3D groundwater equations.

The 2D shallow water module of AdH was used for this work. Future work may expand this model with the application of the 3D shallow water module to examine salinity intrusion.[2]

Initial mesh development and model execution were performed by the Estuarine Engineering Branch of the ERDC as a demonstration project for the USACE SWWRP during Fiscal Year 2010. After the demonstration project, the mesh was modified by CHL to add resolution and to meet the needs of NWP.

The mesh was generated in the Surface-water Modeling System, a graphical user interface that was developed for visualization of model results and mesh generation (Aquaveo 2016).

2.1 Model domain

The model domain, which begins at Bonneville L&D near North Bonneville, WA, includes all 146 river miles of the LCR, and extends more than 30 km beyond the mouth of the river into the Pacific Ocean (Figure 2-1). The lateral extents include the wetted areas for the projected 100-year SLR (USACE 2009) as well as many islands in the LCR. The mesh contains 226,088 nodes and 433,187 elements and has five inflows: the Cowlitz, Lewis, Willamette, and Sandy Rivers, and the Bonneville L&D.

[2] Interested readers are referred to the AdH websites (https://chl.erdc.dren.mil/adaptive-hydraulics and https://chl.erdc.dren.mil/chladh) for the User's Manual and to Savant et al. (2011) for technical details.

Figure 2-1. Extents of model domain.

The LCR is a tidal estuary with a tide range of approximately 2.06 m (6.77 ft) (NOAA gauge 9439040 at Astoria). As the tidal wave propagates inland, its energy is damped, and freshwater inflows begin to dominate the system. At the inland boundary of the mesh domain, little tidal influence can be seen.

Nodal mesh elevations were interpolated from the most current digital elevation model (DEM) available (1 December 2011). The DEM was developed by NWP and was generated using both multibeam and lidar data. The horizontal datum is North American Datum 1983 (NAD83), State Plane Oregon, North and the vertical datum is North American Vertical Datum 1988 (NAVD88) (meters). The elevation contours (in meters) are shown in Figure 2-2 where mean sea level is approximately 1.4 m at Astoria.

Figure 2-2. LCR AdH mesh elevations (NAVD88, State Plane Oregon North, meters).

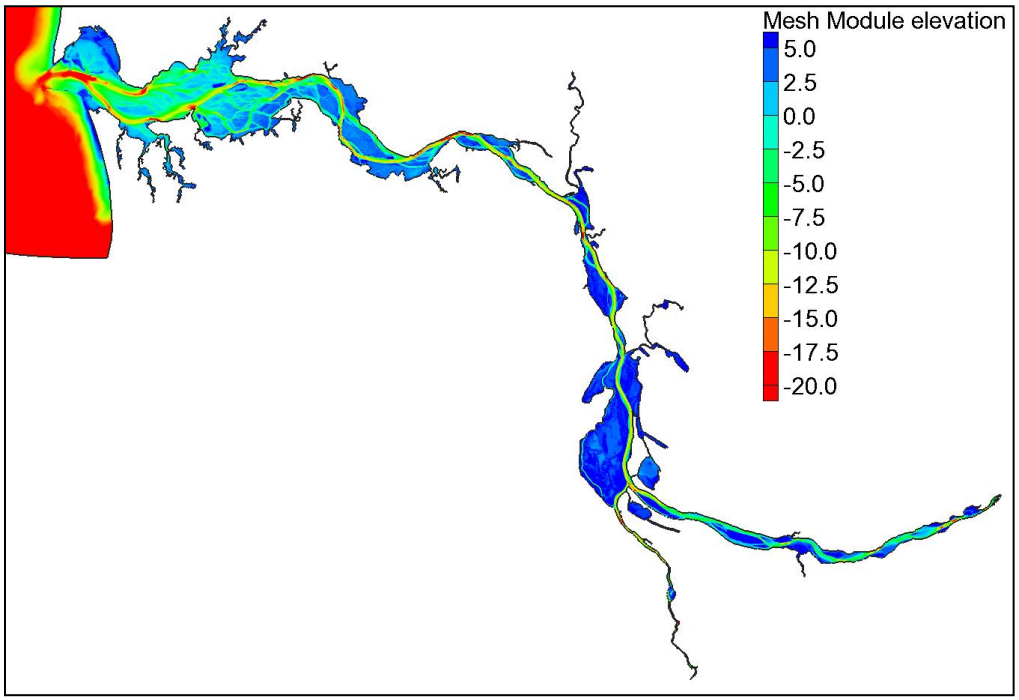

The typical mesh resolution is on the order of 100 m while the tributaries, jetties, pile dikes, and smaller flow paths required a higher resolution (Figure 2-3). The ocean region beyond the mouth of the LCR was not an area of interest and thus was meshed at approximately 1000 m.

Figure 2-3. LCR AdH mesh showing resolution and elevation contouring.

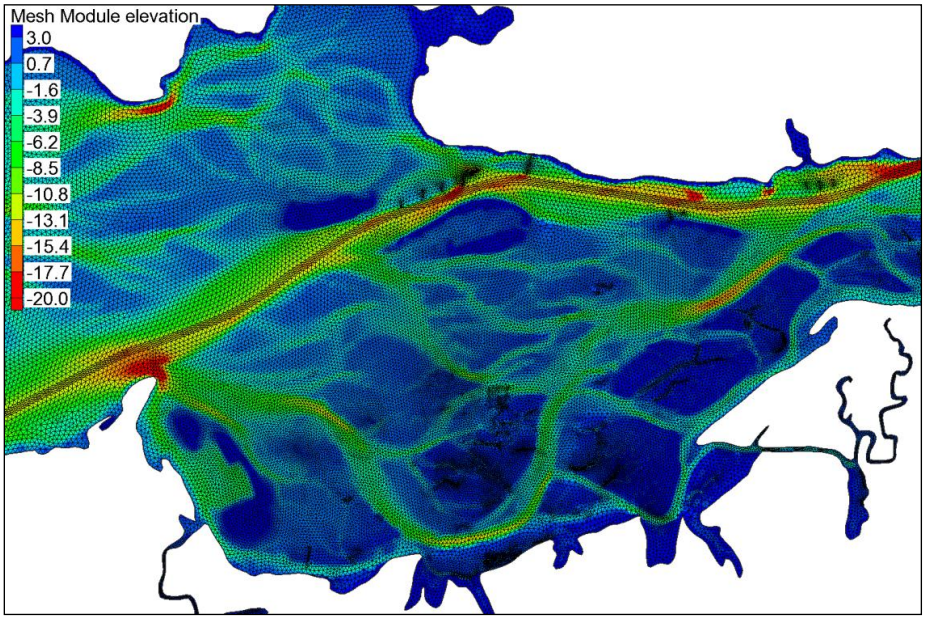

The mesh is comprised of 11 material types, shown in Figure 2-4. The friction associated with each material type was specified in AdH using Manning's *n* with the exception of the pile dikes that were applied as un-submerged vegetation (impenetrable cylinders) (see Section 2.2 for a detailed description of this application). Though Manning's *n* is constant for a given material type, the friction changes with depth. The relationship between friction and depth follows a physically based algorithm that is built into AdH. The friction specifications by material type are listed in Table 2-1. The Manning's *n* values are input using the FR MNG card in the AdH boundary condition file while the pile dikes are specified as un-submerged vegetation using the FR URV card. The FR URV card requires three parameters: bed roughness height, average stem/pile diameter, and average stem/pile density (Berger 2011).[3]

Figure 2-4. LCR mesh material types.

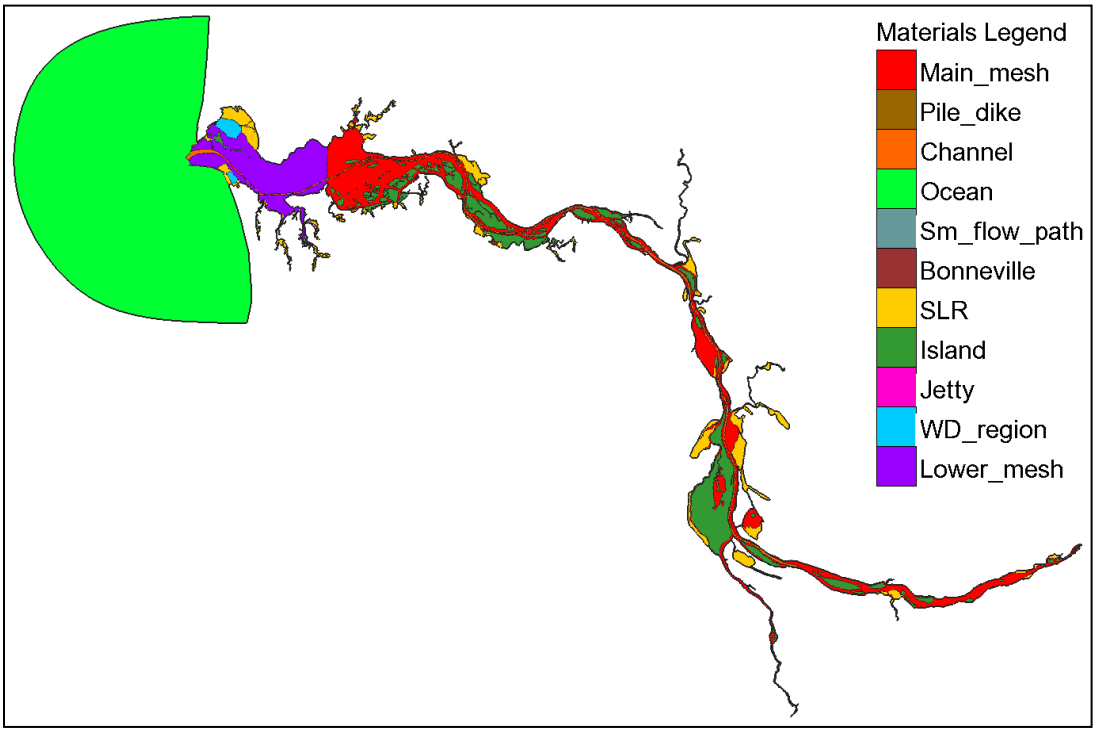

[3] Further discussion of the material type specification can be found in Section 3, Model Calibration.

Table 2-1. Material type specification in AdH.

Material type	AdH Card	Value
Main_mesh	FR MNG	0.025
Pile_dike	FR URV	0.050 0.3048 1.52
Channel	FR MNG	0.025
Ocean	FR MNG	0.015
Sm_flow_path	FR MNG	0.025
Bonneville	FR MNG	0.025
SLR	FR MNG	0.025
Island	FR MNG	0.080
Jetty	FR MNG	0.080
WD_region	FR MNG	0.025
Lower_mesh	FR MNG	0.015

At the request of NWP, several areas were refined to include more detail. For potential future project purposes, the Stock Ranch slough and Crim's Island were refined (Figure 2-5). These areas were refined to 50 m for low gradient regions and approximately 10 m for flow paths and levees.

Figure 2-5. Stock Ranch (left) and Crim's Island (right) mesh refinement.

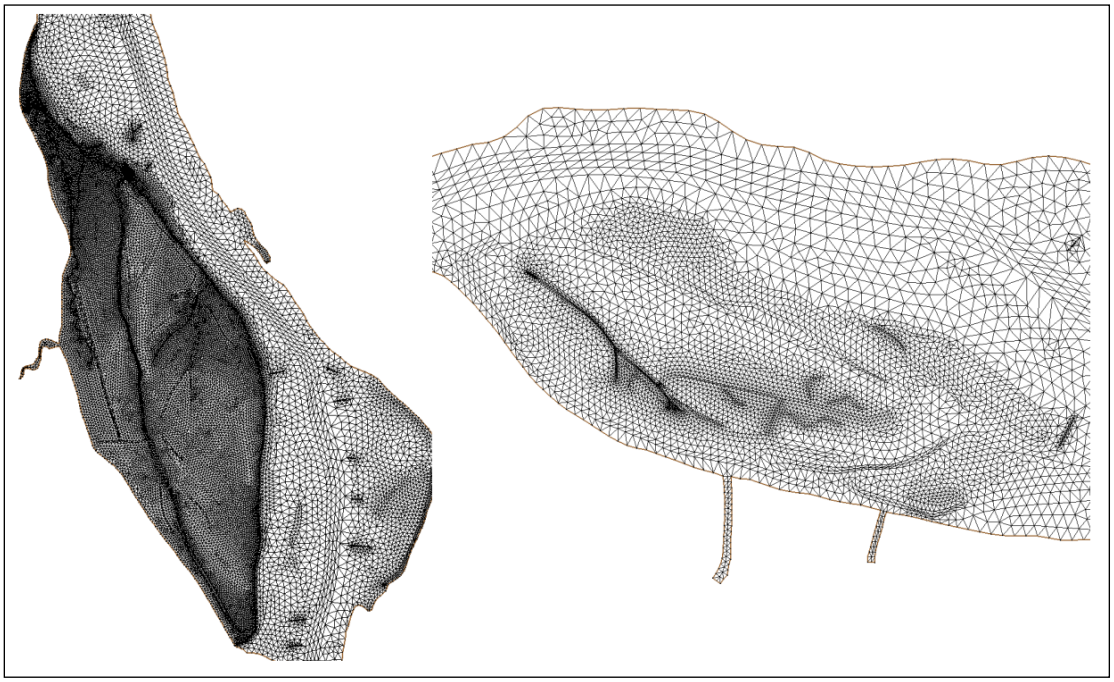

Additionally, the Young's Bay causeway was refined to 10 m to ensure that the roadway was properly defined as impenetrable to flow (Figure 2-6, right). The north and south jetties were refined to enable any future examination of jetty efficiency and jetty restoration or modification (Figure 2-6, left). Mesh resolution along the crest of the jetties is below 5 m, and in some areas, as low 2 m (Figure 2-7). Though the mesh streamlines were based on DEM data, high-resolution TIFF images from NWP were used to aide in visualization.

Figure 2-6. North and south jetty (left) and Young's Bay Causeway (right) mesh refinement.

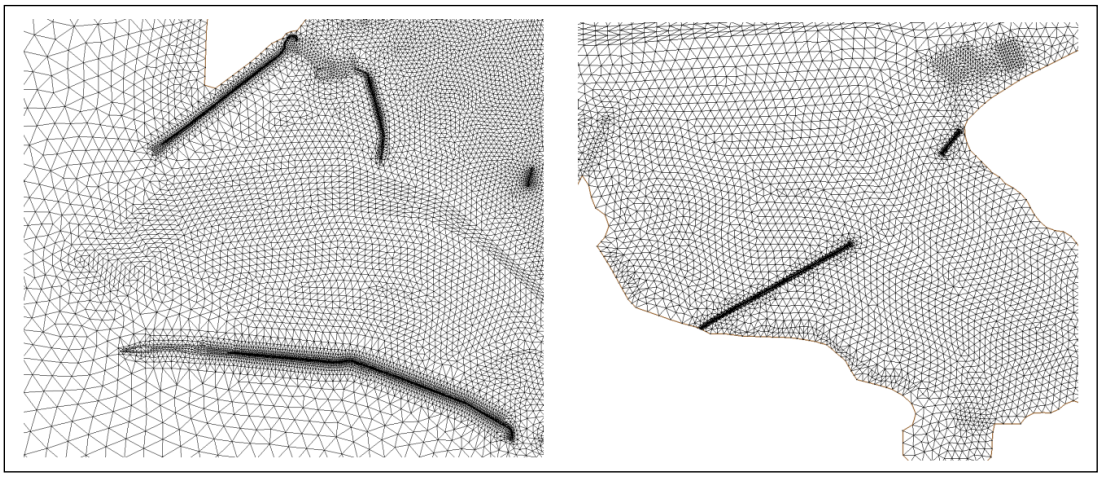

Figure 2-7. North jetty mesh refinement with aerial image underlay.

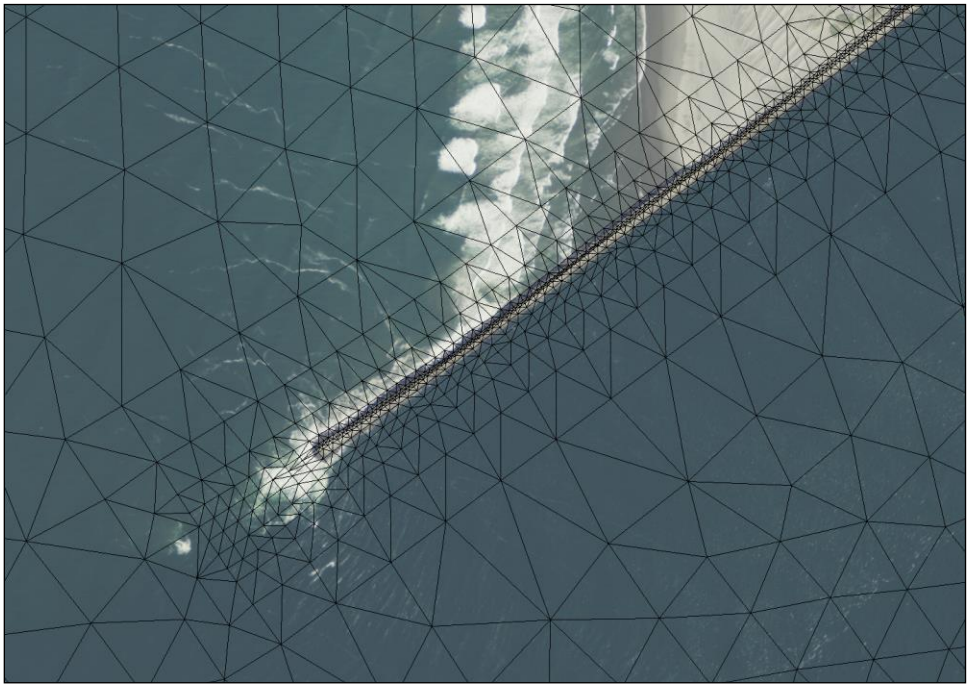

2.2 Pile dike testing

Over two hundred pile dikes are located in the Lower Columbia River and each pile dike field can contain several hundred individual 0.304 to 0.610 m (12- to 24-inch [in.]) diameter piles. If these piles were modeled individually, the resolution requirements at that scale would greatly reduce model efficiency. Though AdH can handle a high-resolution mesh, a simpler and more computationally efficient method is available using AdH's Friction Library.

Friction is defined by material type (specified by each element) in AdH. Each material type can have a different friction type, which is referenced to the Friction Library. Generally, the bed is defined with the FR MNG card which specifies a Manning's *n* value for the element. The Friction Library also contains a card used for modeling un-submerged vegetation (FR URV). This card can be used for stands of marsh grass along the edge of an estuary, or any impenetrable cylinder. In this case, it can be used to model a much larger object, wooden piles. Roughness height, average stem diameter of the vegetation, and average stem density are specified in the FR URV card.

In the LCR mesh, the pile dikes are modeled with the FR URV card, allowing the pile dike areas to be specified simply by a narrow rectangular material region (Figure 2-8). To achieve this using the FR URV card, the construction documents for several pile dikes were examined, and a pile/unit length of pile dike was calculated. This unit density was then divided by the average width of the pile dike material regions across the mesh, giving an average pile density. Because the number of piles on a material region is specified by a density and since the pile dike regions in the mesh are slightly larger than the actual footprint of the real world dikes, the FR URV card effectively spreads the same number of piles over a larger area.

Figure 2-8. LCR mesh showing pile dikes.

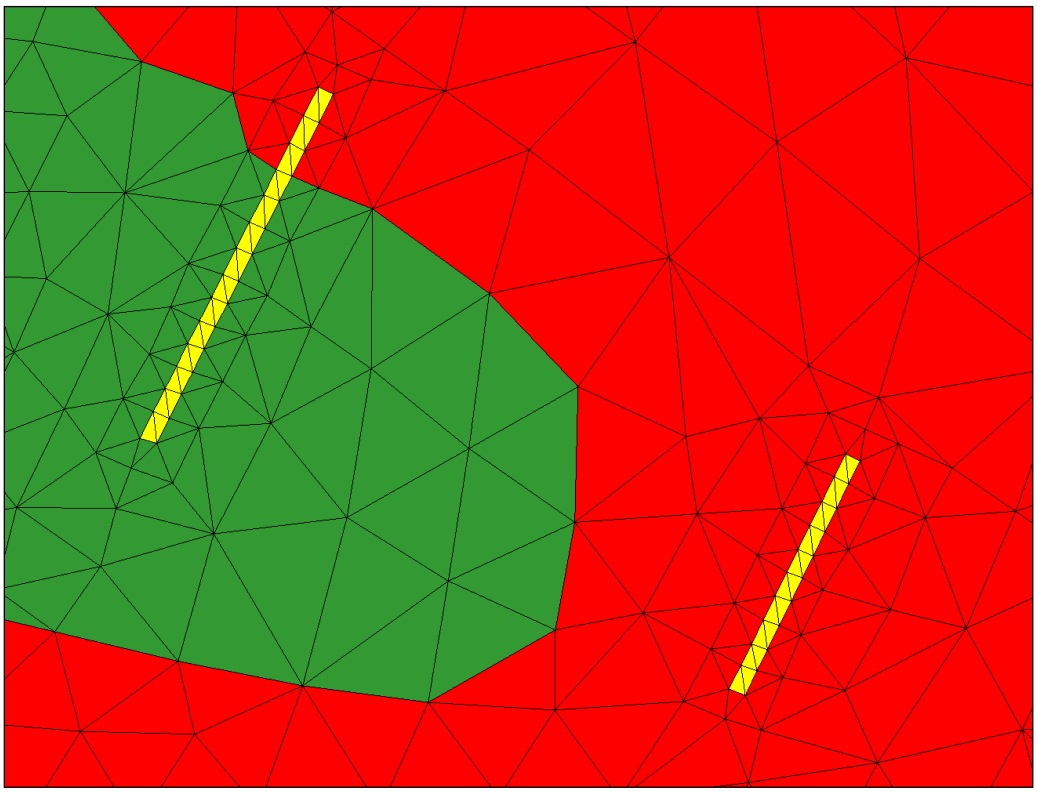

To ensure that this application method did indeed produce the same hydraulic effect as modeling individual piles, two test cases were analyzed. A comparison was made between the pile dike modeled as a material region with the FR URV card and the case in which individual piles are inserted into the flow path (AdH sees each pile as a cylindrical wall within the mesh).

A relatively straight stretch of river in the LCR mesh was chosen as the test region. This subset mesh was modified to increase resolution. Individual piles were meshed at approximately 0.04 m for three consecutive pile dike fields; each containing approximately 300 piles (Figure 2-9).

Figure 2-9. Subset mesh with increased pile dike resolution (left), close view of pile dike resolution (top right), and material type variation (lower right).

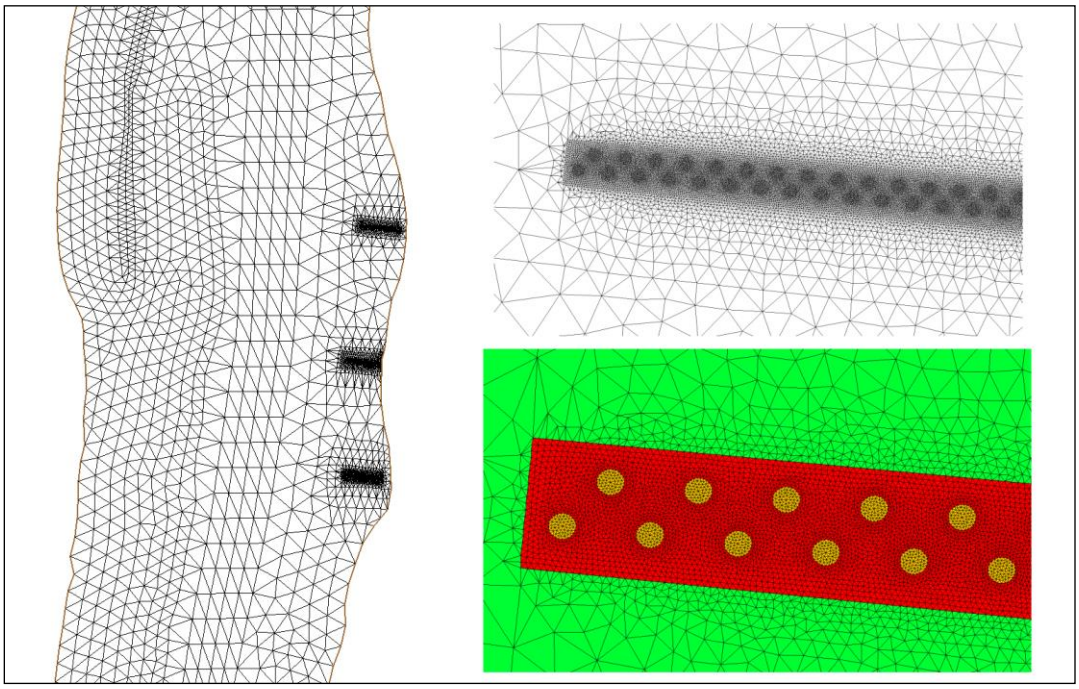

As can be seen in the lower-right image in Figure 2-10, three material types were utilized. The variation in material type allowed for one mesh to be used for the two test case model runs. The first case, where the piles were modeled individually, utilized the OFF card in AdH for the yellow material type (individual piles). By modeling the piles as a separate material type and utilizing the OFF card in AdH, the individual piles were inserted into the mesh. The remaining two material types were modeled as FR MNG with a Manning's *n*. The second case utilized the FR URV card for both the piles (yellow) and the region surrounding the piles (red). This is how the pile dikes are modeled in the larger LCR mesh.

The AdH model was applied to this reach with boundary conditions obtained from full-domain model runs. A high-flow scenario was examined and run at steady state to examine the difference in the velocity fields between the two test cases.

With the pile dikes modeled individually, the water must flow around the piles. When the pile dikes are modeled with the FR URV card, the entire pile dike region (material type) has an increased friction that affects the flow energy, but there are no actual structures to impede the flow. Because of this, near-field differences are to be expected between the two runs

while the far-field (channel) velocities should be approximately the same. The steady-state velocity contouring for each run is shown in Figure 2-10, and the differences between the two velocity magnitudes can be found in Figure 2-11.

Figure 2-10. Velocity comparison (meters per second) of FR URV results (left) to the individual pile dikes (right).

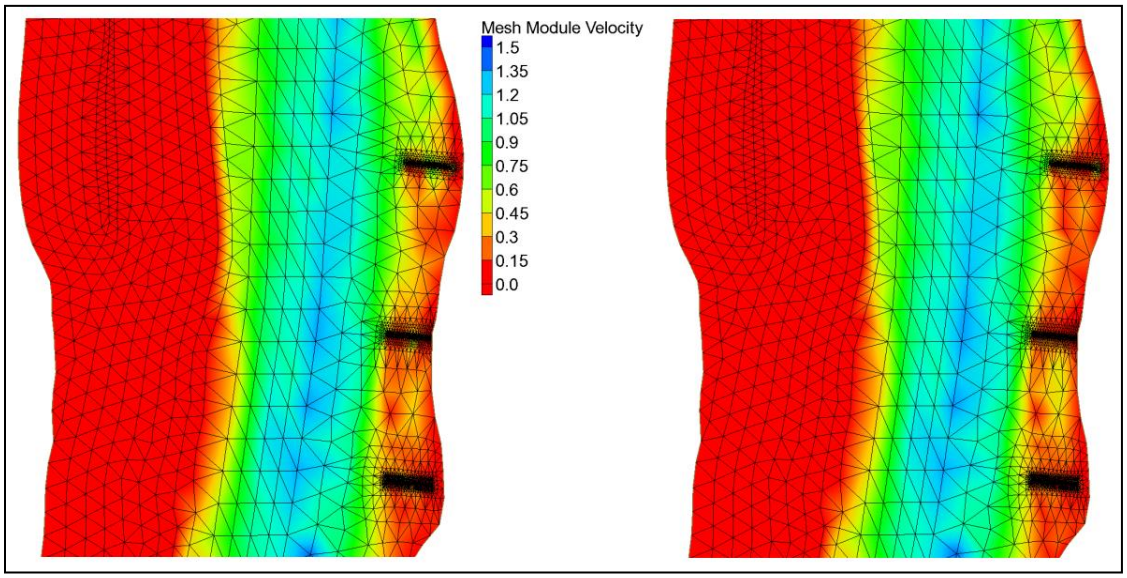

Figure 2-11. Velocity differences (meters per second) between the modeling individual piles and the FR URV card.

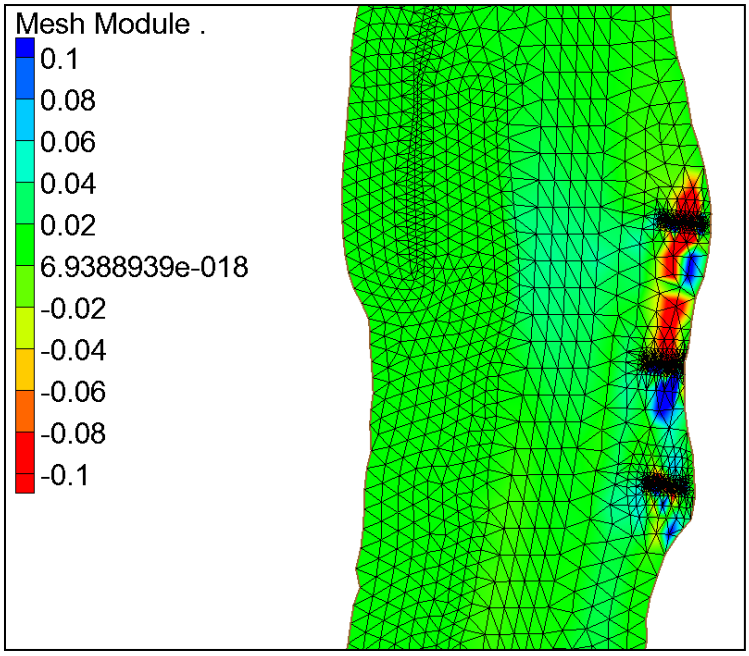

The differences in the velocities in the channel and throughout the majority of the mesh are minimal (approximately 1–2% or less). The test case represents the successful implementation of the FR URV card by effectively reproducing channel and far-field velocities with significantly less resolution. Computational time has been reduced as well as mesh development time.

2.3 Boundary conditions development

The LCR AdH model boundary conditions were developed from field data acquired from the National Oceanic and Atmospheric Administration (NOAA) and U.S. Geological Survey (USGS). The tidal and inflow data are described in this section.

2.3.1 Inflow and elevation data

The USGS streamflow gauges were used to obtain inflow boundary condition data. The gauge locations within the mesh are shown in Figure 2-12. Tabular location information, including the approximate locations of the mouth of each river inflow, is listed in Table 2-2 where river mile is measured relative to the mouth of the Columbia River. The USGS inflow data were implemented using cubic meters per second and Pacific Standard Time (PST).

Figure 2-12. USGS gauge locations.

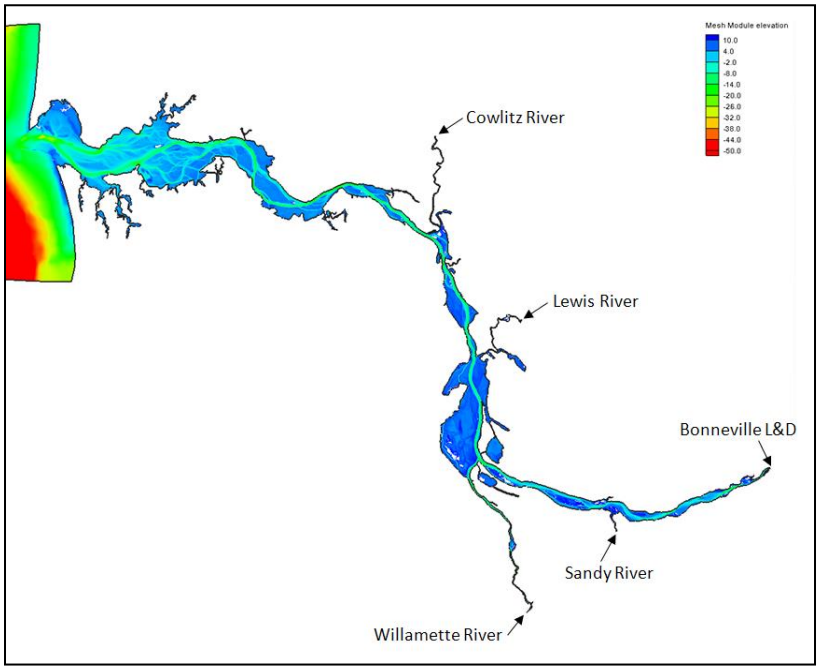

Table 2-2. Inflow boundary condition station information.

Station	Agency	Station ID	Latitude	Longitude	Approximate River Mile
Cowlitz River	USGS	14243000	46° 16’ 30”	122° 54’ 48”	RM 68
Lewis River	USGS	14220000	45° 58’ 12”	122° 34’ 12”	RM 87
Willamette River	USGS	14207740	45° 21’ 00”	122° 37’ 12”	RM 101
Sandy River	USGS	14142500	45° 25’ 48”	122° 13’ 48”	RM 120
Bonneville L&D	USGS	14128870	45° 37’ 48”	121° 57’ 00”	RM 145

NOAA tide gauge data from Astoria were used to drive the ocean boundary of the model. Several other NOAA gauges were used to analyze water surface elevations within the model domain. Gauges that did not have datum information (Columbia River Datum, NAVD88, or NAVD29) were not included. Additionally, water surface elevations at Bonneville were acquired from USGS to analyze model results. Tabular station location information is included in Table 2-3, and a graphical representation of the gauge locations within the mesh can be found in Figure 2-13. The vertical water surface elevation datum was NAVD88 (meters) and PST.

Figure 2-13. NOAA tide gauge locations.

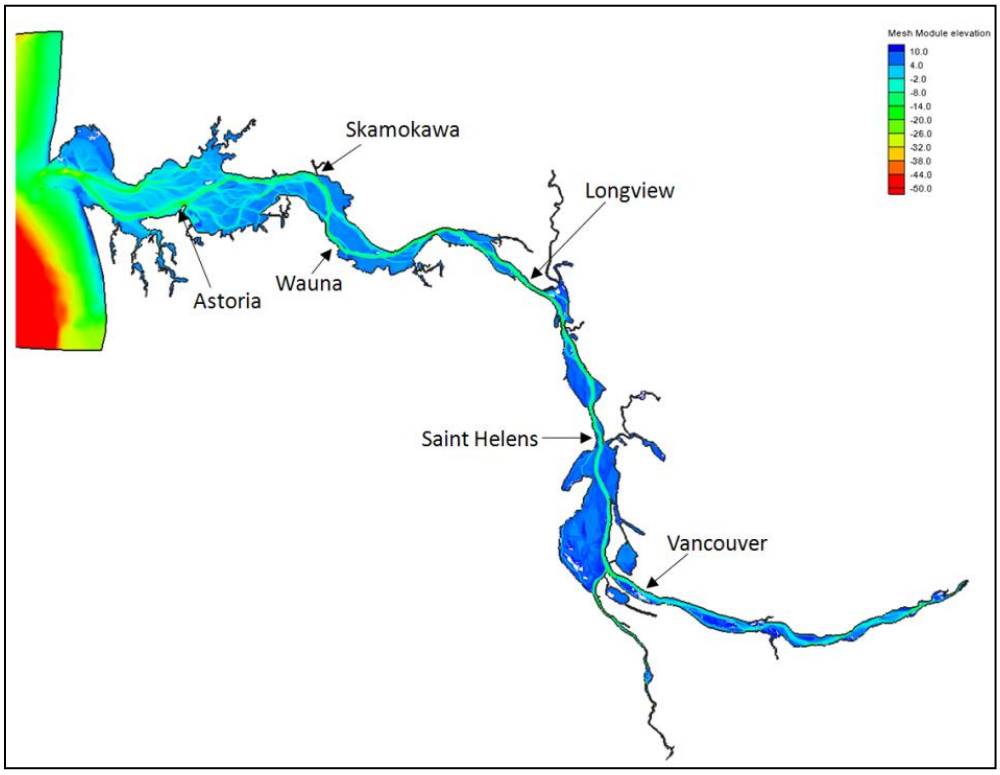

Table 2-3. NOAA tide gauge station information.

Station Name	Agency	Station ID	Latitude	Longitude	State Plane East, m	State Plane North, m	River Mile
Astoria	NOAA	9439040	46° 12' 24"	123° 46' 06"	2247313.6	287548.5	RM 8
Skamokawa	NOAA	9440569	46° 16' 00"	123° 27' 06"	2272473.4	293031.7	RM 34
Longview	NOAA	9440422	46° 06' 18"	122° 57' 12"	2310340.5	273845.7	RM 66
St. Helens	NOAA	9439201	45° 51' 54"	122° 47' 48"	2321851.1	246853.9	RM 86
Bonneville	USGS	14128870	45 37’ 59”	121 57’ 39”	2386107.8	219541.0	RM 145

2.3.2 Tidal boundary conditions

The model tidal boundary (shown in Figure 2-14 with a solid red line) was specified using the NOAA-measured tidal signal at Astoria, OR. The analysis period includes a 2-year river flow event (~9.91 thousand cubic meters per second [kcms] at Bonneville), which occurred in 2009. The boundary condition file contains data from 1 November 2008 to 31 January 2010 to fully encompass the calendar year surrounding this event.

Figure 2-14. LCR ADH mesh extents (NAVD88, SPCS Oregon North, meters).

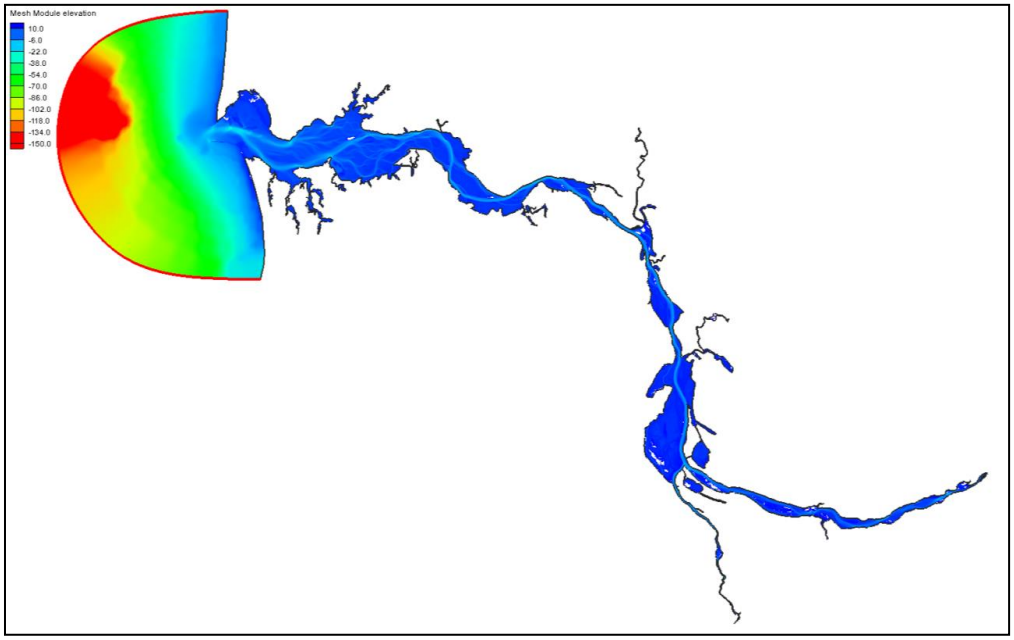

The tidal data were filtered to remove any extraneous noise signals with periods fewer than 4 hours. A comparison of the raw and filtered tide data can be seen in Figure 2-15 as nearly identical.

Figure 2-15. Comparison plot of raw (solid blue) and filtered (dashed green) tide data.

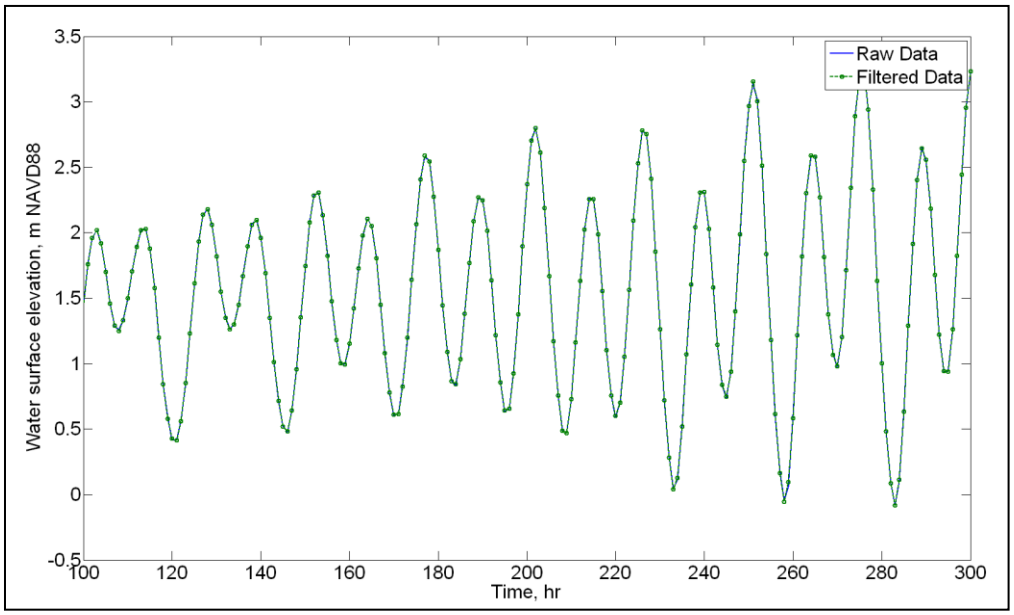

Though Astoria was the closest gauge to the boundary with available data for the time period, it was located a significant distance inland (24 km inland, 57 km from the ocean boundary). Due to this distance, it was necessary to shift the measured gauge data before applying at the tidal boundary (Table 2-4). The mean of the measured tidal data at Astoria required a vertical shift of -0.027 m and a scaling factor due to the tidal wave being amplified by the mouth of LCR. The scaling factor essentially reduces the amplitude of the tidal signal while the vertical shift adjusts the mean of the signal. Additionally, due to the distance between the tidal boundary and the Astoria gauge, the phase lag of 1.1 hours was applied. The resulting model water surface elevation at Astoria closely matches the observed field data.

Table 2-4. Tidal data applied shifts.

	Shift
Vertical shift	-0.027 m
Phase lag	-1.1 hour
Scaling factor	0.95

2.3.3 Inflow boundary conditions

There are five inflows into the model domain: the Cowlitz, Lewis, Willamette, and Sandy Rivers, and the Bonneville L&D (Figure 3-2). Hourly discharge data (cubic meters per second) were collected for the all river inflows, with the exception of the Lewis River where only daily discharge data were available. These inflows were incorporated into the boundary condition file.

The model year 2009 was chosen due to the 2-year event (~9.91 kcms), which occurred during the spring freshet on the Columbia River. During this same time period, the Willamette flow rates were also elevated, which achieved the requirement for high flows during the calibration period. Winds and salinity were not included in this model.

2.3.4 Flow parameters

Roughness (friction) in the AdH model was used as a calibration parameter. Standard accepted values were initially specified, and then slight adjustments were made during calibration to ensure accurate reproduction of the field data.

In general, the material types in the LCR mesh are separated by elevation with different material types for the channel, the main portion of the mesh, islands, and SLR regions. This allows for a higher Manning's *n* value to be applied to vegetated regions such as the islands. A series of friction values were tested to obtain optimal performance.

The kinematic eddy viscosity is a measure of the turbulent smearing occurring at a resolution finer than that of the mesh. It is a flow parameter that ensures that the turbulence is not improperly estimated due to low resolution. In AdH, the eddy viscosity is specified for each material type. The eddy viscosity values for some areas of the mesh, which contain wetting and drying or eddy formations, required slightly higher region-specific values.

3 Model Calibration

3.1 Water surface elevation calibration

Water surface elevations were calculated for the period beginning 1 April 2009 and ending 1 July 2009 and compared with station data in Table 2-3. The 60-day period was chosen to include the spring freshet. The model was run for a 2-week spin-up period to allow the system energy to equilibrate.

The only adjustments made in the calibration process were to the Manning's *n* values. Calibrating the model friction, or roughness, ensured that energy was distributed properly throughout the system.

The water surface elevation comparisons are shown in time-series plots and box plot correlations (Figure 3-1 through Figure 3-10). The 45-degree line on each box plot indicates perfect correlation between the observed and model datasets.

Figure 3-1. Water surface elevation comparison between model (blue) and field (green) for Astoria.

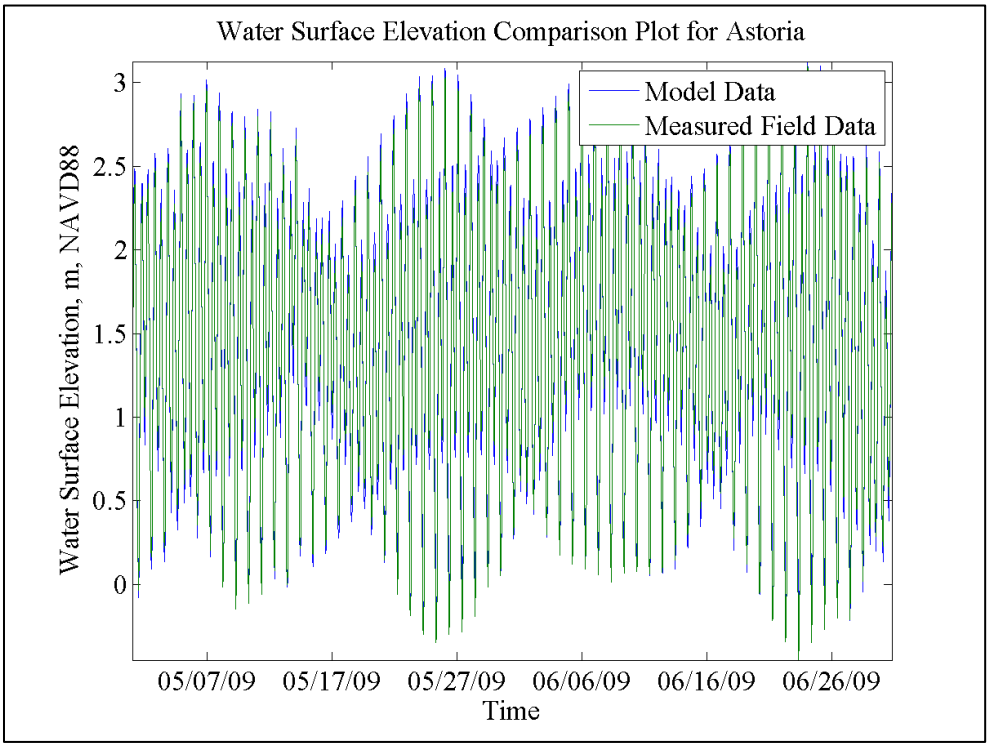

Figure 3-2. Water surface elevation box plot comparison for Astoria.

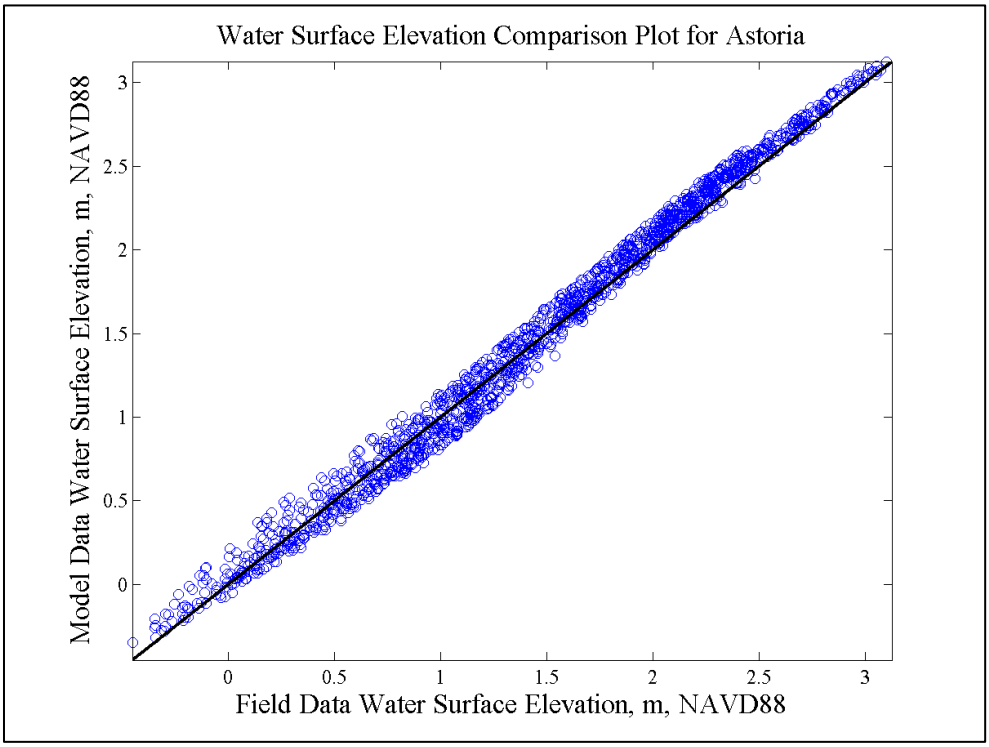

Figure 3-3. Water surface elevation comparison between model (blue) and field (green) for Skamokawa.

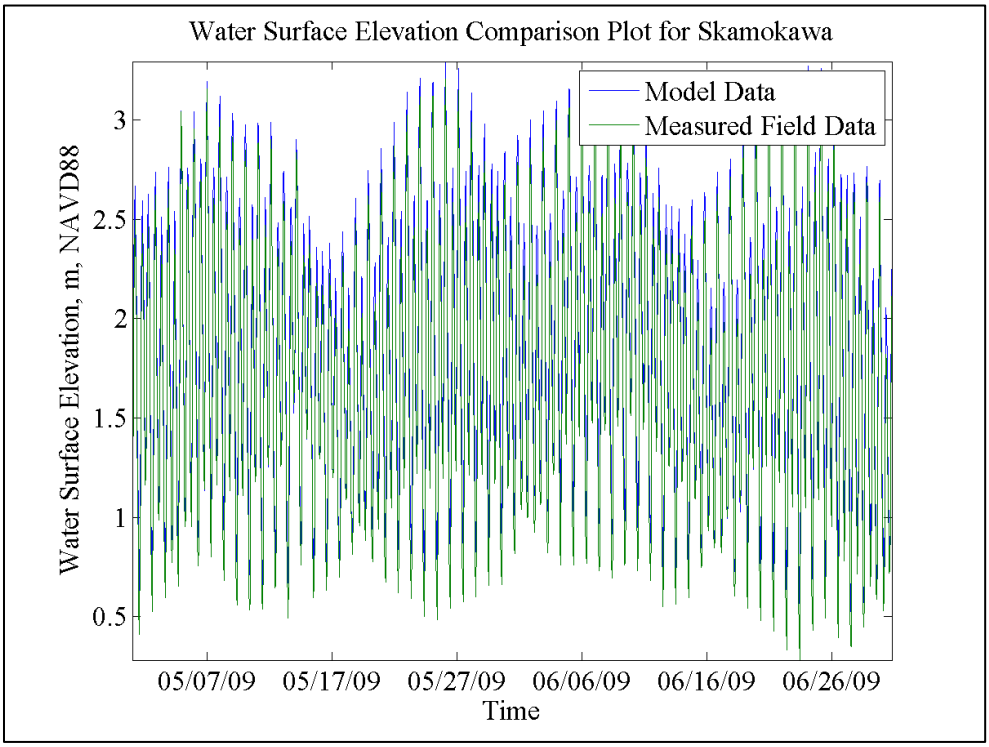

Figure 3-4. Water surface elevation box plot comparison for Skamokawa.

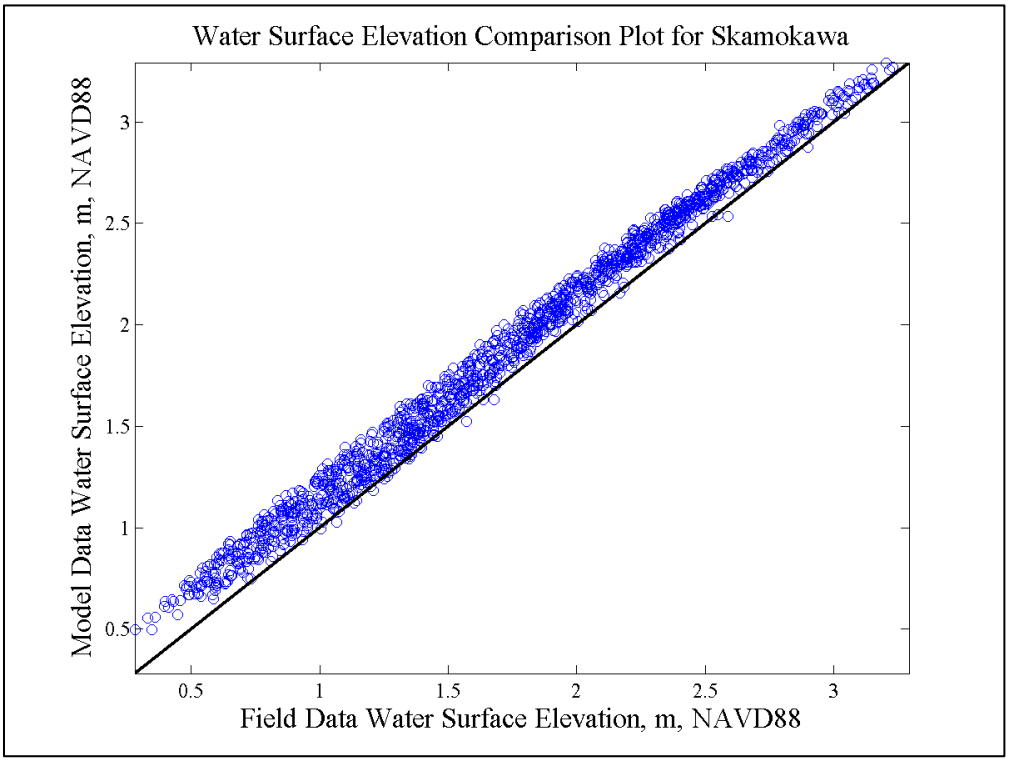

Figure 3-5. Water surface elevation comparison between model (blue) and field (green) for Longview.

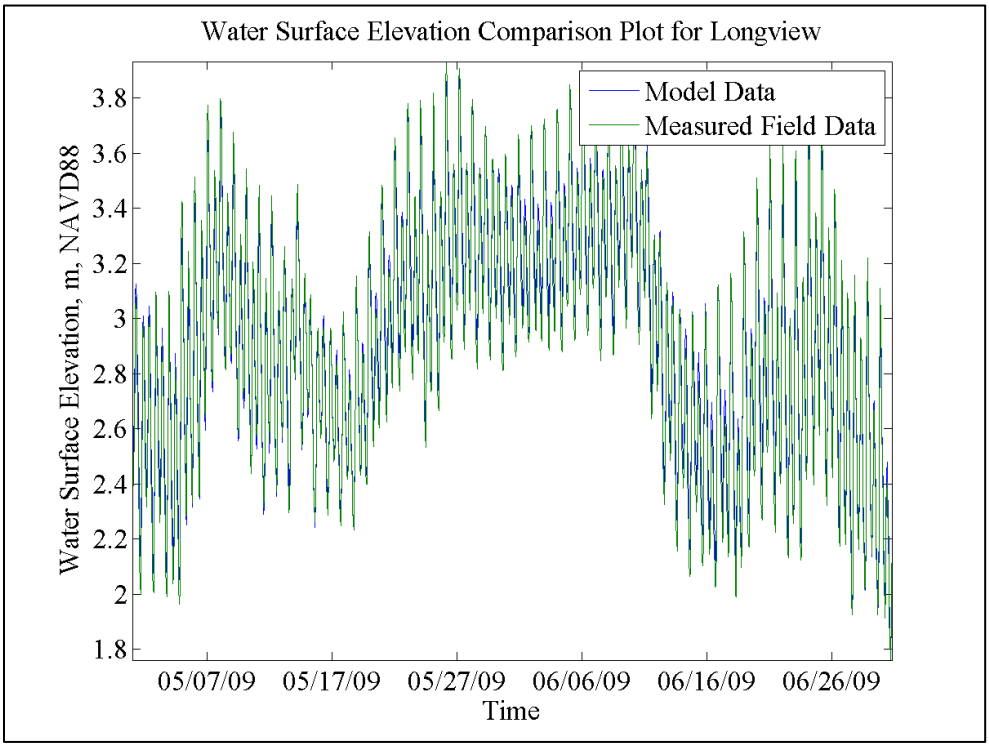

Figure 3-6. Water surface elevation box plot comparison for Longview.

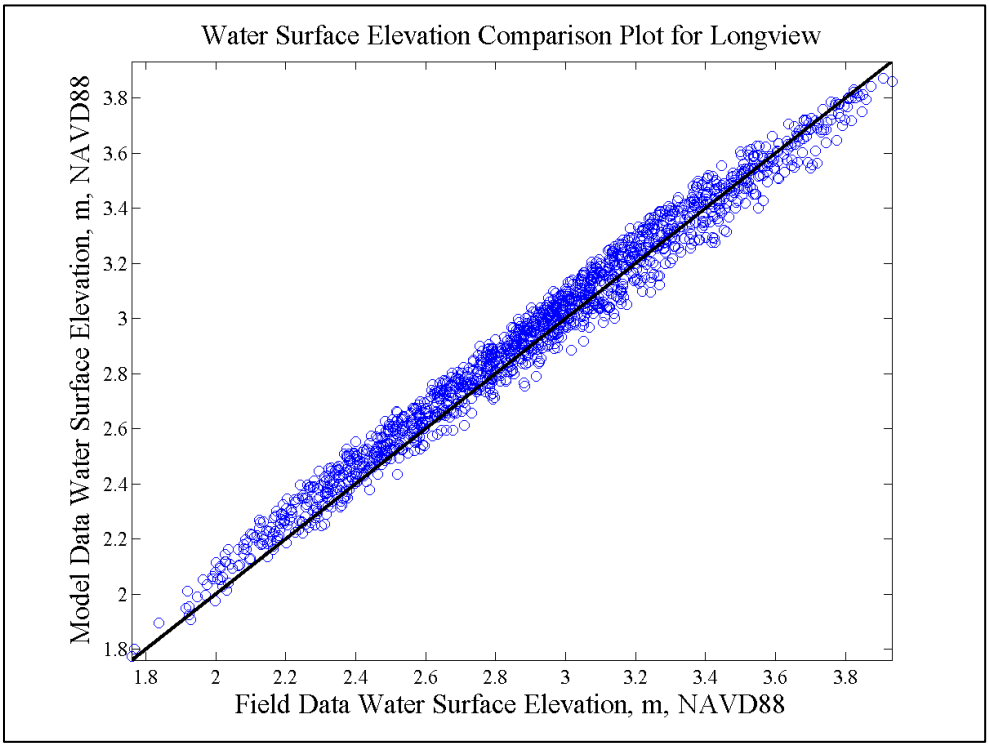

Figure 3-7. Water surface elevation comparison between model (blue) and field (green) for Saint Helens.

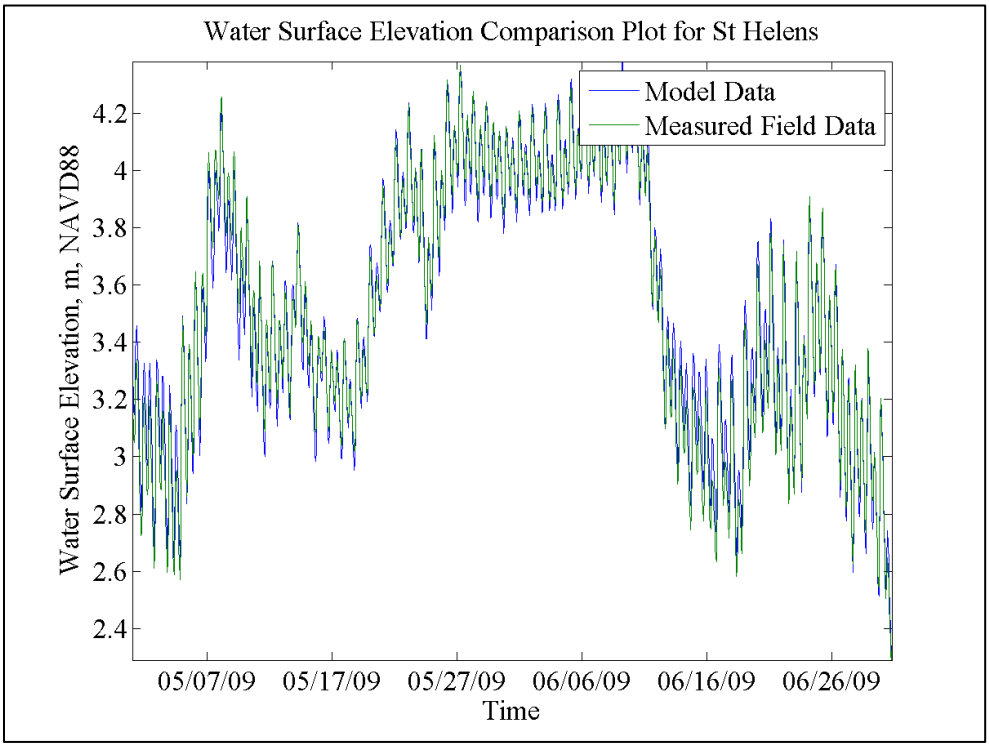

Figure 3-8. Water surface elevation box plot comparison for Saint Helens.

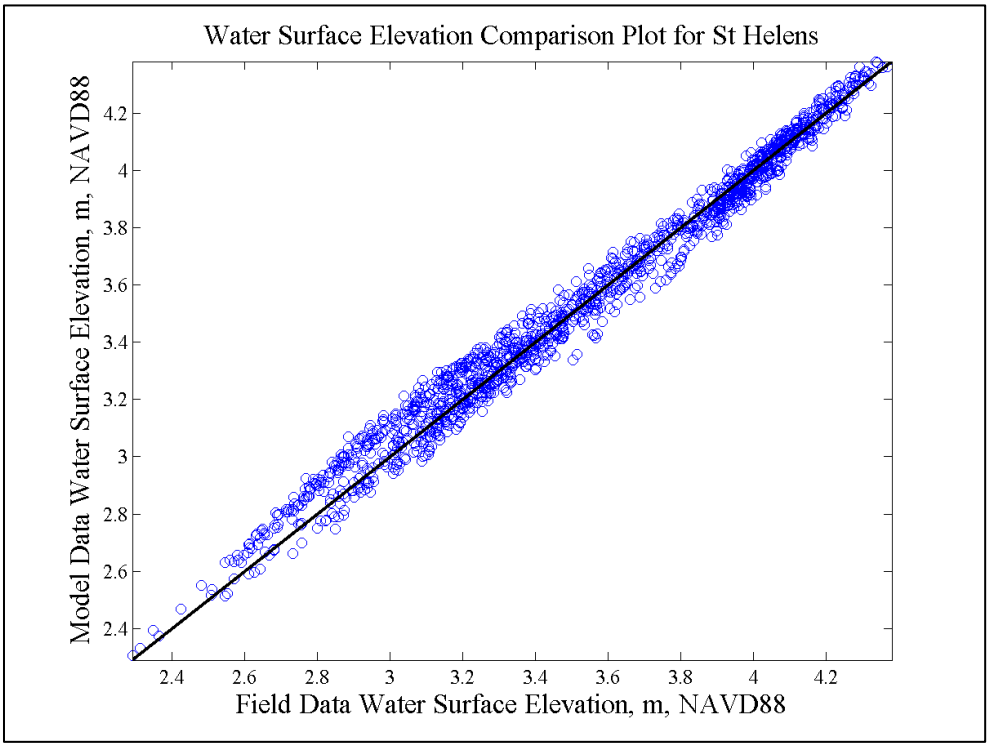

Figure 3-9. Water surface elevation comparison between model (blue) and field (green) for Bonneville.

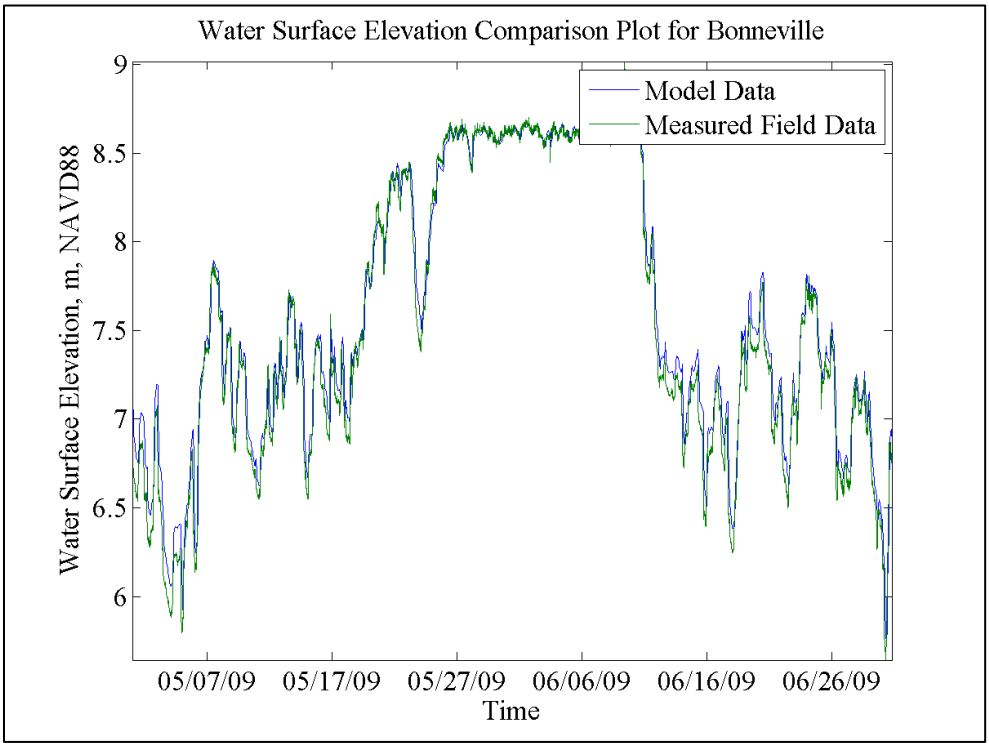

Figure 3-10. Water surface elevation box plot comparison for Bonneville.

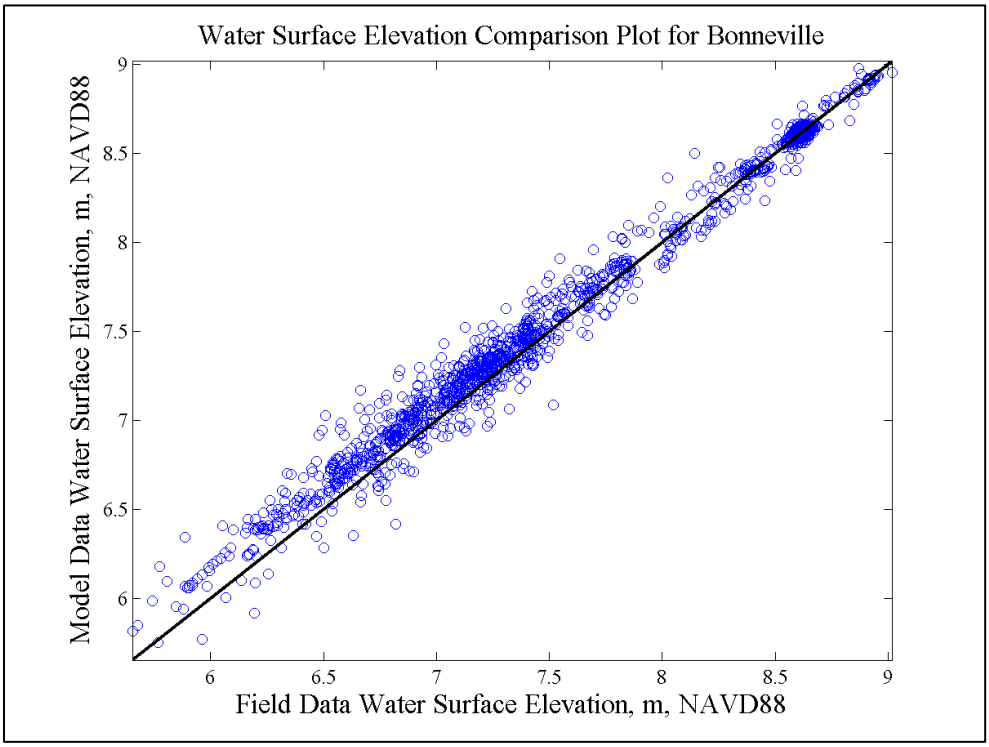

The model data at Astoria show good correlation to the observed field data (Figure 3-1). The model captures both the highs and lows and is phasing well. The box plot comparison at Astoria also shows good correlation by the tight cluster of data points along the 45-degree line.

The model tends to overpredict the water surface at Skamokawa. The likely reason for this is the location on the mesh of the tide gauge at Skamokawa. The NOAA gauge is located in a protected side channel away from the main flow path of the river. The model resolution in this region allows for proper flow patterns on a global scale but does not model the transfer of energy as accurately. This could be due to the resolution in the area being too coarse or to the complex energy losses imparted by the narrow and shallow off-channel flow path to the tide gauge.

The water surface elevations at Astoria and Skamokawa are primarily driven by the ocean tides; thus, the means vary only on a decadal scale. However, as one travels farther upstream, the system transitions from tidally driven to inflow driven. This is can be seen at Longview in Figure 3-5 and at Saint Helens in Figure 3-7 by the damping of the tidal signal and the variation of the mean water surface elevation. Little of the tidal energy is propagated as far inland as Bonneville L&D. As can be seen in Figure 3-9, the system is almost entirely inflow driven at the inland mesh boundary. Throughout this transition period and near the boundary, good correlation continues between the model results and the observed field data.

3.2 Water surface elevation statistical analysis.

Statistical analyses of water surface elevations were included as part of the validation process. The root mean square error (RMSE) was calculated using Equation 1:

$$RMSE = \sqrt{\frac{\sum_{i=1}^{N}(observed_n - model_n)^2}{N}} \quad (1)$$

where N is the number of measurements and n is the index of the given data point. Similarly, the normalized root mean square error (NRMSE) between the field and model data was calculated using Equation 2 (McLaughlin et al. 2003):

$$NRMSE = \frac{\sqrt{\frac{\sum_{i=1}^{N}(observed_n - model_n)^2}{N}}}{Standard\ Deviation} \quad (2)$$

Lower values for NRMSE indicate lower error values and a more accurate representation of the field date. Higher NRMSE values correspond to higher errors between the observed and model data.

The Nash-Sutcliffe Coefficient (Nash and Sutcliffe 1970), Willmott Coefficient (Wilmott et al. 1985), and the Correlation Coefficient (Higgins 2006) were also calculated; the equations can be found in Equations 3, 4, and 5, respectively. For these coefficients, a value of one indicates a perfect replication of the field data while a value of zero indicates little to no correspondence between the observed field data, x, and the model data, y.

$$Correlation\ Coefficient = \frac{N\sum_{n=1}^{N} x_n y_n - \left(\sum_{n=1}^{N} x_n\right)\left(\sum_{n=1}^{N} y_n\right)}{\sqrt{N\left(\sum_{n=1}^{N} x_n^2\right) - \left(\sum_{n=1}^{N} x_n\right)^2}\sqrt{N\left(\sum_{n=1}^{N} y_n^2\right) - \left(\sum_{n=1}^{N} y_n\right)^2}} \quad (3)$$

$$Nash\ Sutcliffe\ coefficient = 1 - \frac{\sum_{n=1}^{N}(observed_n - model_n)^2}{\sum_{n=1}^{N}(observed_n - \overline{observed})^2} \quad (4)$$

$$Wilmott\ coefficient = 1 - \frac{\sum_{n=1}^{N}(model_n - observed_n)^2}{\sum_{n=1}^{N}\left((|observed_n - \overline{observed}|) + (|model_n - \overline{observed}|)\right)^2} \quad (5)$$

The results from the water surface elevation statistical analysis for error, covariance, and coefficients, can be found in Table 3-1. Comparisons between the model and field data at each gauge location were also made and can be found in Table 3-2.

Table 3-1. Water surface elevation statistical analysis for calibration period.

Error Metric	Location				
	Astoria	Longview	Skamokawa	St. Helens	Bonneville
Root Mean Square Error (m)	0.09	0.07	0.15	0.06	0.12
Norm. Root Mean Sq. Error (m)	0.12	0.16	0.23	0.13	0.15
Nash-Sutcliffe Coefficient	0.99	0.98	0.95	0.98	0.98
Willmott Coefficient	1.00	0.99	0.99	1.00	0.99
Covariance	0.66	0.18	0.45	0.20	0.61
Correlation Coefficient	0.99	0.99	1.00	0.99	0.99

Table 3-2. Water surface elevation statistical analysis comparisons for calibration period.

Error Metric	Location				
	Astoria	Longview	Skamokawa	St. Helens	Bonneville
Standard Deviation (Field, m)	0.80	0.44	0.68	0.46	0.81
Standard Deviation (Model, m)	0.83	0.42	0.67	0.44	0.76
Variance (Field, m)	0.64	0.19	0.46	0.21	0.65
Variance (Model, m)	0.69	0.17	0.44	0.20	0.58
Mean (Field, m)	1.44	2.91	1.72	3.53	7.56
Mean (Model, m)	1.47	2.95	1.86	3.54	7.62
Median (Field, m)	1.45	2.93	1.70	3.50	7.38
Median (Model, m)	1.47	2.97	1.85	3.51	7.44
Max (Field, m)	3.10	3.93	3.23	4.37	9.02
Max (Model, m)	3.13	3.87	3.29	4.38	8.98
Min (Field, m)	-0.45	1.76	0.28	2.29	5.65
Min (Model, m)	-0.35	1.77	0.49	2.31	5.75

The statistical analysis results found in Table 3-1 and Table 3-2 quantify the model's ability to accurately represent field data during the calibration period. In Table 3-1, a color ranking was arbitrarily assigned based on the general goodness of fit of each variable. The color rankings in Table 3-2 were assigned based on quantifiable goodness of fit. The blue values indicate results for error and coefficient values or a variation in elevation of less than 0.05 m. For instance, at Astoria, the standard deviation of the water surface of the field data is 0.80 m while the model produced 0.83 m. The difference between these values is 0.03 m which is highlighted in blue indicating variation less than 0.05 m. The green values indicate results in the error and coefficient values or a variation in the elevation between 0.05 m and 0.10 m. The values in orange indicate values for error and coefficients or a variation in the elevation between 0.10 m and 0.15 m. The statistical analysis did not find variation to be more than 0.15 m for any value. The majority of the results shows the model data and the field data within 0.05 m of one another.

The model results at Astoria, Longview, and Saint Helens correlated well with the observed field data. Nearly all of these water surface comparisons were within 0.05 m . The gauge at Bonneville was also reproduced well in the model; this is particularly notable because the gauge was located near the upper boundary of the mesh and the near the boundary inflow.

The statistical analysis shows that the model performs the poorest at Skamokawa. As discussed previously, this could be due the resolution in the area being too coarse or to the complex energy losses imparted by the narrow and shallow off-channel flow path.

The variability of the water surface elevation along the LCR channel centerline during the AdH model calibration period (1 April – 1 July 2009) can be found in Figure 3-11. The range in observed river flowrate for the Columbia and Willamette Rivers during this period is shown in the bottom-right corner of the figure. The profiles were generated by querying the AdH water surface elevation solution file for the minimum, average, and maximum at each model nodal point within the LCR model domain. Note that each of the profiles shown may not reflect a realized instantaneous condition along the LCR. Each water surface elevation profile is a construct of minimum, average, and maximum values that may occur at different times within the April–July simulation. Additionally, the dramatic increase in water surface elevation which occurs near RM 143 can also be seen in field data.

Figure 3-11. Range of water surface elevation profiles along LCR channel centerline during calibration period.

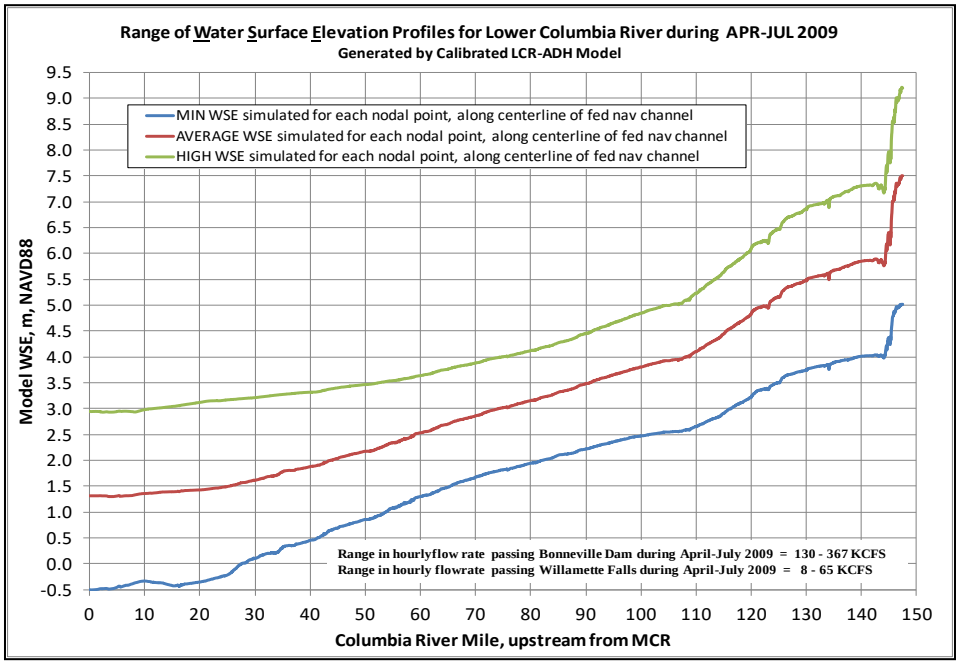

3.3 Harmonic analysis for calibration period

The tide is the change in water surface elevation due, primarily, to gravitational effects of the sun and the moon as the earth rotates on its axis. When the gravitational effects are combined, a period of larger amplitudes, known as spring tide, can be seen. When the effects of the moon and sun negate one another, the resulting period of reduced amplitudes is known as neap tide. Estuarine geometry and fresh-water inflows can also alter the tidal signal.

The tide is often referred to as a tidal signal since the water surface elevation can be viewed as a long-wave signal. Additionally, the tidal signal can be considered to be composed of harmonic constituents. Each constituent represents a different effect and has a unique amplitude and phase for a given location. The tidal signal may be decomposed into a series of major tidal constituents by applying Equation 6:

$$h(t) = H_o + \sum_{i=1\ to\ n} f_i\, H_i \cos(a_i t - \kappa_i) \tag{6}$$

where $h(t)$ is the water surface elevation, H_o is the mean water level above the datum, f is the nodal factor for tidal constituent i, a is the constituent frequency, t is the time from the initial epoch, and κ is the epoch (phase lag) of the tidal constituent.[4] By conducting a harmonic frequency analysis on both the model and observed field data, a more detailed examination of the tidal signal can be achieved. The harmonic analysis conducted in this work applied the MATLAB program T-Tide which uses Fast Fourier Transform to decompose the tidal signal. The 35 components with the largest amplitudes are output. The tabular results can be found in Table 3-3 where the four harmonic constituents with the largest amplitudes are in bold. Bar chart comparisons between the model (black) and the observed field data (white) for amplitude and phase can be found in Figure 3-12 through Figure 3-21.

[4] For more information on tides and harmonic analyses, refer to NOAA Special Publication NOS CO-OPS 3 NOAA (2007).

Table 3-3. Harmonic constituent amplitude comparisons (meters).

Harmonic Constituent	Location									
	Astoria		Longview		Skamokawa		St. Helens		Bonneville	
	Field	Model	Field	Model	Field	Model	Field	Model	Field	Model
MM	0.05	0.05	0.12	0.10	0.06	0.06	0.16	0.12	0.08	0.07
MSF	0.06	0.08	0.23	0.22	0.12	0.13	0.29	0.26	0.34	0.32
ALP1	0.01	0.01	0.01	0.01	0.01	0.01	0.01	0.01	0.01	0.01
2Q1	0.01	0.01	0.02	0.01	0.01	0.01	0.01	0.00	0.03	0.03
Q1	0.05	0.04	0.03	0.02	0.04	0.03	0.02	0.02	0.01	0.01
O1	0.26	0.22	0.07	0.06	0.18	0.14	0.04	0.04	0.01	0.01
NO1	0.02	0.02	0.02	0.02	0.02	0.03	0.02	0.01	0.02	0.02
K1	0.50	0.45	0.19	0.17	0.40	0.35	0.11	0.12	0.06	0.05
J1	0.01	0.01	0.01	0.00	0.01	0.00	0.01	0.01	0.02	0.02
OO1	0.02	0.02	0.02	0.01	0.03	0.02	0.01	0.01	0.01	0.01
UPS1	0.00	0.00	0.00	0.00	0.00	0.00	0.00	0.00	0.02	0.01
EPS2	0.01	0.01	0.01	0.01	0.01	0.01	0.01	0.01	0.01	0.01
MU2	0.02	0.03	0.02	0.02	0.03	0.04	0.01	0.01	0.01	0.01
N2	0.19	0.20	0.08	0.07	0.16	0.16	0.04	0.04	0.01	0.01
M2	0.93	1.00	0.35	0.32	0.79	0.79	0.16	0.18	0.01	0.02
L2	0.06	0.08	0.02	0.02	0.06	0.07	0.00	0.01	0.01	0.01
S2	0.15	0.15	0.04	0.03	0.11	0.10	0.01	0.02	0.01	0.01
ETA2	0.01	0.01	0.01	0.00	0.01	0.01	0.01	0.01	0.00	0.01
MO3	0.04	0.07	0.04	0.04	0.06	0.08	0.02	0.02	0.00	0.00
M3	0.01	0.01	0.02	0.01	0.01	0.01	0.01	0.01	0.00	0.00
MK3	0.05	0.07	0.07	0.06	0.09	0.10	0.03	0.03	0.00	0.00
SK3	0.01	0.02	0.01	0.01	0.02	0.02	0.00	0.00	0.01	0.01
MN4	0.01	0.02	0.03	0.02	0.03	0.03	0.01	0.01	0.01	0.00
M4	0.02	0.03	0.06	0.06	0.07	0.09	0.03	0.03	0.00	0.00
SN4	0.00	0.00	0.01	0.01	0.01	0.01	0.00	0.00	0.00	0.00
MS4	0.01	0.02	0.01	0.01	0.02	0.03	0.01	0.01	0.00	0.00
S4	0.00	0.00	0.00	0.00	0.00	0.00	0.00	0.00	0.01	0.01
2MK5	0.01	0.02	0.02	0.02	0.01	0.02	0.01	0.01	0.00	0.00

Harmonic Constituent	Location									
	Astoria		Longview		Skamokawa		St. Helens		Bonneville	
	Field	Model	Field	Model	Field	Model	Field	Model	Field	Model
SDK5	0.00	0.00	0.00	0.00	0.00	0.00	0.00	0.00	0.00	0.00
SMN6	0.01	0.01	0.00	0.00	0.00	0.01	0.00	0.00	0.00	0.00
M6	0.01	0.02	0.01	0.01	0.01	0.01	0.00	0.00	0.00	0.00
2MS6	0.00	0.01	0.00	0.00	0.00	0.00	0.00	0.00	0.00	0.00
2SM6	0.00	0.00	0.00	0.00	0.00	0.00	0.00	0.00	0.00	0.00
3MK7	0.00	0.01	0.01	0.00	0.00	0.01	0.00	0.00	0.00	0.00
M8	0.00	0.00	0.00	0.00	0.00	0.00	0.00	0.00	0.00	0.00

Figure 3-12. Harmonic constituent amplitude comparisons between model (black) and field (white) for Astoria.

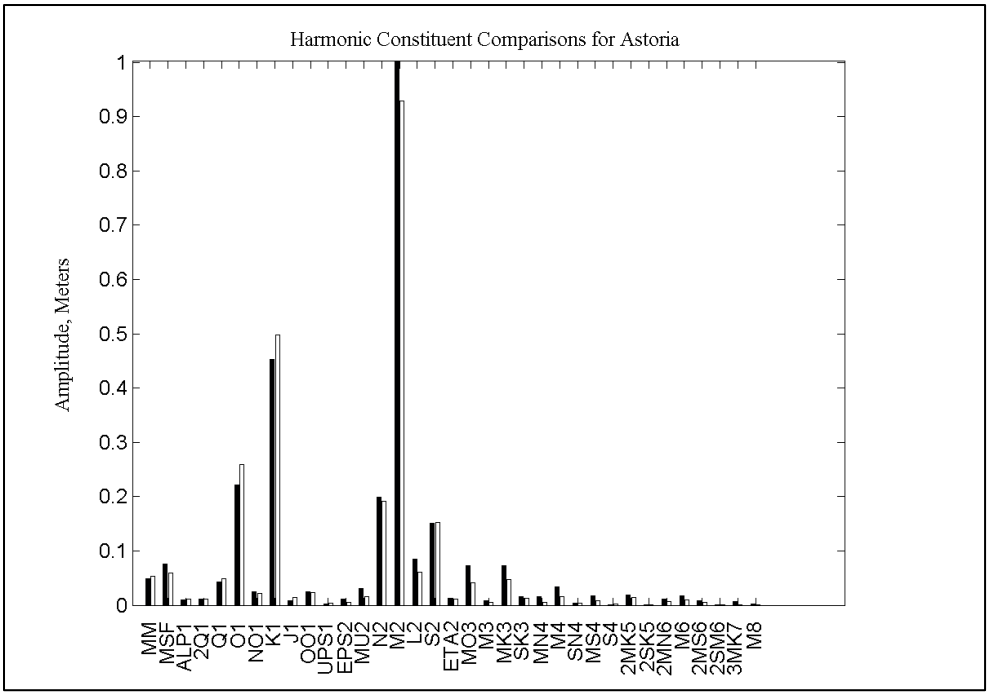

Figure 3-13. Harmonic constituent phase comparisons between model (black) and field (white) for Astoria.

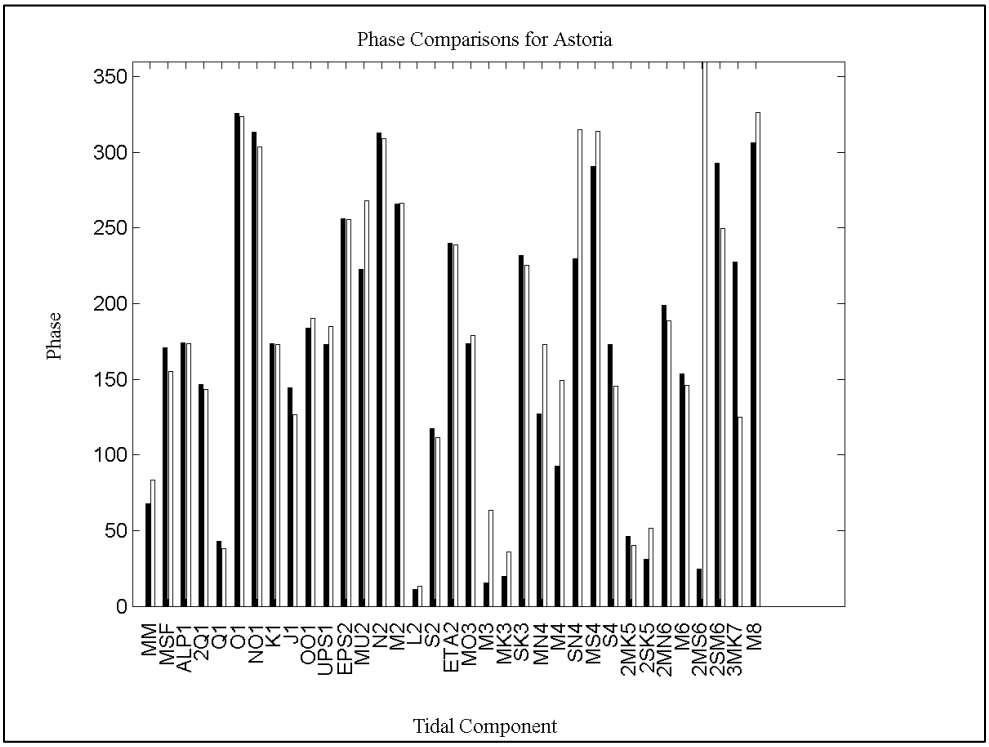

Figure 3-14. Harmonic constituent amplitude comparisons for Skamokawa.

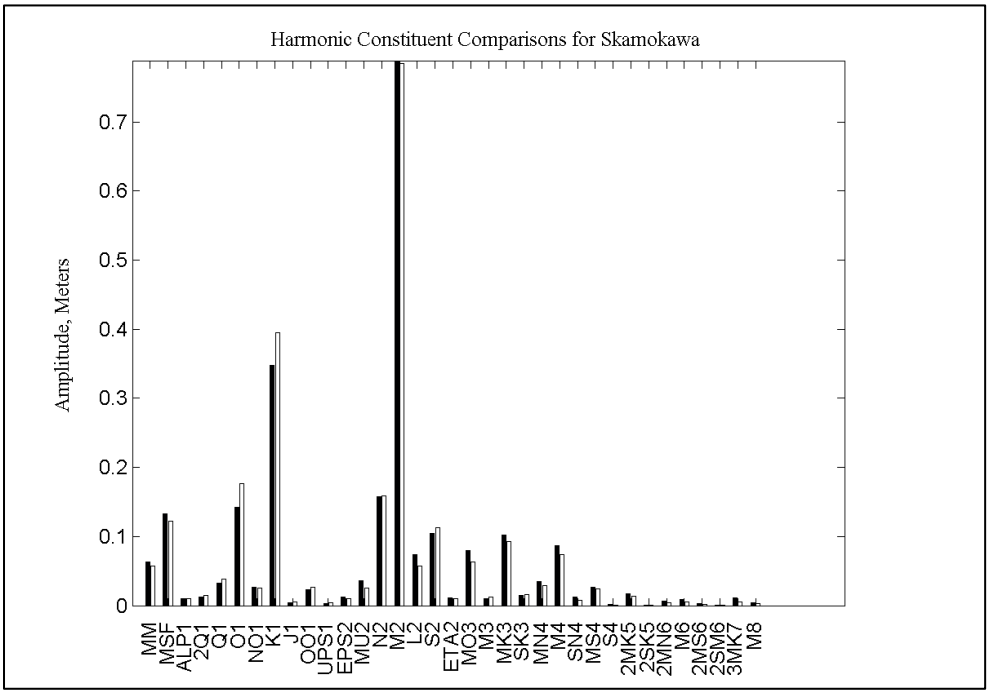

Figure 3-15. Harmonic constituent phase comparisons for Skamokawa.

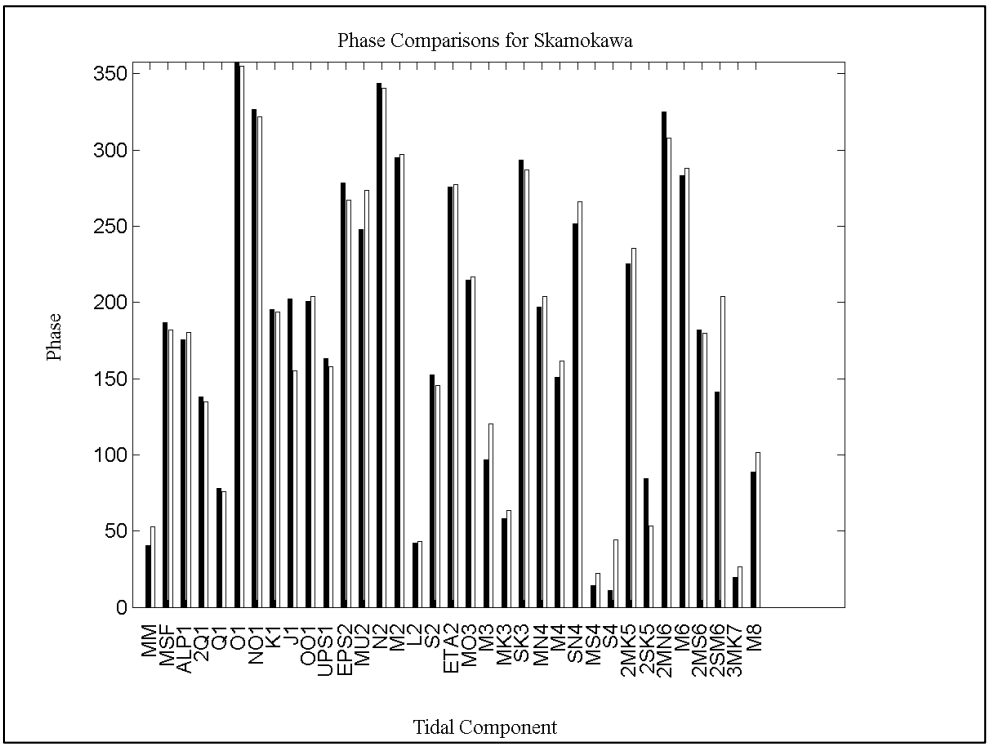

Figure 3-16. Harmonic constituent amplitude comparisons for Longview.

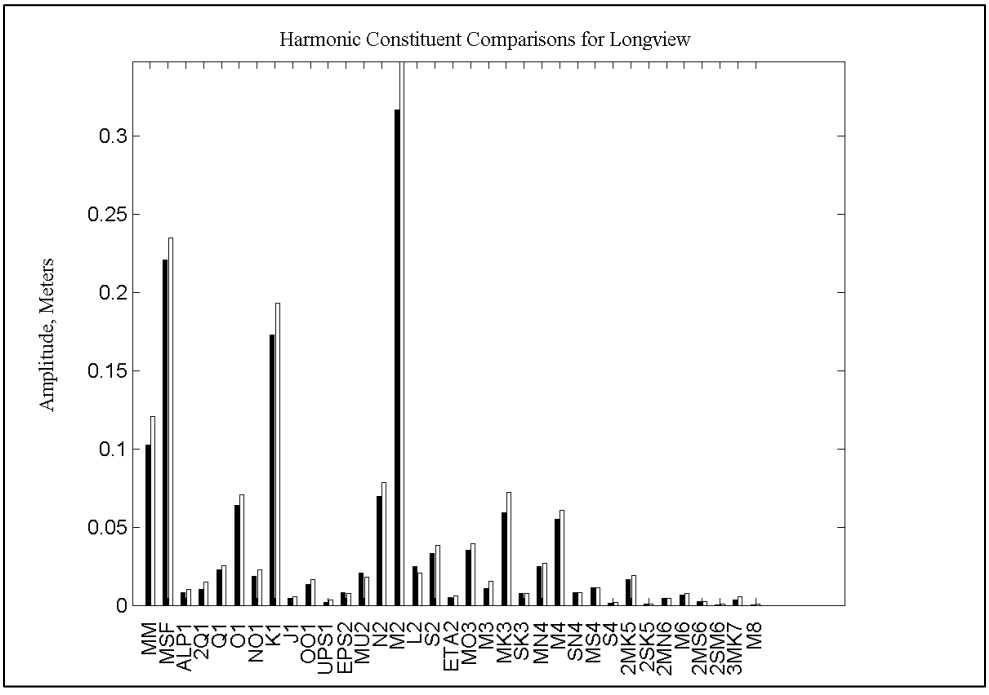

Figure 3-17. Harmonic constituent phase comparisons for Longview.

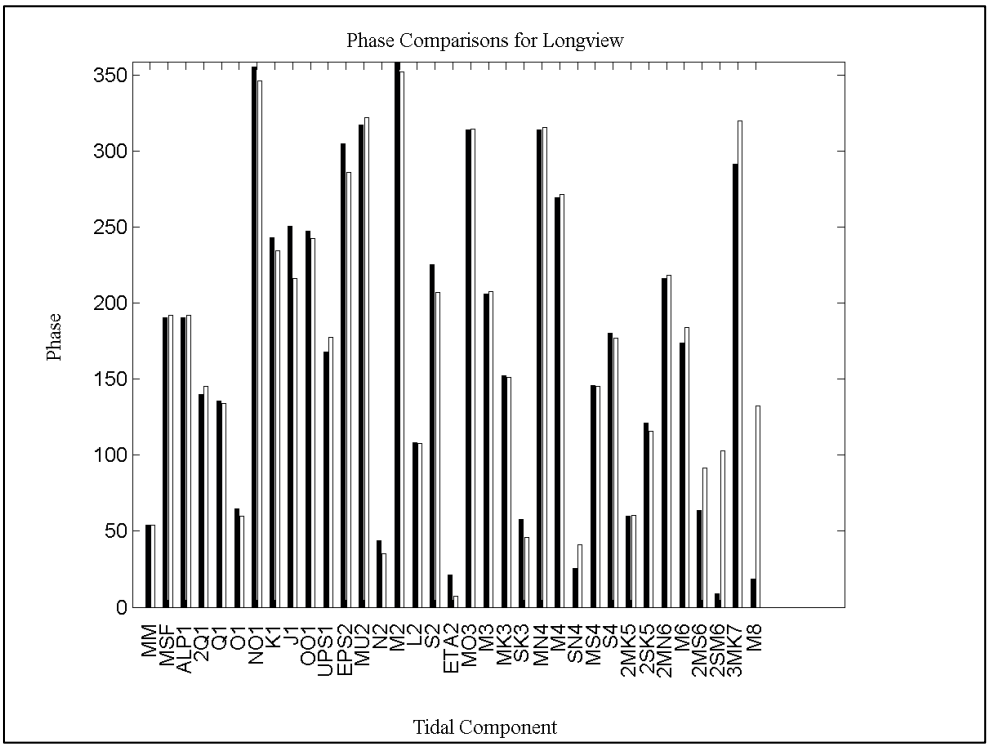

Figure 3-18. Harmonic constituent amplitude comparisons for Saint Helens.

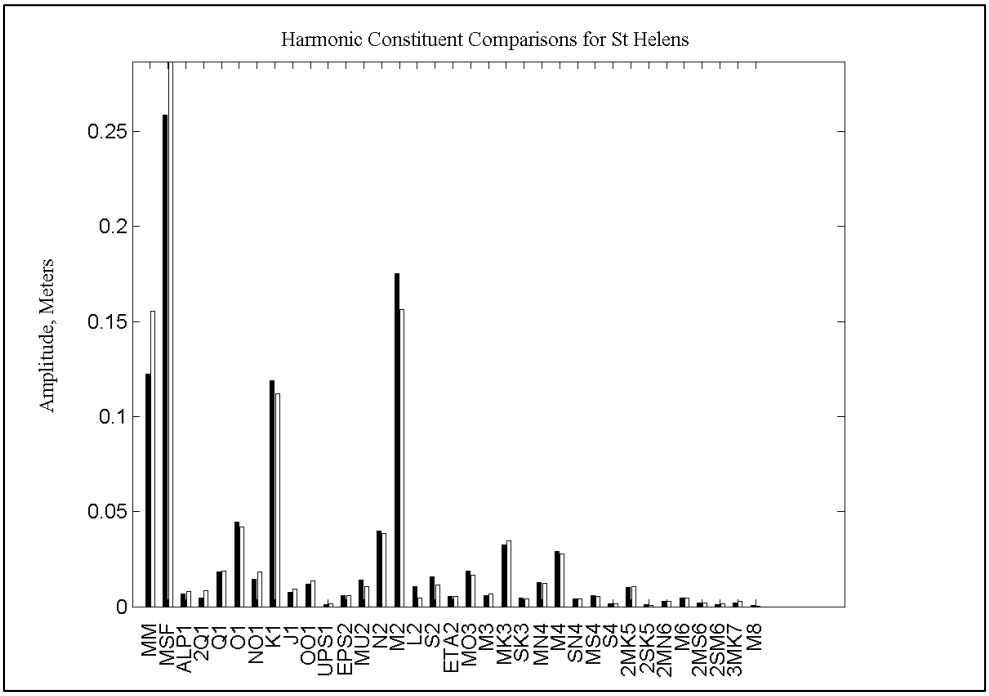

Figure 3-19. Harmonic constituent phase comparisons for Saint Helens.

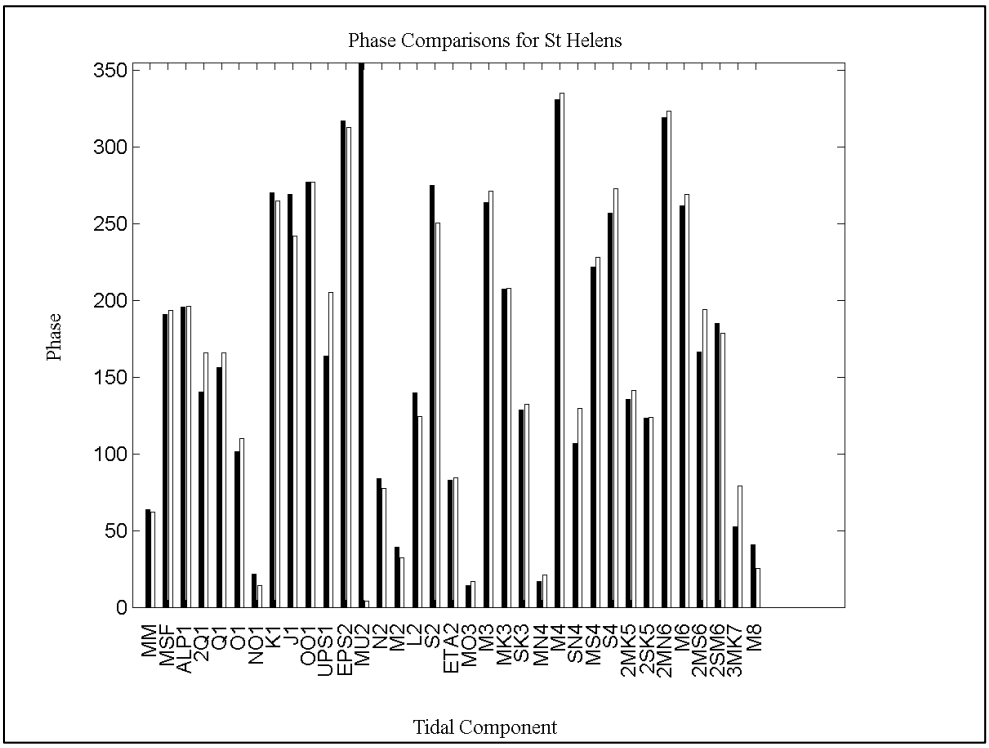

Figure 3-20. Harmonic constituent amplitude comparisons for Bonneville.

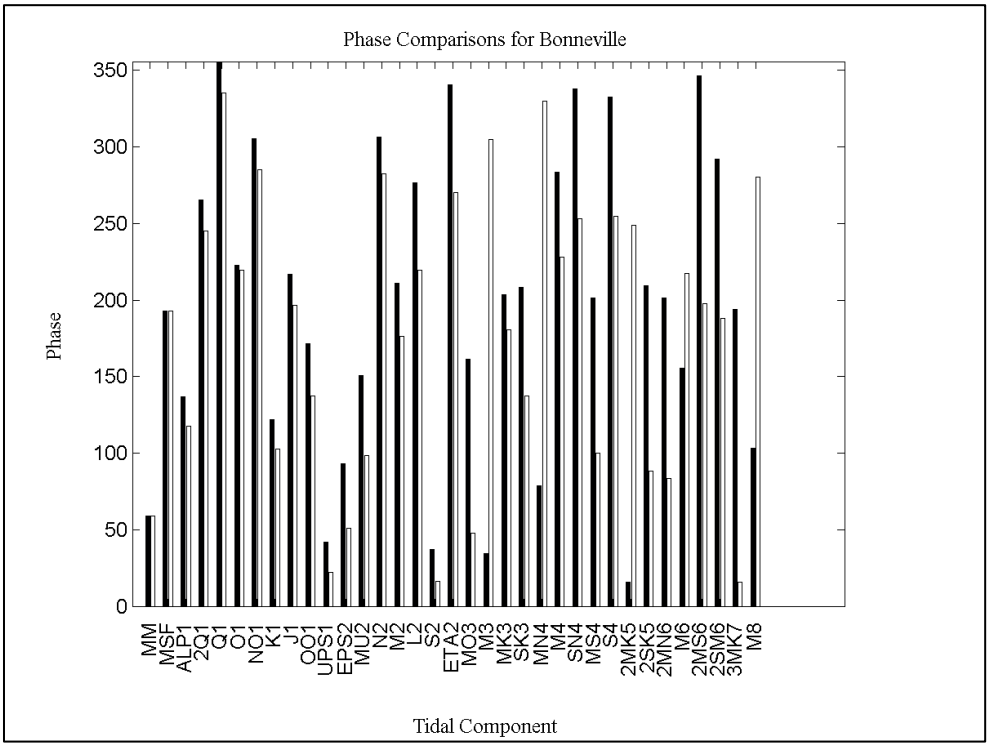

Figure 3-21. Harmonic constituent phase comparisons for Bonneville.

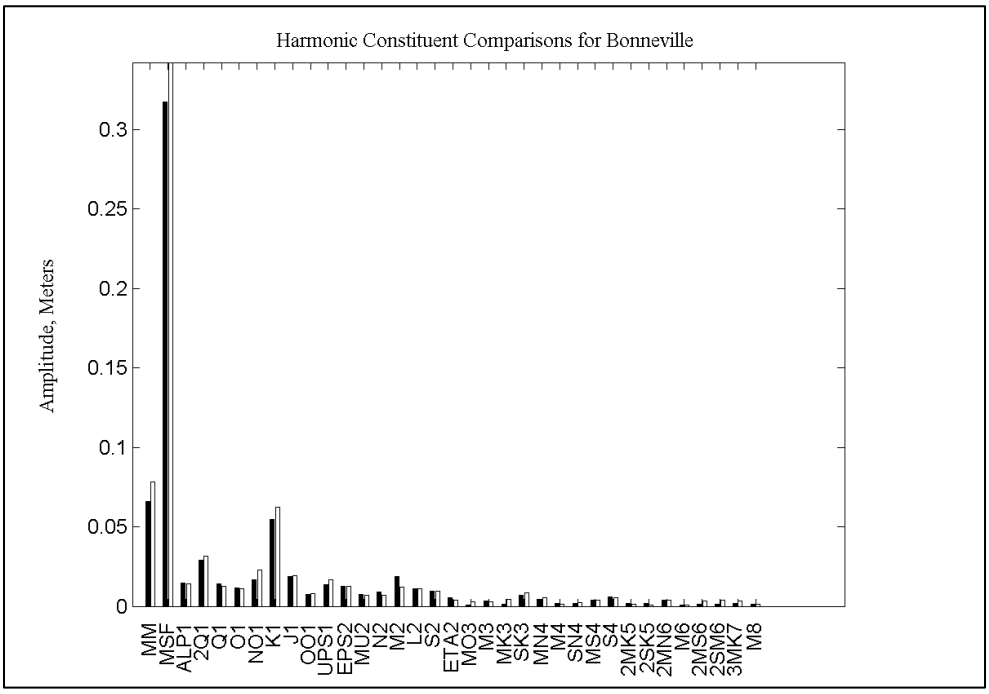

The comparison between the harmonic constituent amplitude for the model and the field data shows good correlation. The variations observed were within the anticipated range. The largest difference between amplitudes was found in the M2 (12.42 hours) comparison at the Astoria gauge of 0.07 m.

As expected, the magnitude of the amplitudes generally decreases farther upstream due to reduced tidal influence. Additionally, higher frequencies were not expected to be captured by the model since these can be largely affected by winds. This accounts for much of the larger differences in the comparison.

Finally, the power spectrum of the observed field data and the model were compared. The results at Astoria (Figure 3-22) and Longview (Figure 3-23) are representative of the entire model. In these figures, the peaks in power represent the frequency of a major tidal component. It can be seen that the lower frequencies that contain the majority of the tidal energy have an excellent correlation. As the frequencies are increased, non-tidal components begin to be seen, resulting in slight differences in power between the model and the field.

Figure 3-22. Power spectrum comparison between the model (blue) and the field (red) at Astoria.

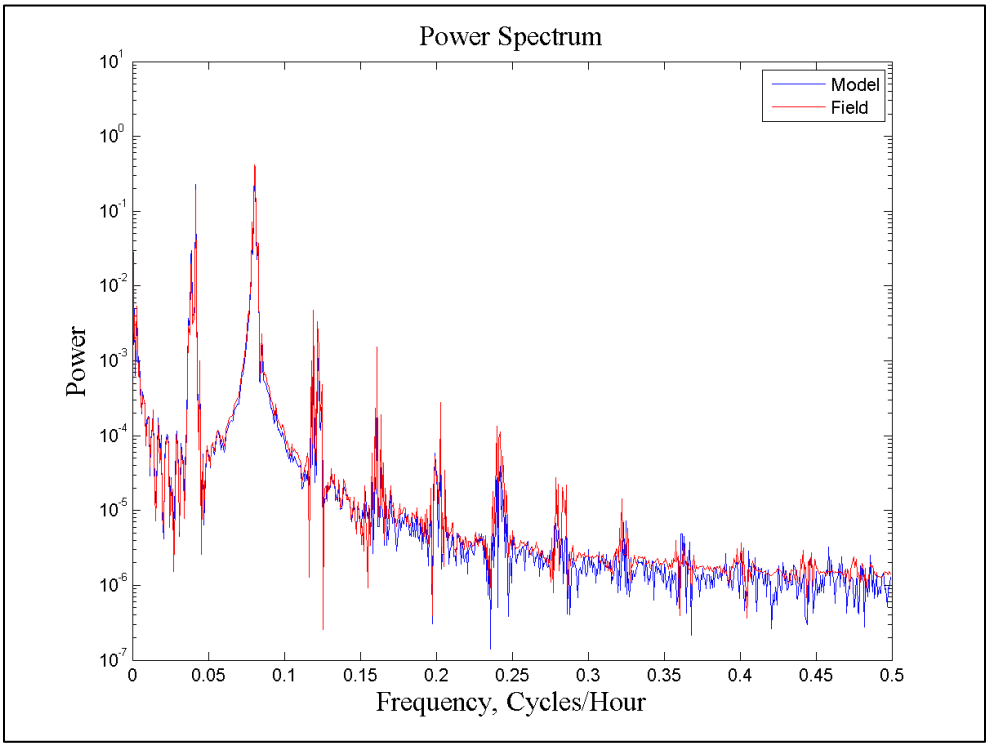

Figure 3-23. Power spectrum comparison between the model (blue) and the field (red) at Longview.

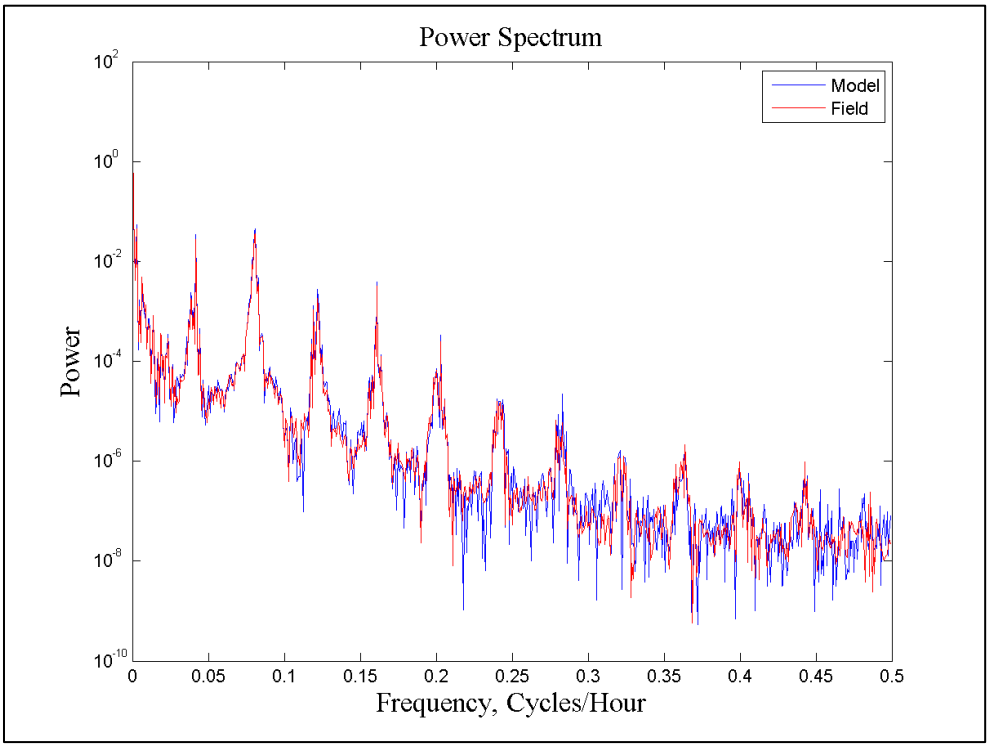

The water surface elevation analysis and the harmonic analysis show good correlation between the model and the measured field data. Overall, variations between the model and field data indicate that the model is accurately representing measured field data.

3.4 Computational environment

The application of AdH for this work was executed on the ERDC High Performance Computing CRAY XT4 (Jade) parallel processing supercomputer using 400 processors. The model was run continuously for the entirety of the calibration-validation period, a total of 5,544 model hours. The simulation required approximately 122 clock hours with a model output of 1 hour and a variable time-step between 30 to 100 seconds. Model spinup had a time-step of 50 seconds. During the spring freshet, the time-step was 30 seconds while the drier periods were modeled at 100 seconds. AdH is capable of much larger computational time-steps; however, the level of detail required to adequately capture the bathymetric features of interest to NWP required a restriction of time-step primarily to adequately capture the wetting-drying of the intertidal areas. AdH is capable of time-step adaption to ensure accuracy of the computed results (Savant et al. 2011). In this study, AdH adapted the time-step by reducing it as needed for convergence.

4 Model Validation

The purpose of model validation is to ensure that the model adequately reproduces observed field data using the friction parameters determined during calibration. The analysis of the model results for the validation period was exclusive of the calibration period of the model. This chapter discusses the model validation and accompanying water surface analysis for the LCR AdH model.

The model validation period was chosen to be a typically drier time of the year (1 September 1 2009 through 31 October 31 2009). Although there are several months in between the calibration period and the validation period, the model was run continuously from April 2009 through the end of October 2009 with a 2-week spin-up period.

4.1 Water surface elevation comparisons for the validation period.

A statistical analysis of the water surface elevations for the validation period was conducted to quantify the model's ability to accurately represent field data.

The results for the validation period can be found in Table 4-1 and Table 4-2. In Table 4-1, a color ranking was arbitrarily assigned based on the general goodness of fit of each variable. The color rankings in Table 4-2 were assigned based on quantifiable "goodness of fit." The blue values indicate results for error and coefficient values or a variation in elevation of less than 0.05 m. The green values indicate results in the error and coefficient values or a variation in the elevation between 0.05 m and 0.10 m. The values in orange indicate values for error and coefficients or a variation in the elevation between 0.10 m and 0.15 m. Values greater than 0.15 m are shown in white.

The model results at Astoria, Longview, and Saint Helens correlated well with the observed field data. Nearly all of the model results were within 0.05 m of the field results. During the validation period, the model performed better at Skamokawa than during the calibration period. This is likely due to the lower flows found during the validation period. The statistical analysis shows that the model performs the poorest at Bonneville with the difference between the means for the entire validation period varying by 0.15 m.

Table 4-1. Water surface elevation statistical analysis for validation period.

Error Metric	Location				
	Astoria	Longview	Skamokawa	St. Helens	Bonneville
Root Mean Square Error	0.07	0.07	0.11	0.07	0.19
Normalized Root Mean Sq. Error	0.09	0.16	0.15	0.22	0.52
Nash-Sutcliffe Coefficient	0.99	0.98	0.98	0.95	0.73
Willmott Coefficient	1.00	0.99	0.99	0.99	0.93
Covariance	0.66	0.19	0.51	0.11	0.11
Correlation Coefficient	1.00	0.99	1.00	0.99	0.95

Table 4-2. Water surface elevation statistical analysis comparison for validation period.

Error Metric	Location				
	Astoria	Longview	Skamokawa	St. Helens	Bonneville
Standard Deviation (Field, m)	0.81	0.45	0.72	0.34	0.36
Standard Deviation (Model, m)	0.83	0.42	0.71	0.33	0.33
Variance (Field, m)	0.65	0.21	0.52	0.12	0.13
Variance (Model, m)	0.68	0.18	0.50	0.11	0.11
Mean (Field, m)	1.37	1.97	1.45	2.13	3.62
Mean (Model, m)	1.34	1.98	1.54	2.19	3.77
Median (Field, m)	1.39	1.93	1.46	2.12	3.57
Median (Model, m)	1.36	1.95	1.54	2.18	3.71
Max (Field, m)	3.12	3.17	3.13	3.09	4.81
Max (Model, m)	3.09	3.03	3.08	3.07	4.82
Min (Field, m)	-0.38	1.03	0.10	1.28	2.89
Min (Model, m)	-0.38	1.08	0.21	1.39	3.10

The majority of the results shows the model data and the field data within 0.05 m of one another. As compared to the results from the calibration period, the validation period also shows good correlation between the model and the observed field data. The model at Astoria produced the most accurate results while the Bonneville results were the least effective at reproducing the field data.

As discussed in Section 3, differences in the results at Bonneville are expected due to the proximity of the NOAA gauge to the model inflow boundary. During the lower river flows of the validation period, reflection or interaction of the tidal wave with the model boundary may be effecting the

water surface elevation; whereas, during the higher flows of the calibration period, the riverine flow dominated the upstream system energy.

Time series and box plots of the water surface elevation comparisons are included in Figure 4-1 through Figure 4-10. In the time series plots, the model data are represented in blue and the observed field data are in green.

Much of the differences between the calibration results and the validation results can be explained by the flow regimes. During the high-flow period, the model must calculate overbank flow across areas not wetted during low flows and the division of the flow between the channel and overbank. The overbank friction is a more challenging parameter to determine than the channel roughness (for example). For this reason, the model typically is more accurate at recreating field data (see results at Astoria, Skamokawa, and Saint Helens).

Figure 4-1. Water surface elevation comparison between model (blue) and field (green) for Astoria.

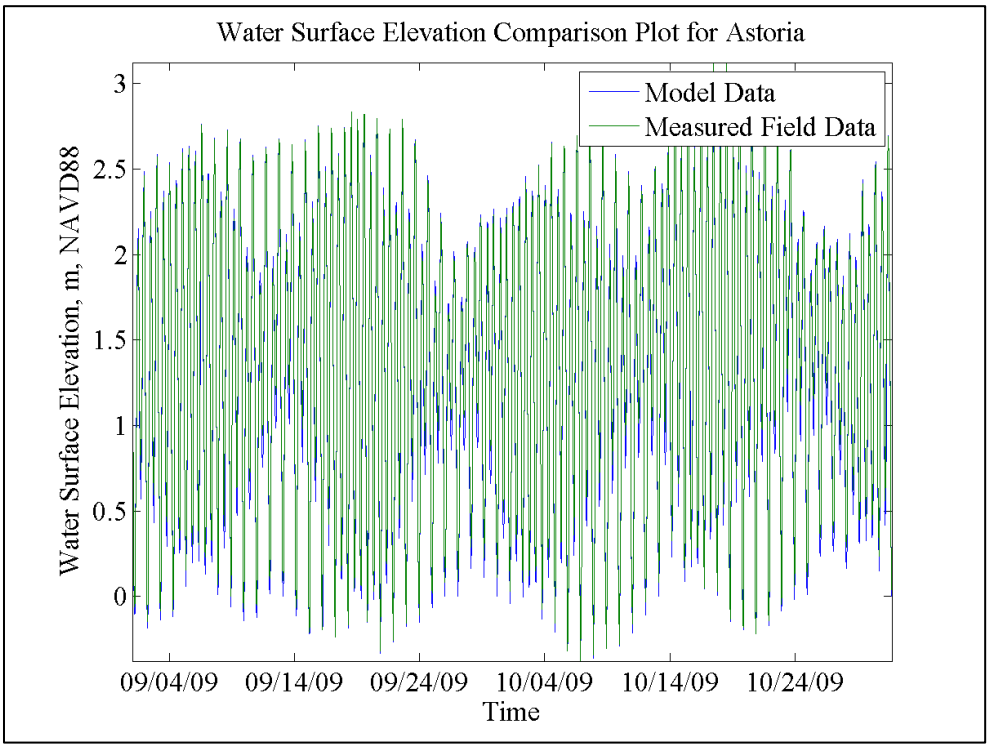

Figure 4-2. Water surface elevation box plot comparison for Astoria.

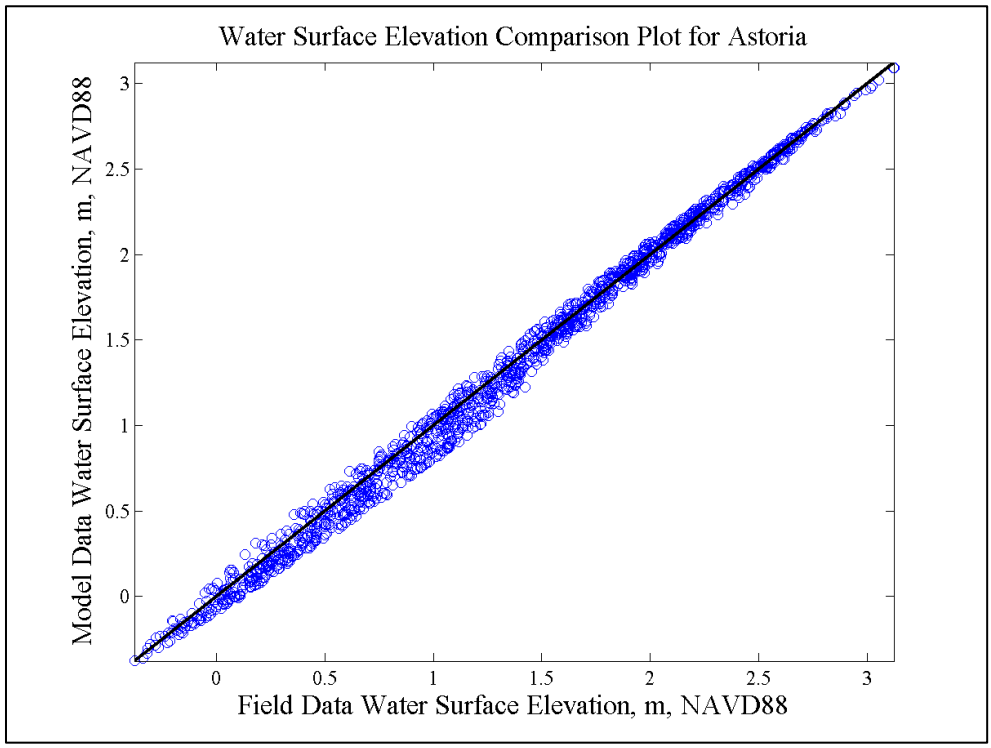

Figure 4-3. Water surface elevation comparison between model (blue) and field (green) for Skamokawa.

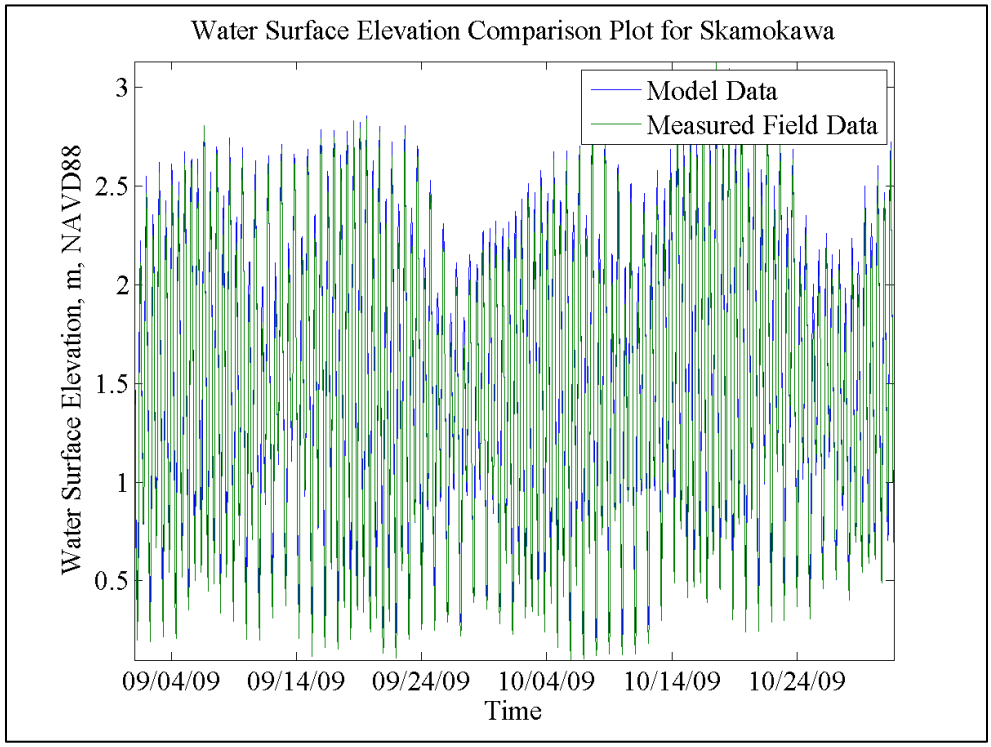

Figure 4-4. Water surface elevation box plot comparison for Skamokawa.

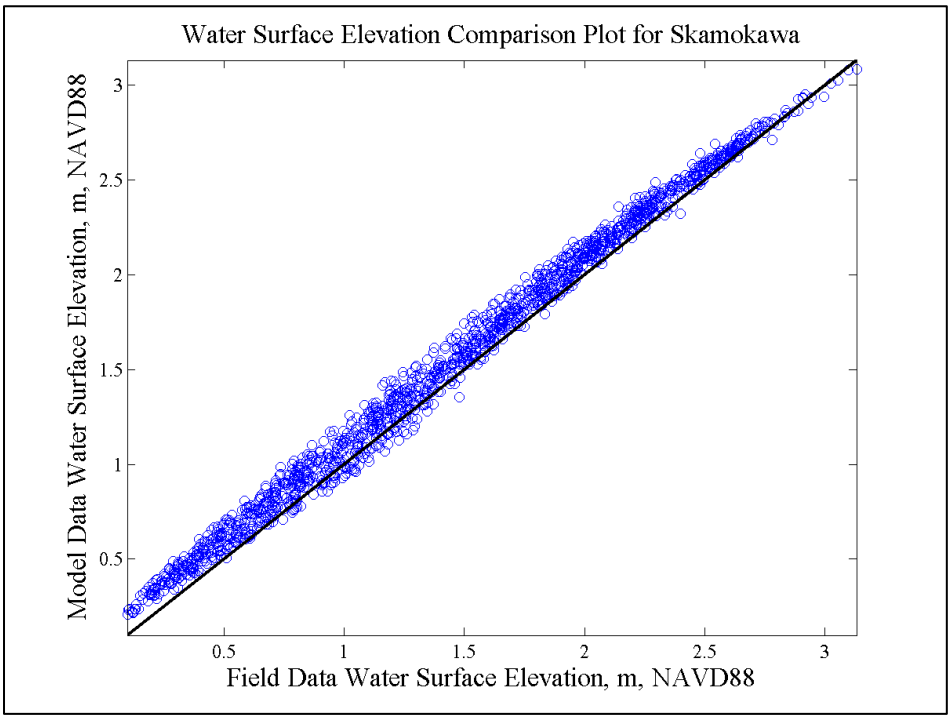

Figure 4-5. Water surface elevation comparison between model (blue) and field (green) for Longview.

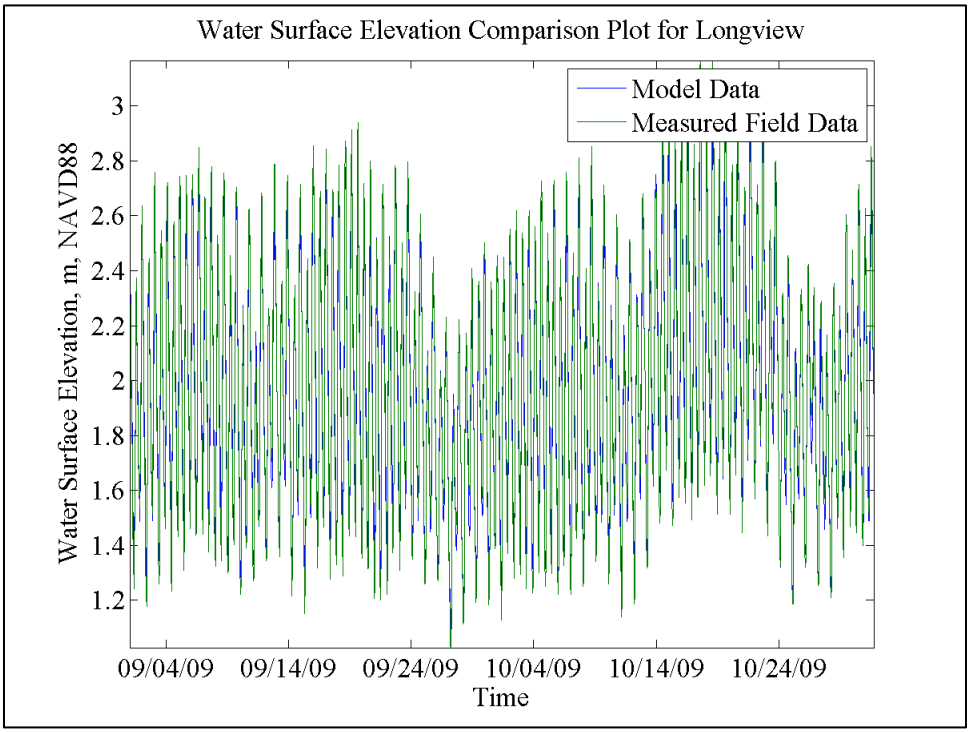

Figure 4-6. Water surface elevation box plot comparison for Longview.

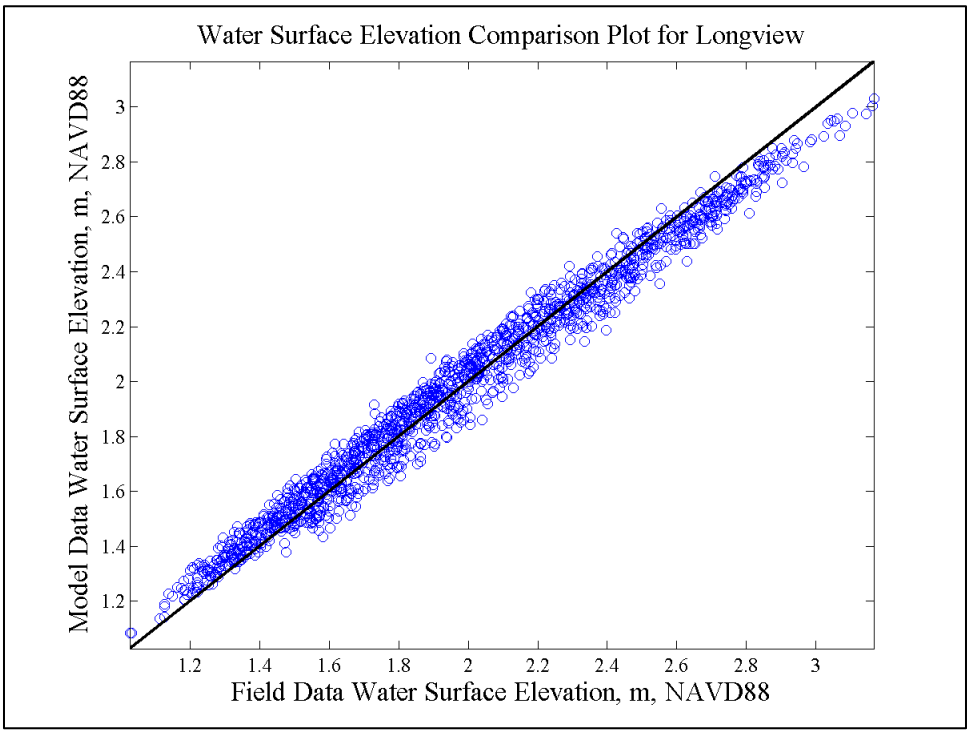

Figure 4-7. Water surface elevation comparison between model (blue) and field (green) for Saint Helens.

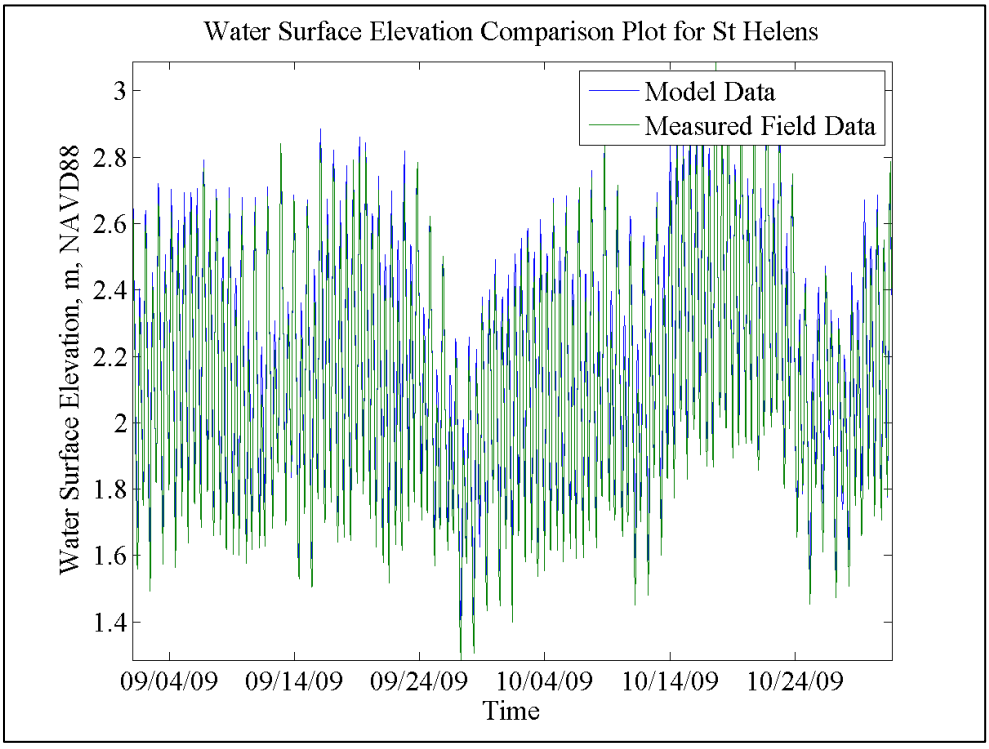

Figure 4-8. Water surface elevation box plot comparison for Saint Helens.

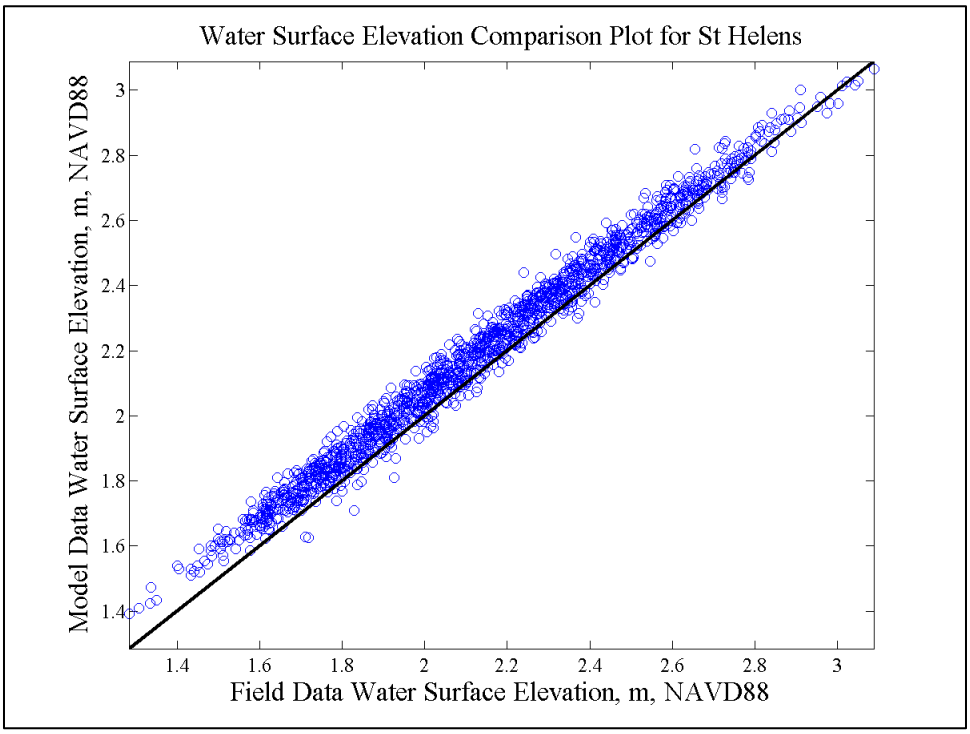

Figure 4-9. Water surface elevation comparison between model (blue) and field (green) for Bonneville.

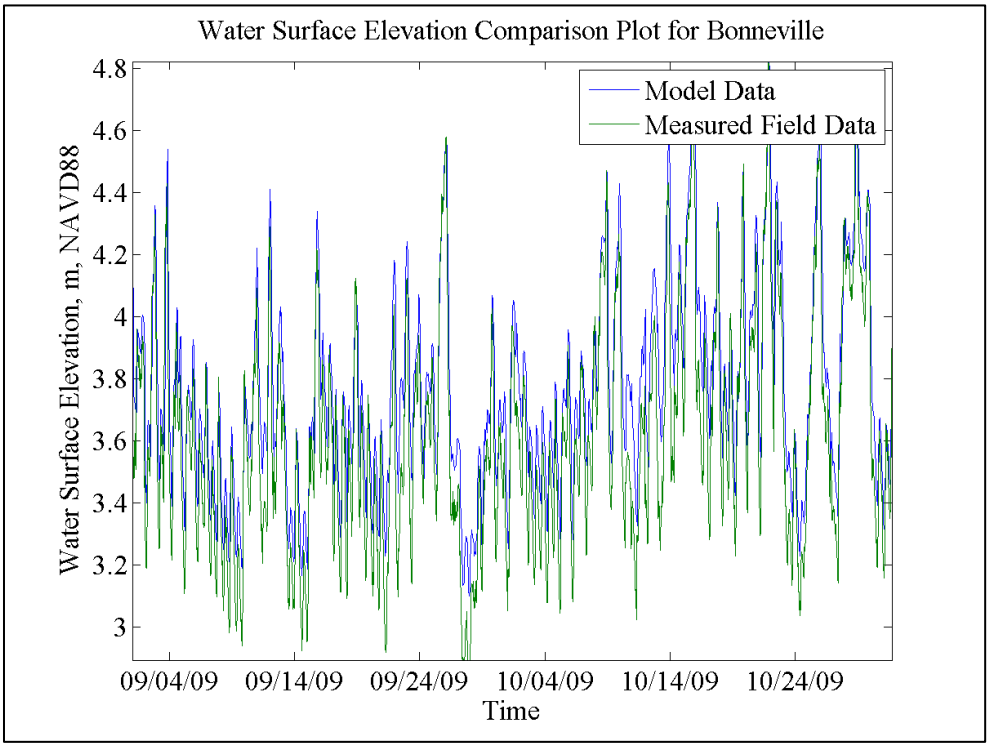

Figure 4-10. Water surface elevation box plot comparison for Bonneville.

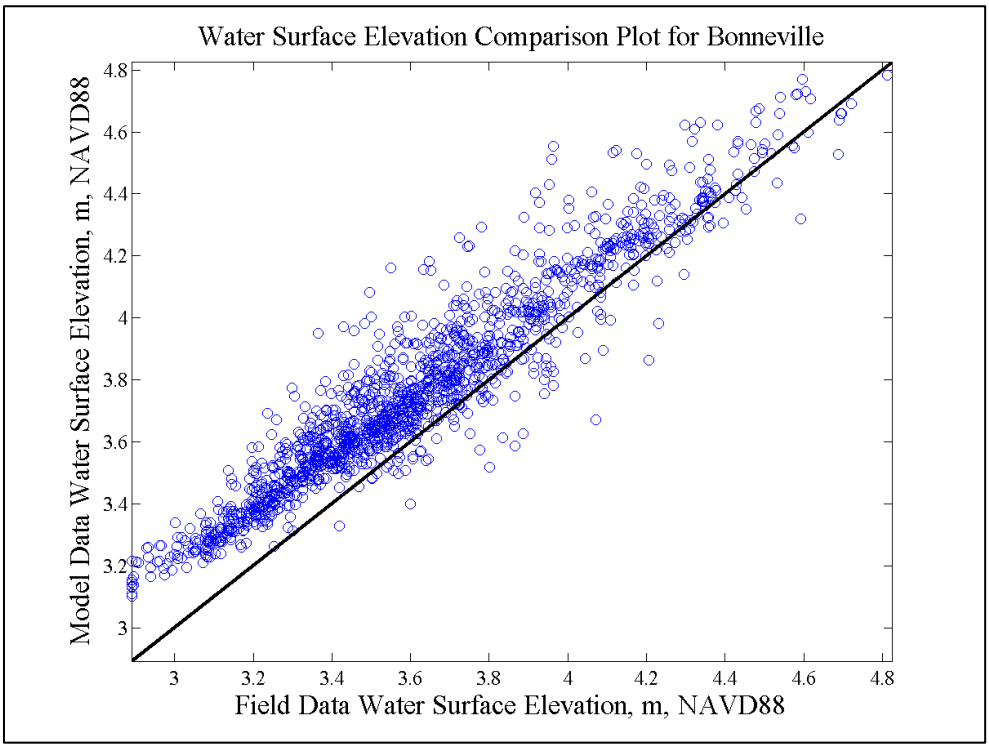

The water surface elevation comparisons show good correlation between the model and field data. The worst gauge for the validation period was the Bonneville gauge, which consistently overpredicts the water surface elevation. This is most likely a result of the calibration period being during the spring freshet as well as possible inflow effects (reflection of the boundary not damped by high inflow). The Astoria gauge appears to produce the most accurate model results.

4.2 Harmonic analysis for validation period

As discussed in Section 3.3 the harmonic analysis was conducted using the MATLAB code T-Tide. The graphical comparison between the harmonic constituent amplitude and phase can be found in Figure 4-11 through Figure 4-20. The tabulated results can be found in Table 4-3, with the four largest constituents shown in bold.

Table 4-3. Harmonic constituent amplitude comparisons for validation (meters).

Harmonic Constituent	Location									
	Astoria		Longview		Skamokawa		St. Helens		Bonneville	
	Field	Model	Field	Model	Field	Model	Field	Model	Field	Model
MM	0.07	0.07	0.10	0.10	0.08	0.09	0.10	0.11	0.09	0.09
MSF	0.03	0.04	0.10	0.11	0.06	0.08	0.11	0.11	0.04	0.05
ALP1	0.01	0.01	0.00	0.00	0.01	0.01	0.01	0.00	0.02	0.01
2Q1	0.02	0.02	0.01	0.01	0.02	0.02	0.00	0.01	0.04	0.03
Q1	0.04	0.03	0.02	0.02	0.03	0.03	0.02	0.02	0.02	0.02
O1	0.28	0.24	0.12	0.10	0.22	0.19	0.09	0.08	0.06	0.05
NO1	0.00	0.00	0.01	0.01	0.00	0.00	0.01	0.01	0.03	0.03
K1	0.35	0.32	0.18	0.14	0.30	0.25	0.16	0.12	0.15	0.14
J1	0.03	0.03	0.01	0.01	0.02	0.02	0.01	0.01	0.05	0.04
OO1	0.01	0.01	0.01	0.01	0.01	0.01	0.01	0.01	0.03	0.03
UPS1	0.01	0.01	0.00	0.00	0.00	0.00	0.00	0.01	0.02	0.02
EPS2	0.02	0.02	0.01	0.01	0.02	0.02	0.01	0.01	0.02	0.01
MU2	0.05	0.08	0.04	0.05	0.06	0.09	0.03	0.04	0.00	0.01
N2	0.16	0.15	0.07	0.06	0.13	0.12	0.05	0.05	0.02	0.01
M2	0.98	1.03	0.51	0.48	0.88	0.88	0.36	0.36	0.12	0.10
L2	0.05	0.06	0.04	0.04	0.05	0.06	0.03	0.03	0.00	0.01
S2	0.31	0.30	0.15	0.13	0.26	0.24	0.10	0.10	0.08	0.06
ETA2	0.01	0.01	0.01	0.01	0.01	0.01	0.01	0.00	0.01	0.01
MO3	0.02	0.04	0.06	0.06	0.06	0.07	0.04	0.04	0.02	0.01
M3	0.01	0.01	0.01	0.01	0.01	0.02	0.01	0.01	0.01	0.00
MK3	0.01	0.02	0.06	0.06	0.05	0.06	0.04	0.04	0.01	0.01
SK3	0.01	0.01	0.02	0.01	0.02	0.02	0.01	0.01	0.01	0.00
MN4	0.01	0.01	0.03	0.02	0.02	0.02	0.01	0.01	0.01	0.01
M4	0.01	0.03	0.11	0.10	0.06	0.08	0.06	0.06	0.03	0.03
SN4	0.00	0.01	0.02	0.02	0.01	0.01	0.01	0.01	0.00	0.00
MS4	0.01	0.02	0.06	0.06	0.03	0.05	0.03	0.04	0.02	0.02
S4	0.00	0.00	0.01	0.01	0.00	0.00	0.00	0.00	0.00	0.00
2MK5	0.01	0.01	0.01	0.01	0.01	0.01	0.01	0.01	0.00	0.00

Harmonic Constituent	Location									
	Astoria		Longview		Skamokawa		St. Helens		Bonneville	
SDK5	0.00	0.00	0.00	0.00	0.00	0.00	0.00	0.00	0.00	0.00
SMN6	0.01	0.01	0.00	0.00	0.01	0.01	0.00	0.00	0.00	0.00
M6	0.02	0.02	0.01	0.00	0.02	0.02	0.00	0.01	0.01	0.01
2MS6	0.02	0.02	0.01	0.01	0.02	0.02	0.01	0.01	0.01	0.00
2SM6	0.00	0.01	0.00	0.00	0.00	0.01	0.01	0.00	0.00	0.00
3MK7	0.00	0.00	0.01	0.00	0.00	0.01	0.01	0.01	0.00	0.00
M8	0.00	0.00	0.01	0.01	0.01	0.01	0.00	0.00	0.00	0.00

Figure 4-11. Harmonic constituent amplitude comparisons between model (black) and field (white) at Astoria.

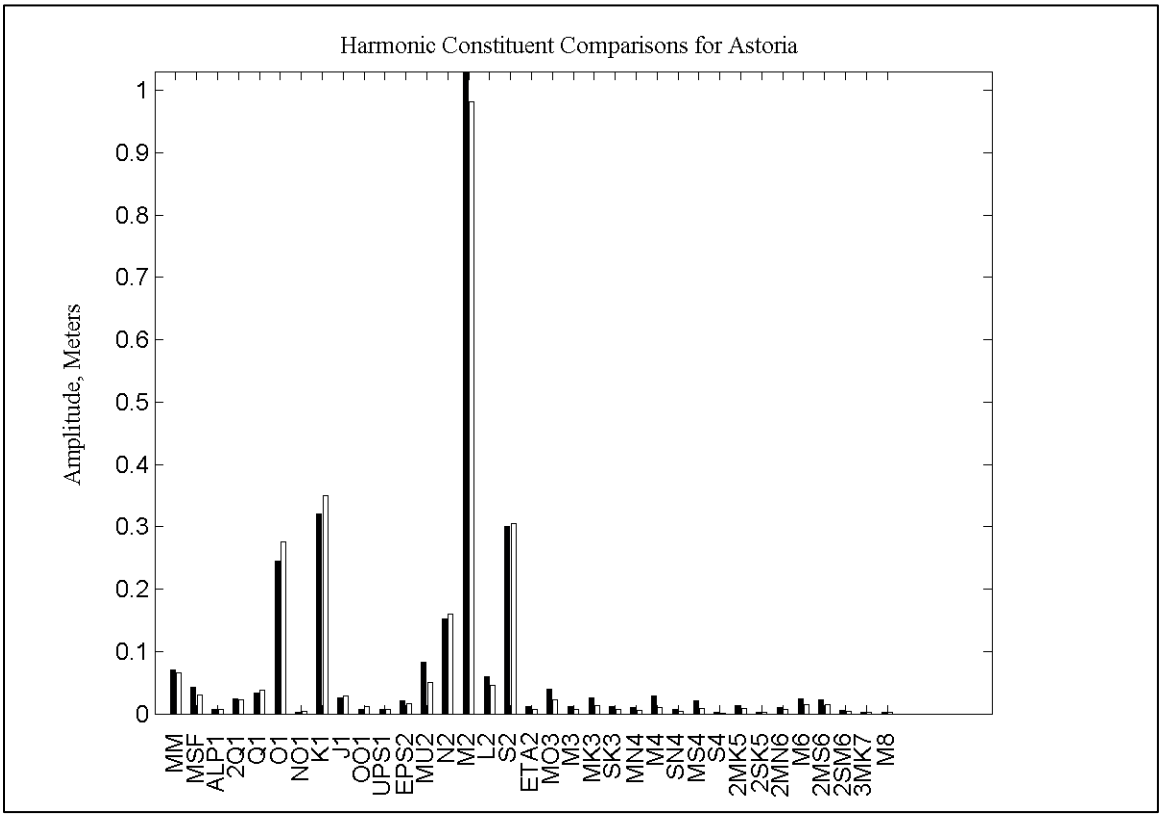

Figure 4-12. Harmonic constituent phase comparisons between model (black) and field (white) at Astoria.

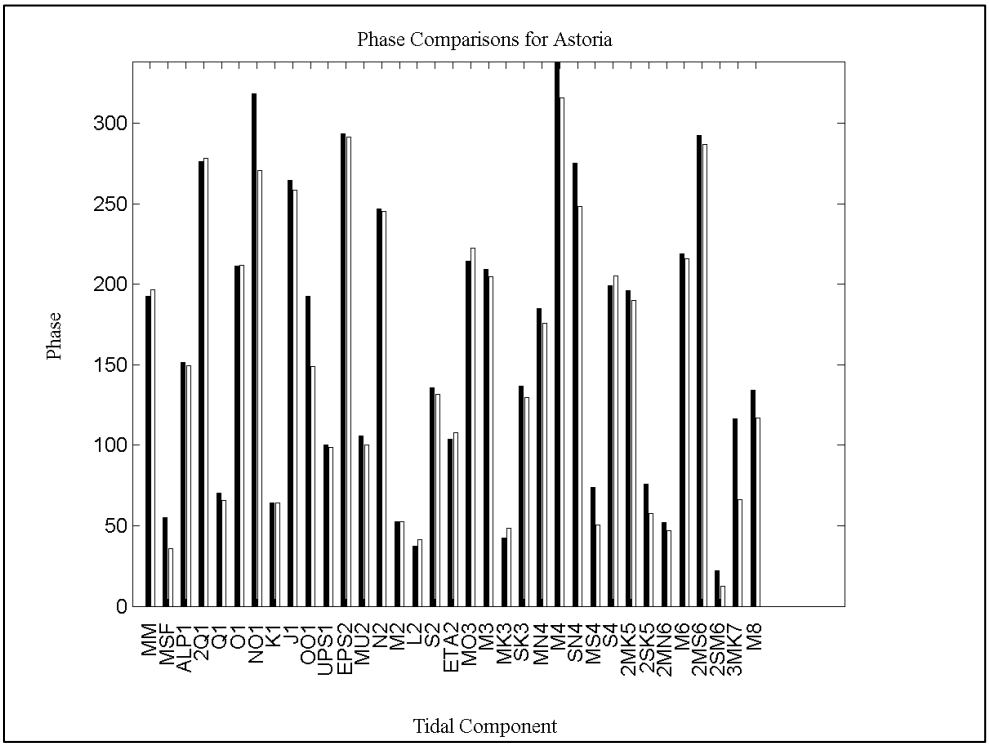

Figure 4-13. Harmonic constituent amplitude comparisons for Skamokawa.

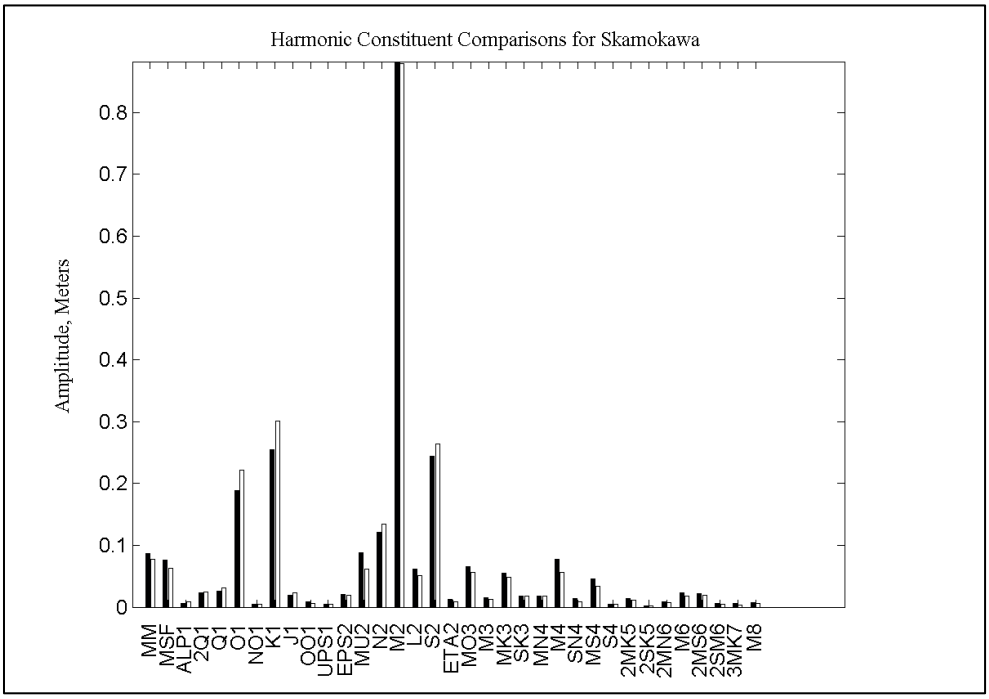

Figure 4-14. Harmonic constituent phase comparisons for Skamokawa.

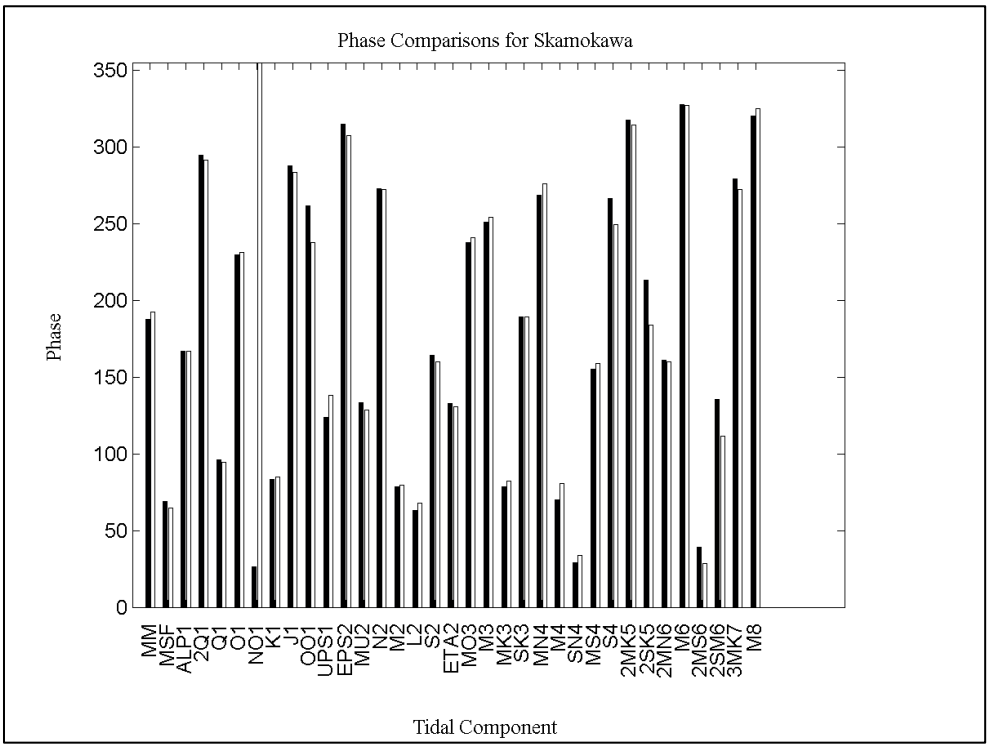

Figure 4-15. Harmonic constituent amplitude comparisons for Longivew.

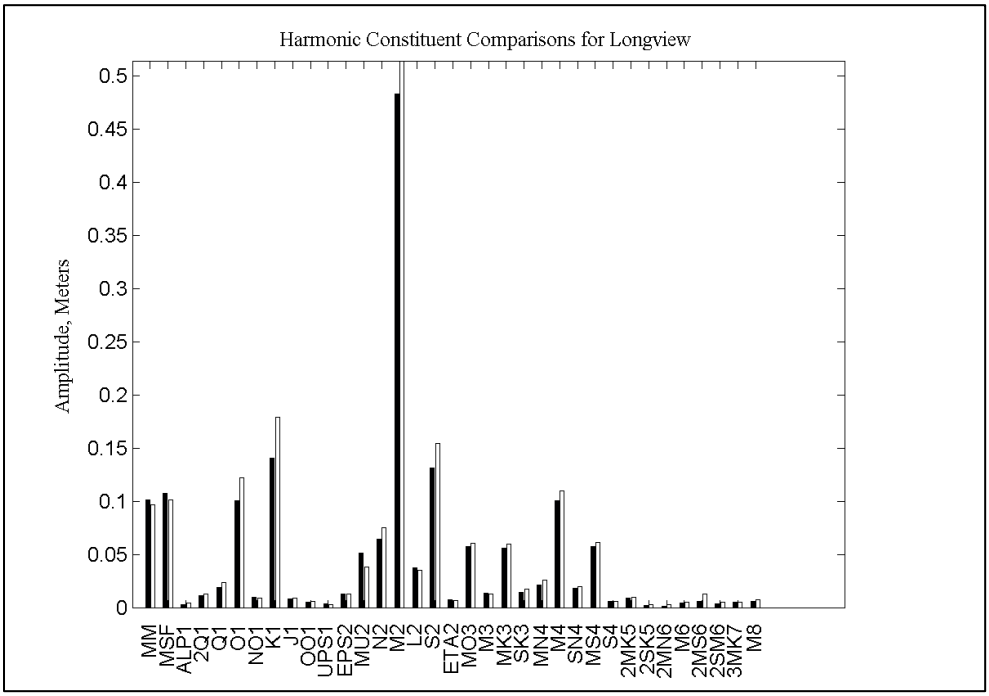

Figure 4-16. Harmonic constituent phase comparisons for Longview.

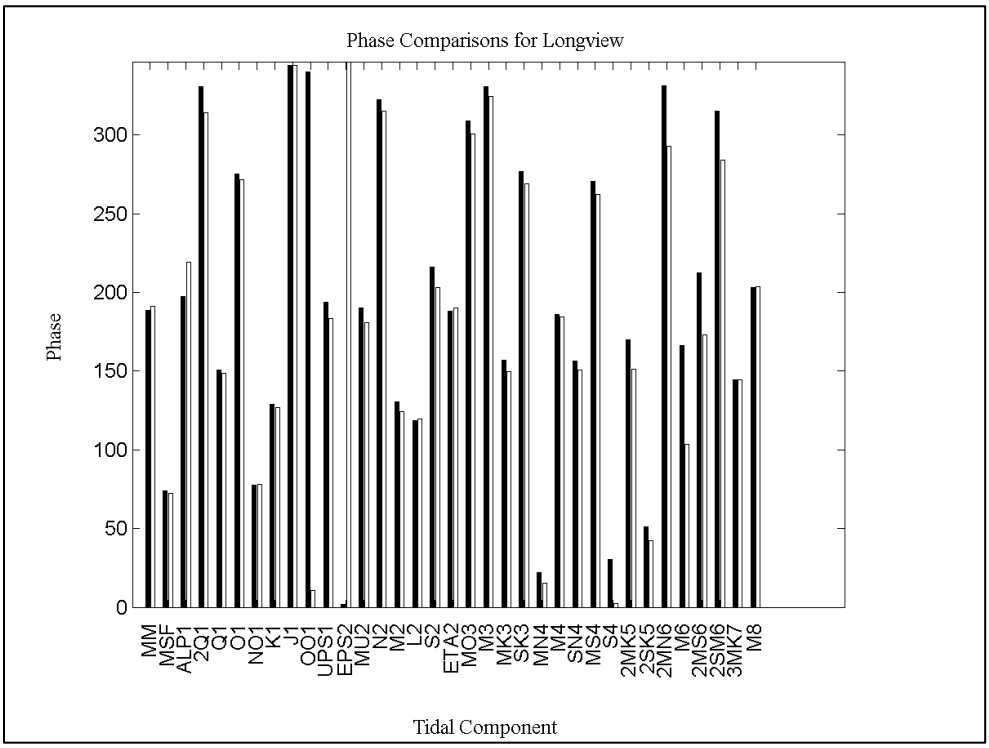

Figure 4-17. Harmonic constituent amplitude comparisons for Saint Helens.

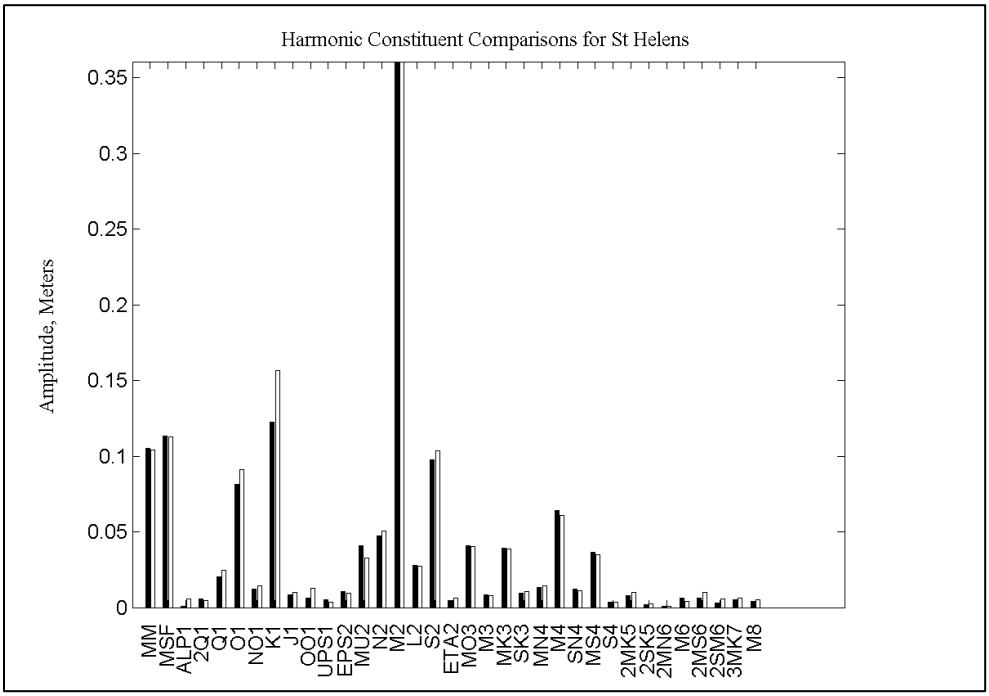

Figure 4-18. Harmonic constituent phase comparisons for Saint Helens.

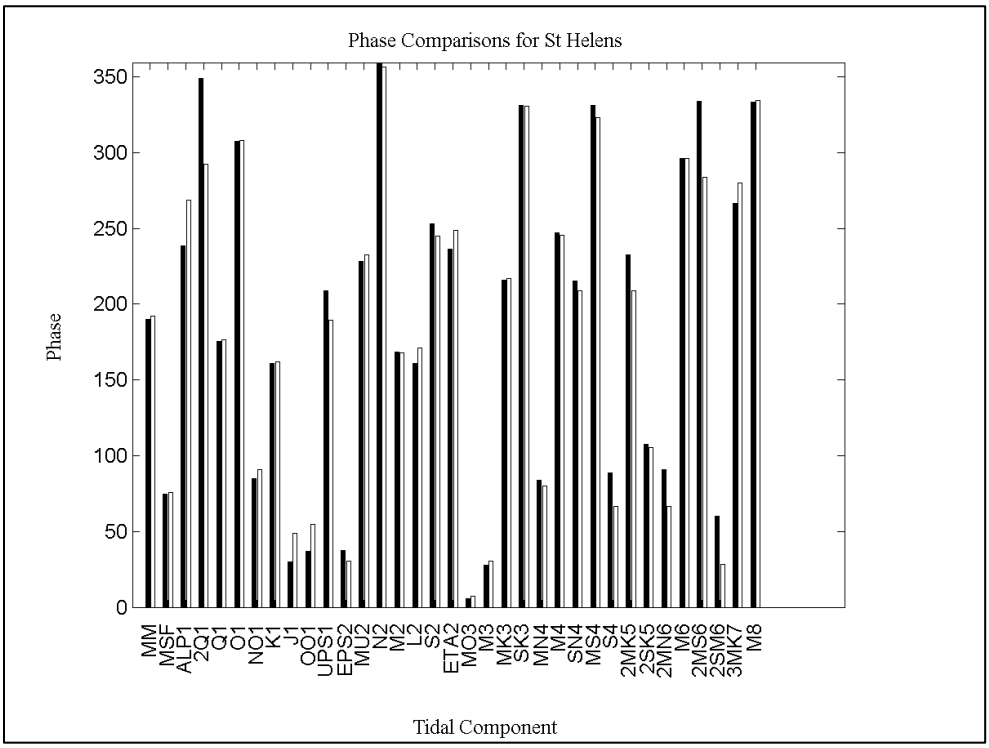

Figure 4-19. Harmonic constituent amplitude comparisons for Bonneville.

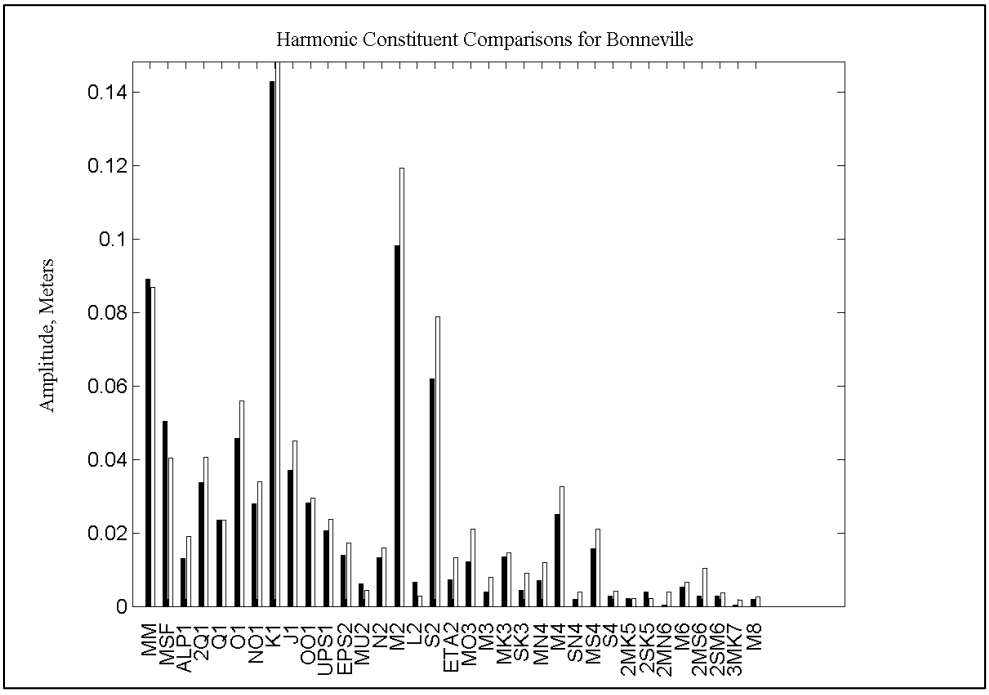

Figure 4-20. Harmonic constituent phase comparisons for Bonneville.

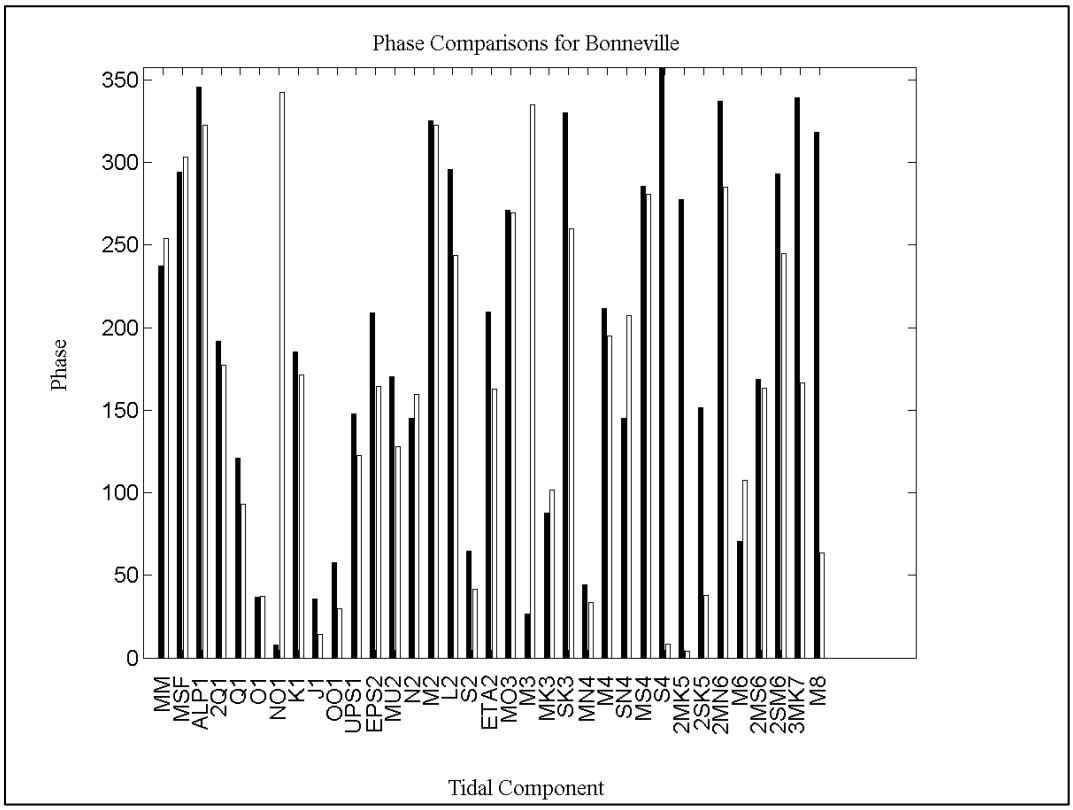

The amplitude and phase of the harmonic constituents show a close correlation between the field and model data. Again, the reduction in amplitudes can be seen moving upstream. Overall, the harmonic analysis for the validation period was slightly better than the results for the calibration period. The period of major flooding is the likely reason the model constituents for the calibration period were not as accurate as in the validation period.

The power spectrum comparison for Astoria and Longview can be found in Figure 4-21 and Figure 4-22, respectively.

Figure 4-21. Power spectrum comparison between the model (blue) and the field (red) at Astoria.

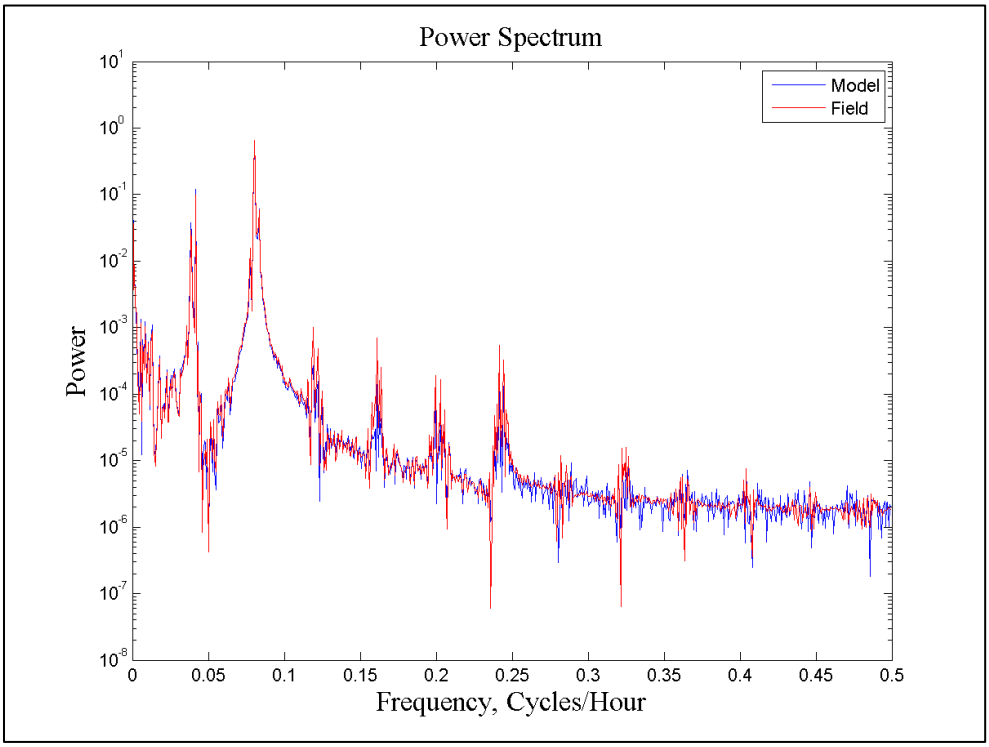

Figure 4-22. Power spectrum comparison between the model (blue) and the field (red) at Longview.

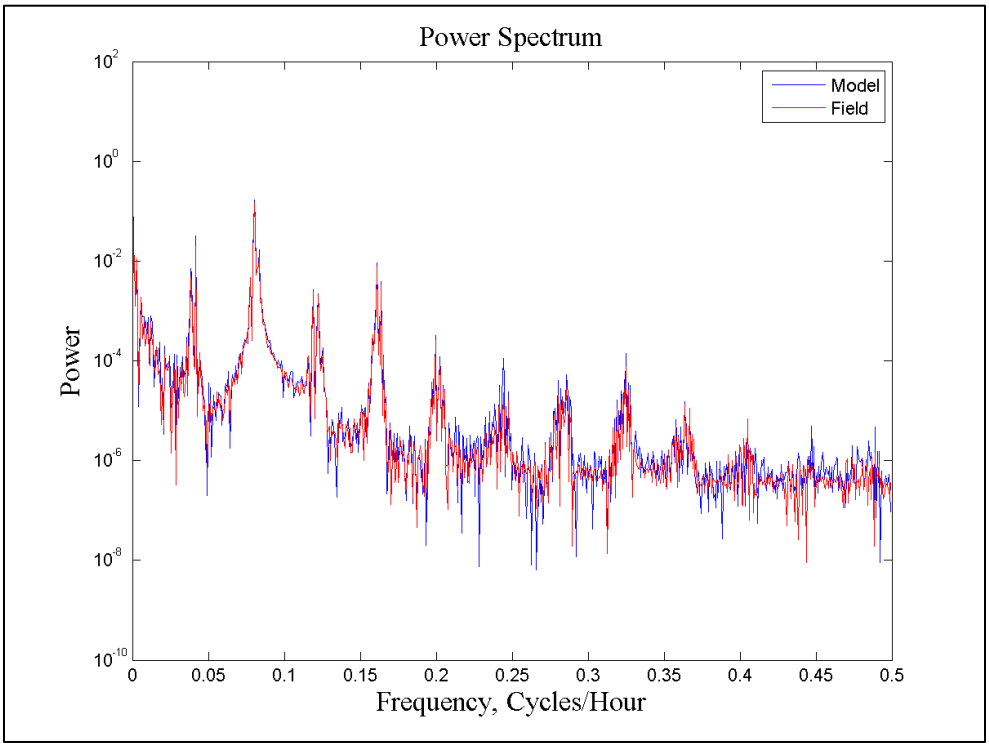

The power spectrum comparisons show the model accurately reproducing the power at the tidal constituent frequencies. As expected, the model is incapable of capturing the higher, non-tidal frequencies but continues to do well at the specific higher harmonic constituent frequencies throughout the power spectrum.

5 Long-Term Analysis

Since the model was run continuously from April through October, it lends itself to the opportunity to examine the model results as a whole. Statistical analysis, shown in Table 5-1, as well as water surface elevation comparisons, and harmonic analysis were conducted.

Table 5-1. Water surface elevation statistical analysis for the long-term model run.

Error Metric	Location				
	Astoria	Skamokawa	Longview	St. Helens	Bonneville
Root Mean Square Error	0.08	0.13	0.08	0.08	0.16
Normalized Root Mean Sq. Error	0.10	0.18	0.13	0.12	0.09
Nash-Sutcliffe Coefficient	0.99	0.97	0.98	0.99	0.99
Willmott Coefficient	1.00	0.99	1.00	1.00	1.00
Covariance	0.67	0.50	0.35	0.50	3.03
Correlation Coefficient	1.00	1.00	0.99	1.00	1.00
Standard Deviation (Field, m)	0.81	0.71	0.60	0.72	1.77
Standard Deviation (Model, m)	0.83	0.71	0.59	0.69	1.72
Variance (Field, m)	0.65	0.51	0.37	0.52	3.12
Variance (Model, m)	0.69	0.50	0.35	0.48	2.96
Mean (Field, m)	1.38	1.54	2.33	2.67	5.33
Mean (Model, m)	1.38	1.66	2.36	2.73	5.45
Median (Field, m)	1.40	1.54	2.30	2.51	4.79
Median (Model, m)	1.39	1.66	2.33	2.59	4.92
Max (Field, m)	3.12	3.23	3.93	4.37	9.02
Max (Model, m)	3.13	3.29	3.87	4.38	8.98
Min (Field, m)	-0.58	0.06	1.03	1.28	2.89
Min (Model, m)	-0.53	0.12	1.08	1.39	3.10

The statistical analysis shows results similar to the calibration and validation periods. The model is accurately representing the field data over the long-term period of 7 months. The majority of values is within 0.05 m of one another and the error values are minimal.

The following are selected water surface elevation comparisons at Astoria and Longview for the long-term model run (Figures 5-1 through 5-4). These two gauges were chosen as representing the remaining gauges well.

Figure 5-1. Water surface elevation comparison between model (blue) and field (green) for Astoria.

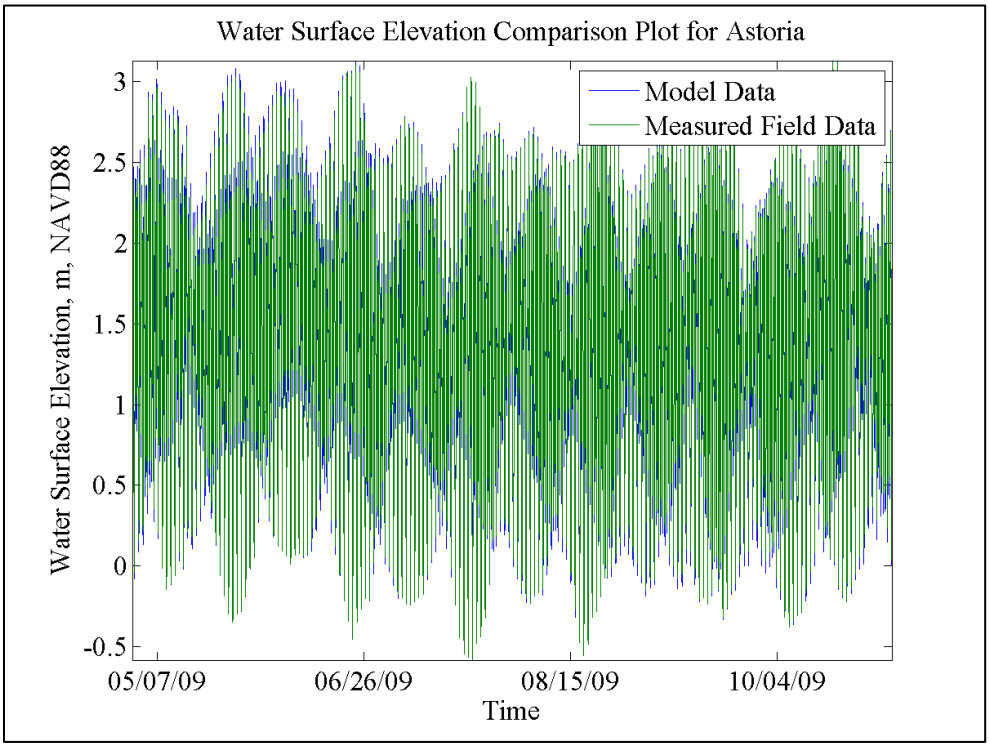

Figure 5-2. Water surface elevation box plot comparison for Astoria.

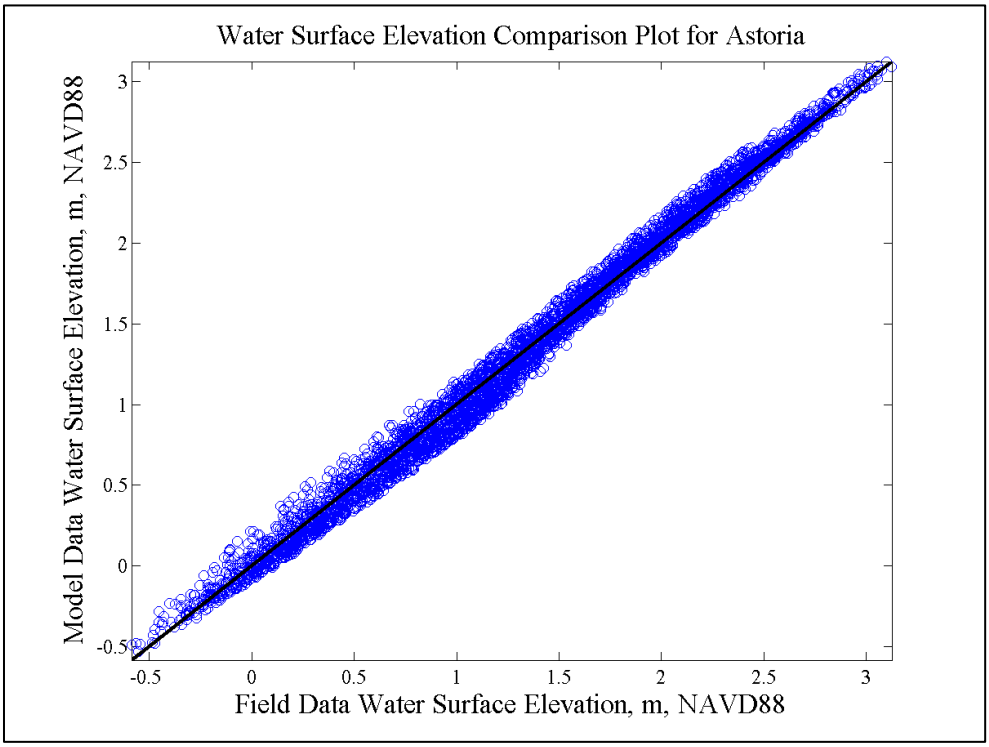

Figure 5-3. Water surface elevation comparison between model (blue) and field (green) for Longview.

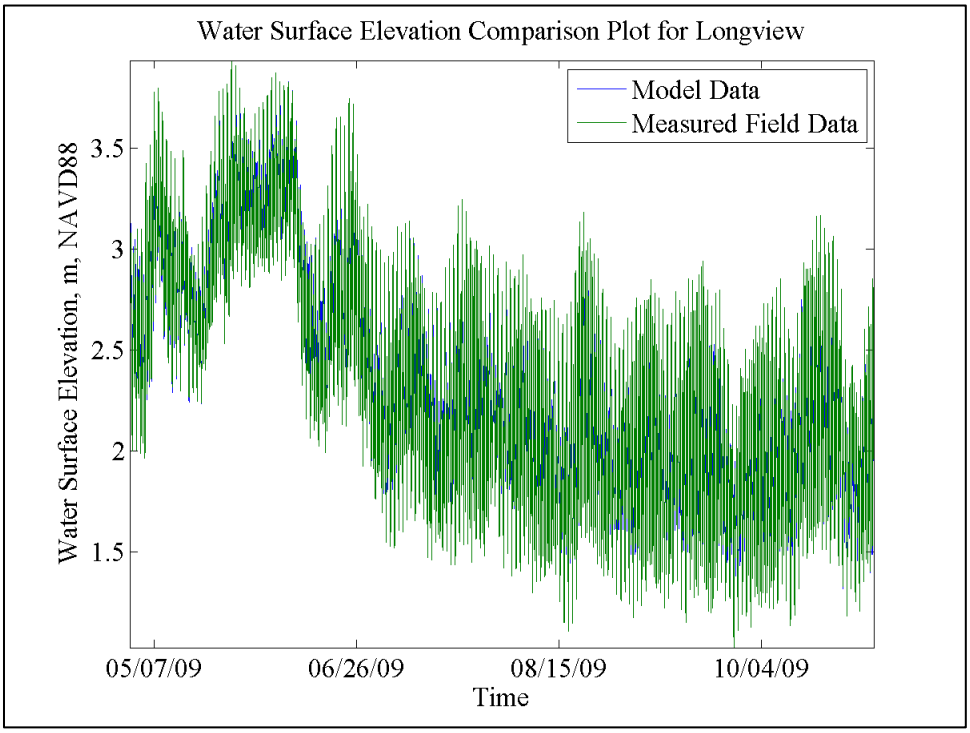

Figure 5-4. Water surface elevation box plot comparison for Longview.

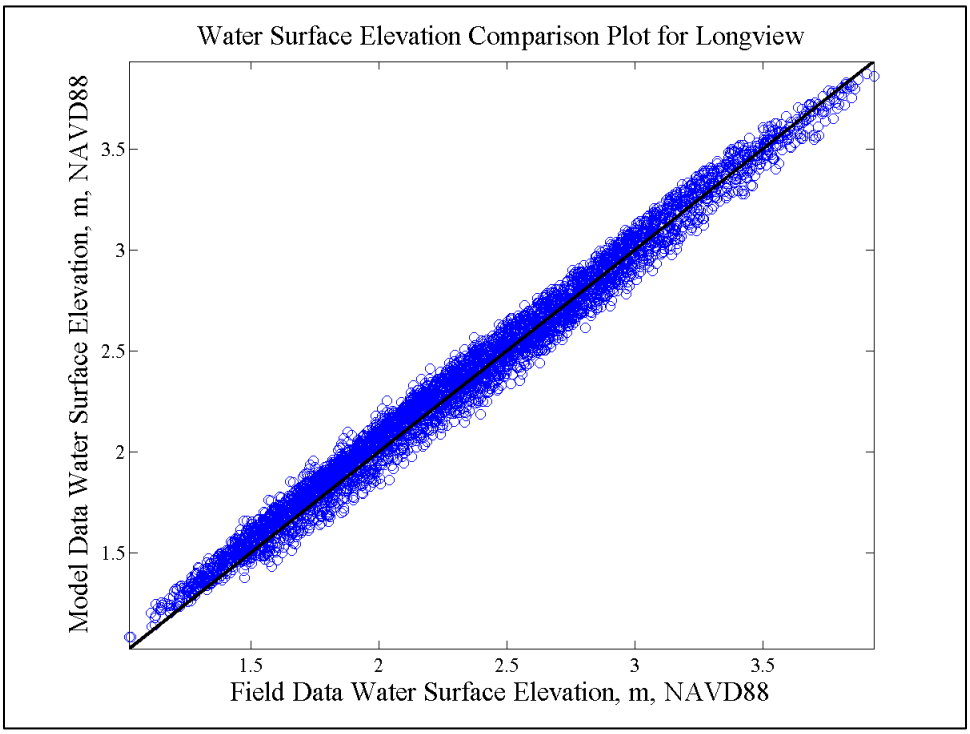

Harmonic analysis was also conducted for the long-term model run to compare the amplitude and phase of the harmonic constituents. Tabular results can be found in Table 5-2 and bar charts can be found in Figures 5-5 through 5-8.

Table 5-2. Harmonic constituent amplitude comparisons for long-term model run (meters).

Harmonic Constituent	Location									
	Astoria		Skamokawa		Longview		St. Helens		Bonneville	
	Field	Model	Field	Model	Field	Model	Field	Model	Field	Model
MM	0.04	0.04	0.06	0.07	0.12	0.11	0.15	0.13	0.22	0.21
MSF	0.04	0.05	0.09	0.10	0.15	0.15	0.18	0.16	0.13	0.12
ALP1	0.01	0.00	0.00	0.00	0.00	0.00	0.00	0.00	0.01	0.01
2Q1	0.01	0.01	0.02	0.01	0.01	0.01	0.00	0.00	0.03	0.02
Q1	0.05	0.04	0.04	0.03	0.02	0.02	0.02	0.02	0.02	0.02
O1	0.28	0.24	0.21	0.18	0.11	0.09	0.08	0.07	0.01	0.01
NO1	0.01	0.01	0.00	0.00	0.00	0.00	0.01	0.00	0.01	0.01
K1	0.43	0.39	0.35	0.30	0.20	0.16	0.15	0.13	0.07	0.07
J1	0.02	0.01	0.01	0.01	0.01	0.00	0.00	0.00	0.02	0.02
OO1	0.02	0.01	0.01	0.01	0.00	0.00	0.00	0.00	0.01	0.01
UPS1	0.00	0.00	0.00	0.00	0.00	0.00	0.00	0.00	0.01	0.01
EPS2	0.01	0.02	0.01	0.01	0.01	0.01	0.00	0.00	0.00	0.00
MU2	0.02	0.05	0.03	0.05	0.02	0.03	0.02	0.02	0.00	0.00
N2	0.18	0.18	0.15	0.14	0.08	0.07	0.05	0.05	0.02	0.01
M2	0.96	1.01	0.84	0.84	0.44	0.41	0.28	0.28	0.05	0.05
L2	0.06	0.08	0.06	0.08	0.04	0.04	0.03	0.03	0.01	0.01
S2	0.24	0.23	0.20	0.18	0.10	0.09	0.06	0.06	0.04	0.03
ETA2	0.00	0.00	0.00	0.00	0.00	0.00	0.00	0.00	0.01	0.00
MO3	0.03	0.05	0.06	0.07	0.05	0.05	0.03	0.03	0.01	0.00
M3	0.01	0.01	0.01	0.01	0.01	0.01	0.01	0.01	0.01	0.00
MK3	0.02	0.04	0.06	0.07	0.07	0.06	0.04	0.04	0.01	0.01
SK3	0.01	0.01	0.02	0.02	0.02	0.01	0.01	0.01	0.00	0.00
MN4	0.00	0.01	0.02	0.03	0.03	0.02	0.01	0.01	0.00	0.00
M4	0.01	0.03	0.06	0.08	0.09	0.08	0.05	0.05	0.01	0.01

Harmonic Constituent	Location									
	Astoria		Skamokawa		Longview		St. Helens		Bonneville	
	Field	Model	Field	Model	Field	Model	Field	Model	Field	Model
SN4	0.00	0.00	0.00	0.00	0.01	0.01	0.00	0.00	0.00	0.00
MS4	0.01	0.02	0.03	0.04	0.04	0.04	0.02	0.02	0.01	0.01
S4	0.00	0.00	0.00	0.00	0.00	0.00	0.00	0.00	0.00	0.00
2MK5	0.01	0.02	0.01	0.01	0.01	0.01	0.01	0.01	0.00	0.00
2SDK5	0.00	0.00	0.00	0.00	0.00	0.00	0.00	0.00	0.00	0.00
2MN6	0.01	0.01	0.01	0.01	0.00	0.00	0.00	0.00	0.00	0.00
M6	0.01	0.02	0.01	0.02	0.00	0.00	0.00	0.00	0.00	0.00
2MS6	0.01	0.02	0.01	0.01	0.00	0.00	0.00	0.00	0.00	0.00
2SM6	0.00	0.00	0.00	0.00	0.00	0.00	0.00	0.00	0.00	0.00
3MK7	0.00	0.00	0.00	0.01	0.00	0.00	0.00	0.00	0.00	0.00
M8	0.00	0.00	0.00	0.01	0.00	0.00	0.00	0.00	0.00	0.00

Figure 5-5. Harmonic constituent amplitude comparisons for Astoria.

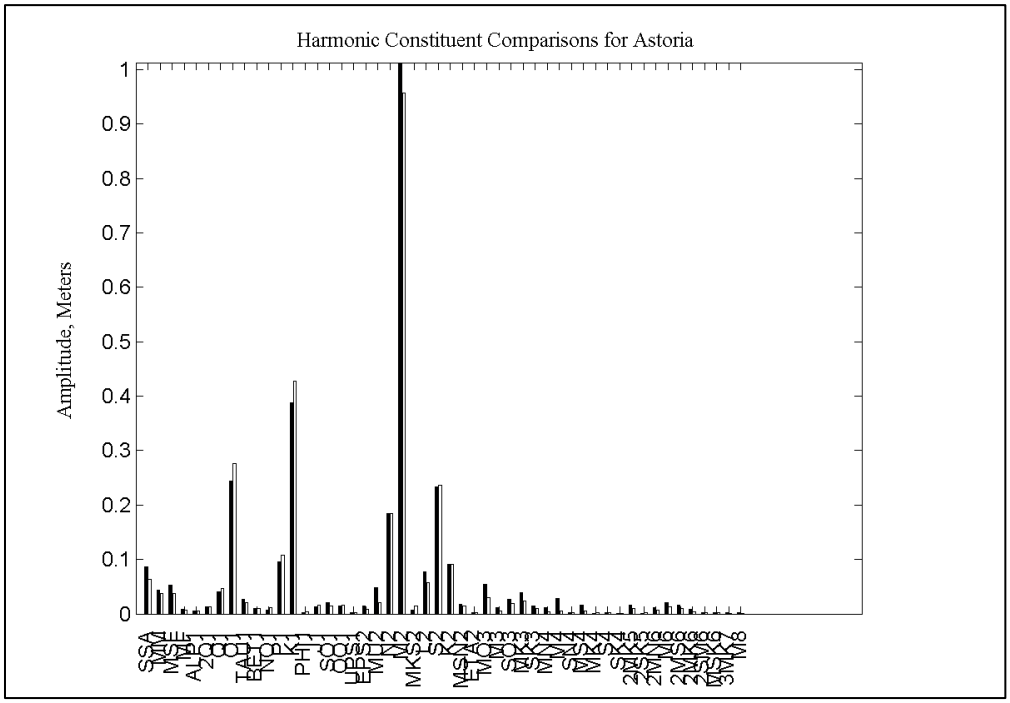

Figure 5-6. Harmonic constituent phase comparisons for Astoria.

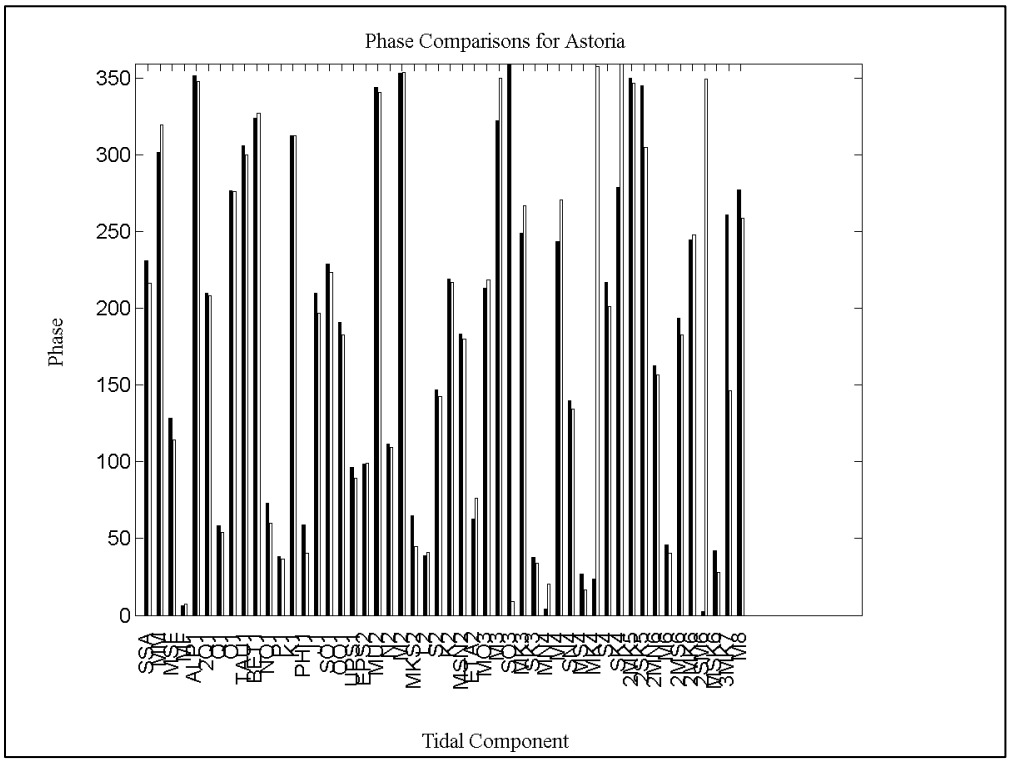

Figure 5-7. Harmonic constituent amplitude comparisons for Longview.

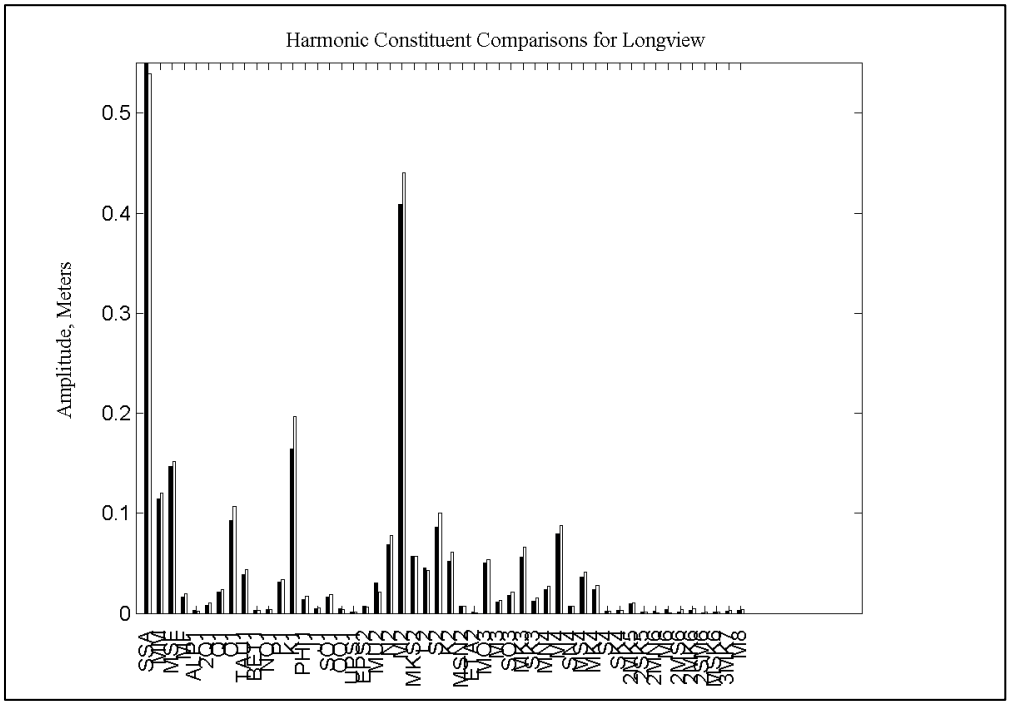

Figure 5-8. Harmonic constituent phase comparisons for Longview.

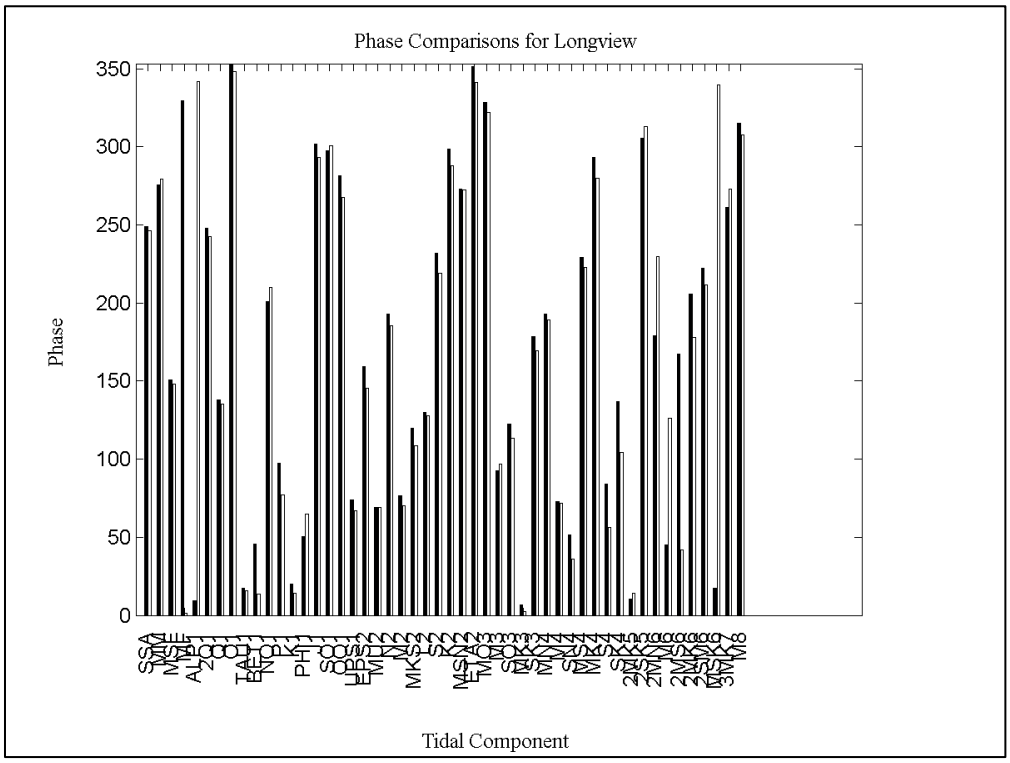

The results from the harmonic analysis for the long-term period show good correlation between the model results and the observed field data. Overall, the model produces excellent results as has been demonstrated through water surface elevation analysis and harmonic analysis.

6 Sea Level Rise (SLR)

The validated LCR AdH model was utilized in estimating predicted SLR in accordance with EC-1165-2-211 (USACE 2009), applicable to Astoria, OR. The observed ocean tidal boundary condition was adjusted to emulate the effect of SLR for each of three scenarios:

- SLR scenario "A" = +0.50 m above present condition (SLR curve #3 at 50 years from present or SLR curve #2 at 70 years from present)
- SLR scenario "B" = +1.0 m above present condition (SLR curve #3 at 75 years from present)
- SLR scenario "C" = +1.5 m above present condition (SLR curve #3 at 100 years from present)

The AdH model simulations are based on the assumption that the riverbed morphology remains constant through time (morphology does not respond to SLR conditions). SLR was estimated using EC-1165-2-211 (USACE 2009), applicable to Astoria, OR. The minimum, maximum, and average water surface elevation along the channel centerline for each SLR scenario can be found in Figures 6-1 through 6-3. Additionally, the minimum, maximum, and average water surface elevation for each SLR scenario was plotted with the 2009 calibration period results (Figures 6-4 through 6-6).

Figure 6-1. Minimum, maximum, and average water surface elevation along LCR channel for SLR scenario A.

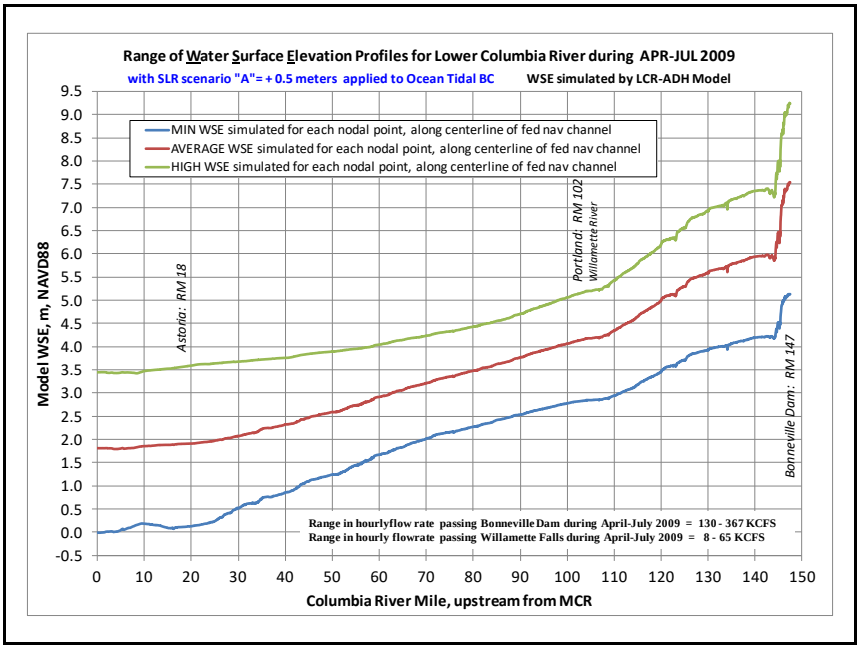

Figure 6-2. Minimum, maximum, and average water surface elevation along LCR channel for SLR scenario B.

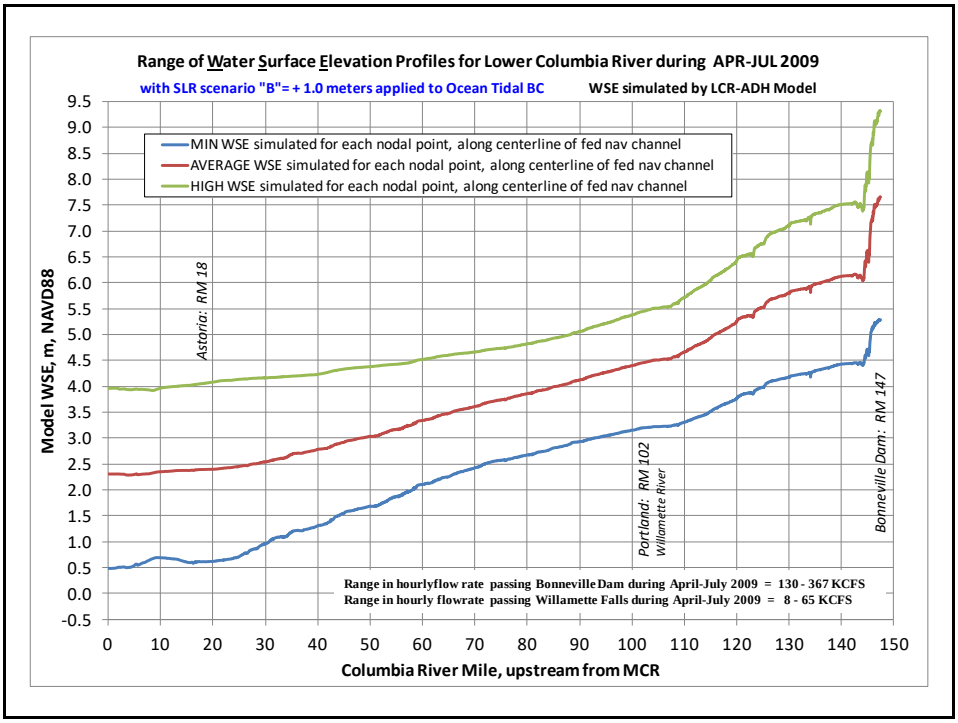

Figure 6-3. Minimum, maximum, and average water surface elevation along LCR channel for SLR scenario C.

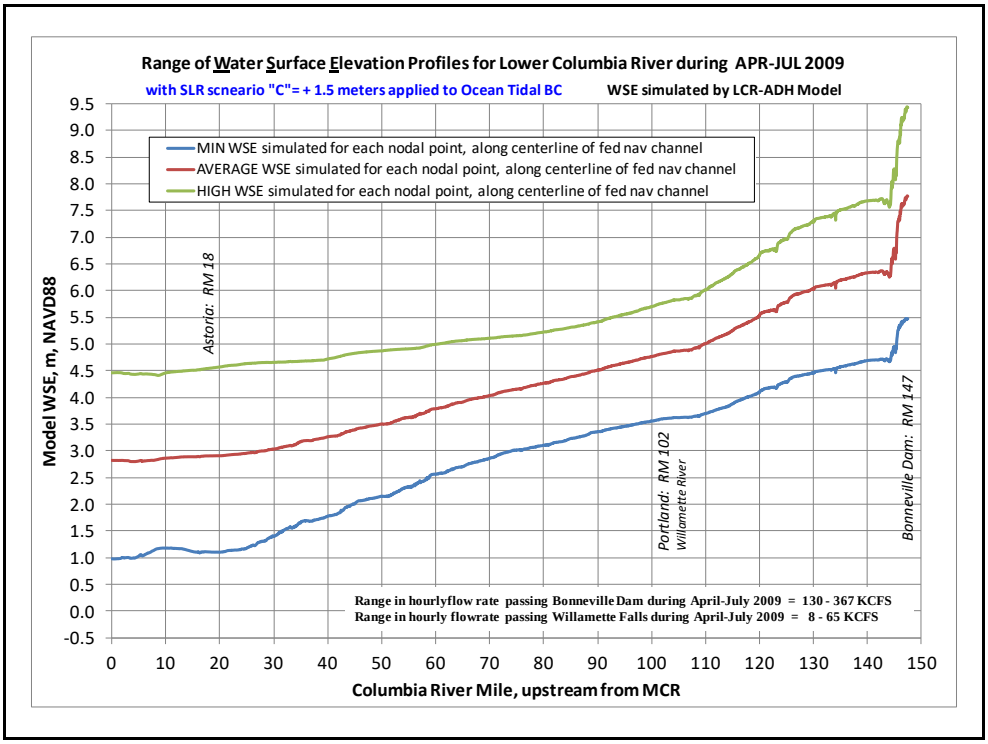

Figure 6-4. Minimum water surface elevation for actual and three SLR scenarios along LCR channel.

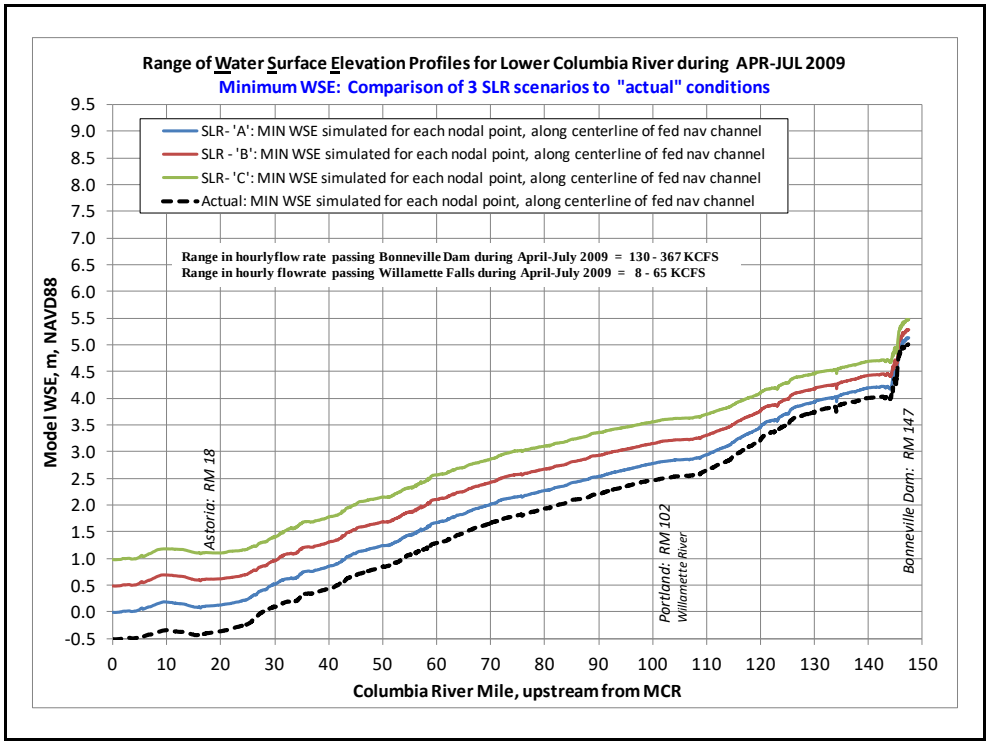

Figure 6-5. Maximum water surface elevation for actual and three SLR scenarios along LCR channel.

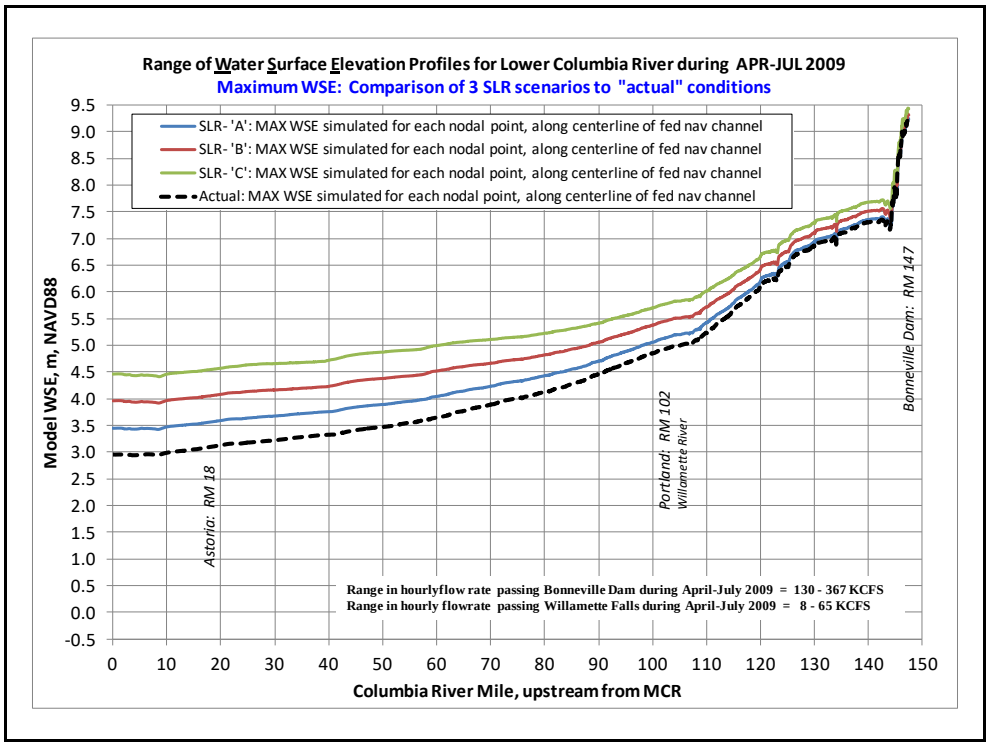

Figure 6-6. Average water surface elevation for actual and three SLR scenarios along LCR channel.

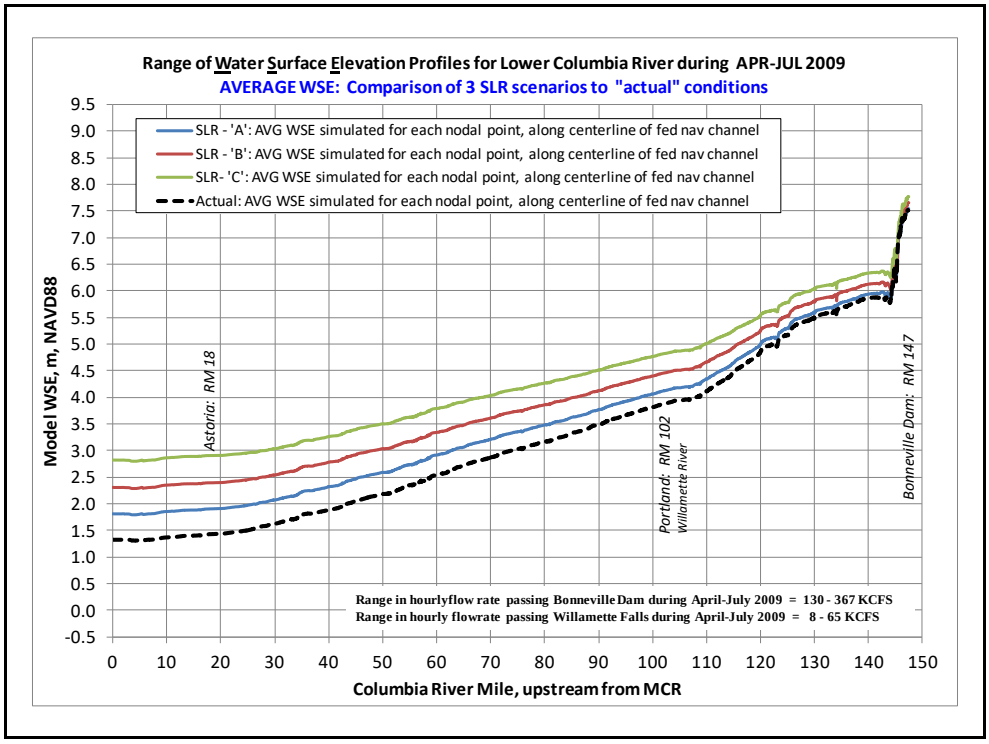

7 Summary and Conclusion

The SWWRP LCR AdH model mesh was modified to meet the needs of NWP. Mesh resolution was added in the Stock Ranch region, Crim's Island, the jetties, and the Young's Bay Causeway. The most current (December 2011) DEM, obtained from NWP, was utilized for mesh elevation interpolation.

Testing was conducted on the approach to modeling pile dikes. The pile dikes in the LCR AdH mesh are modeled as unsubmerged vegetation rather than the computationally intensive method of meshing individual 0.30 m (12 in.) piles. This approach was shown to be effective and accurate at simulating far-field hydraulics through model tests. As anticipated, the near-field hydraulics are not properly captured; however, this was deemed acceptable for the full-domain, global model approach and for modeling effects in the navigation channel and other areas away from pile dike fields.

The water surface elevation calibration and validation were completed for the LCR AdH model. The results from calibration and validation periods are similar and show that the model is accurately reproducing observed field data. The error in the water surface elevations is well within acceptable and anticipated values. The statistical analyses show that the majority of the water surface elevations produced by the model is within 0.05 m of the field data.

Additionally, since the model was run continuously for 7 months (April through October 2009), a statistical analysis was conducted on this entire long-term run. The results were very similar to the calibration and validation results and show that the model is accurately representing the observed field data over the entire long-term model run.

In conclusion, the LCR AdH model is accurately reproducing observed water surface elevations at several locations within the model domain and is an adequate tool for calculating water surface elevations in the LCR system, particularly for restoration efforts.

References

Aquaveo. 2016. Surface-Water Modeling System (SMS). https://www.aquaveo.com/software/sms-surface-water-modeling-system-introduction

Fox, D. S., S. Bell, W. Nehlsen, and J. Damron. 1984. *The Columbia River Estuary: Atlas of Physical and Biological Characteristic*s. Columbia River Estuary Data Development Program, Columbia River Estuary Study Taskforce, Astoria, Oregon.

Higgins, J. 2006. *The Radical Statistician: A Beginners Guide to Unleashing the Power of Applied Statistics in the Real World* (5th Edition). https://www.management-advantage.com/products/RadicalStatistician.htm

McLaughlin, J. W., A. Bilgili, and D. R. Lynch. 2003. "Numerical Modeling of Tides in the Great Bay Estuarine System: Dynamical Balance and Spring-Neap Residual Modulation." *Estuarine, Coastal, and Shelf Science* 57(1–2)A: 283–296.

Nash, J. E., and J. V. Sutcliffe. 1970. "River Flow Forecasting through Conceptual Models Part I – A Discussion of Principles." *Journal of Hydrology* vol. 10: 282–290.

National Oceanic and Atmospheric Administration (NOAA). 2007. *Tidal Analysis and Predication*. NOAA Special Publication NOA CO-OPS 3. July 2007. https://tidesandcurrents.noaa.gov/pub.html

Savant, G., R. C. Berger, T. O. McAlpin, and J. N. Tate. 2011. "An Efficient Implicit Finite Element Model for Dam and Levee Breaches." *Journal of Hydraulic Engineering* 137(9). https://ascelibrary.org/doi/abs/10.1061/(ASCE)HY.1943-7900.0000372

Sherwood, C. R., D. A. Jay, R. B. Harvey, P. Hamilton, and C. A. Simenstad. 1990. "Historical Changes in the Columbia River Estuary." *Progress in Oceanograrphy* 25: 299–352.

Simenstad, C. A., L. F. Small, C. D. McIntire, D. A. Jay, and C. Sherwood. 1990. "Columbia River Estuary Studies: An Introduction to the Estuary, a Brief History, and Prior Studies." *Progress in Oceanography* 25(1–4): 1–13.

U.S. Army Corps of Engineers (USACE). 2009. *Water Resource Policies and Authorities Incorporating Sea-Level Change Considerations in Civil Works Programs*. Circular No. 1165-2-211. Washington, DC.

U.S. Army Corps of Engineers (USACE), Northwestern Division, North Pacific Region. (n.d.). *Water Management for the Pacific Northwest Reservoir System*. http://www.nwd-wc.usace.army.mil/pdf/wmbroch.pdf

Willmott, C. J., S. G. Ackleson, R. E. Davis, J. J. Feddema, K. M. Klink, D. R. Legares, J. O'Donnell, and C. M. Rowe. 1985. "Statistics for the Evaluation and Comparison of Models." *Journal of Geophysical Research* 90(C5): 8995–9005.

Unit Conversion Factors

Multiply	By	To Obtain
cubic feet	0.02831685	cubic meters
feet	0.3048	meters
miles (U.S. statute)	1,609.347	meters

Acronyms and Abbreviations

2D	two-dimensional
3D	three-dimensional
AdH	Adaptive Hydraulics
CHL	Coastal and Hydraulics Laboratory
DEM	digital elevation model
ERDC	U.S. Army Engineer Research and Development Center
FCRPS	Federal Columbia River Power System
FY	fiscal year
L&D	lock and dam
LCR	Lower Columbia River
NAD83	North American Datum of 1983
NAVD88	North American Vertical Datum of 1988
NOAA	National Oceanic and Atmospheric Administration
NRMSE	normalized root mean square error
NWP	Portland District
PST	Pacific Standard time
RM	River Mile
RMSE	root mean square error
SLR	sea level rise
SWWRP	System Wide Water Resource Program
USACE	U.S. Army Corps of Engineers
USGS	U.S. Geological Survey

REPORT DOCUMENTATION PAGE

Form Approved
OMB No. 0704-0188

1. REPORT DATE	2. REPORT TYPE	3. DATES COVERED *(From - To)*
April 2020	Final Report	

4. TITLE AND SUBTITLE
Lower Columbia River Adaptive Hydraulics (AdH) Model: Development, Water Surface Elevation Validation, and Sea Level Rise Analysis

5a. CONTRACT NUMBER

5b. GRANT NUMBER

5c. PROGRAM ELEMENT NUMBER

6. AUTHOR(S)
Kimberly C. Pevey, Gaurav Savant, Hans Rod Moritz, and Elvon O. Childs

5d. PROJECT NUMBER

5e. TASK NUMBER

5f. WORK UNIT NUMBER

7. PERFORMING ORGANIZATION NAME(S) AND ADDRESS(ES)
Coastal and Hydraulics Laboratory
U.S. Army Engineer Research and Development Center
3909 Halls Ferry Road
Vicksburg, MS 39180-6199

U.S. Army Corps of Engineers, Portland District
333 SW First Avenue
Portland, OR 97208-2946

8. PERFORMING ORGANIZATION REPORT NUMBER
ERDC/CHL TR-20-6

9. SPONSORING/MONITORING AGENCY NAME(S) AND ADDRESS(ES)
U.S. Army Corps of Engineers, Portland District
333 SW First Avenue
Portland, OR 97208-2946

10. SPONSOR/MONITOR'S ACRONYM(S)
USACE NWP

11. SPONSOR/MONITOR'S REPORT NUMBER(S)

12. DISTRIBUTION/AVAILABILITY STATEMENT
Approved for public release; distribution is unlimited.

13. SUPPLEMENTARY NOTES
MIPR W66QKZ11602884, "Lower Columbia River Adaptive Hydraulics (AdH) Model"

14. ABSTRACT
A numerical model of the Lower Columbia River, validated to water surface elevations, has been generated using the Adaptive Hydraulics (AdH) code. The model boundary conditions include an ocean tidal boundary and five inflows: the Lewis, Cowlitz, Willamette, and Sandy Rivers, and the Columbia River at Bonneville Lock and Dam. The model, which spans approximately 146 river miles, accurately reproduces water surface elevations measured in the field at several locations along the model domain.
An examination of the AdH model's Friction Library was also conducted. The Friction Library was used in this application to estimate the effects of pile dikes. Rather than model individual piles in the model mesh, the piles were modeled using the Friction Library's submerged vegetation material type. Through testing of this application, it was determined that the Friction Library approach, which enhances model run time and efficiency, can accurately reproduce the global effects of pile dike fields.
Additionally, the validated model was used to analyze three sea level rise (SLR) scenarios, which correspond to predicted SLR at Astoria, OR, at 50, 75, and 100 years from the present (0.5 meter [m], 1.0 m, and 1.5 m, respectively).

15. SUBJECT TERMS
Columbia River (Ore. And Wash.), Computer simulation, Hydraulic models, Sea level, Water levels

16. SECURITY CLASSIFICATION OF:			17. LIMITATION OF ABSTRACT	18. NUMBER OF PAGES	19a. NAME OF RESPONSIBLE PERSON
a. REPORT	b. ABSTRACT	c. THIS PAGE			Gaurav Savant
Unclassified	Unclassified	Unclassified	SAR	80	19b. TELEPHONE NUMBER *(Include area code)* 601-634-3213